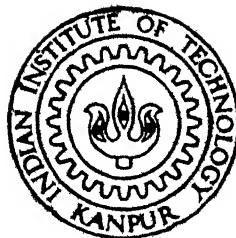


ANALYSIS AND CONTROLLER DESIGN BY POLE PLACEMENT FOR A DC-DC BUCK-BOOST CONVERTER

by

LT. P. P. SACHDEV



DEPARTMENT OF ELECTRICAL ENGINEERING

INDIAN INSTITUTE OF TECHNOLOGY KANPUR

MARCH, 1998

TH
66/1998/m

Salya

8

C

A

**ANALYSIS AND CONTROLLER DESIGN BY POLE
PLACEMENT FOR A DC-DC BUCK-BOOST CONVERTER**

20031

A Thesis Submitted
in Partial Fulfilment of the Requirements
for the Degree of

Master of Technology

by

LT. P.P. SACHDEV

to the

**DEPARTMENT OF ELECTRICAL ENGINEERING
INDIAN INSTITUTE OF TECHNOLOGY, KANPUR**

March 1998

-4 MAY 1998 / EE
CENTRAL LIBRARY
F. T. KANPIL

Case No. A **125358**

EE-1998-M-SAC-ANA

Entered in System

DM
8-5-98




CERTIFICATE

1231

It is certified that the work contained in the thesis entitled **ANALYSIS AND CONTROLLER DESIGN BY POLE PLACEMENT FOR A DC-DC BUCK-BOOST CONVERTER**, by P.P. SACHDEV, has been carried out under my supervision and that this work has not been submitted elsewhere for a degree.

March 1998


Dr. A. JOSHI
Professor
Department of Electrical Engineering
I.I.T. Kanpur

ACKNOWLEDGEMENTS

At this point of time in my life, when it is a dream come true for me, I would like to express my gratitude to my elders and thanks to all my friends, who made it possible for me to accomplish what I once thought as impossible. I would like to thank Gyanender, whose presence always reassured me of “all that begins well. ends well”. On the eve of submission of thesis report, I remember Mr. R.K. Singh (presently in England) who gave a kick start to this work and I am sure he will be proud of what came out of it. I was fortunate to have friends like Rajan, Bhujbal, Srinivas Chandra, G.M. Reddy, Sunil, Malabika Basu and Ramesh Ji. Life has strange ways where people meet to say goodbye, but what’s left with us is sweet memories. “We had joy we had fun and we had seasons in the sun.....(especially the three musketeers of Power Electronics)”.

Though it was towards the end of my tenure in IIT Kanpur, I made another good friend, always smiling Qadeer. As the saying goes he provided that last bit to make it to the end. I shall always miss you. One person who always stood by me during my highs and lows, silently participating in my work was my wife Arti. To whom I dedicate this work.

I thank Mr. Uday Mazumdar, Mr. Ajai Srivastava, Mr. Rajesh, Mr. Ramnath for their kind help and support during the crucial days of this work.

Working under Dr. A. Joshi, was a pleasure. I thank him for the ^{extra} ~~extream~~ patience with which he tolerated my blunders. Much of the finner tips came from him and I could always feel his reassurring hand on my back.

I am extremely grateful to Dr. A.K. Raina, who allowed me free access to his lab facilities.

ABSTRACT

A detailed analysis of modelling and behaviour of buck boost converter has been done. The state space linear differential models are used to study the open loop time domain behaviour of the converter. To enable design of close loop feed back controllers continuous time representation of the converter is achieved by small signal linearized model which are obtained by linearizing the non linear state space averaged equations. Attempt is made to high light the fact that if switching information is neglected then state space average model can represent the converter behaviour for all kinds of perturbation. Using the small signal linearized model a state feed back controller is designed by pole placement and its response for perturbation in V_{ref} , V_{dc} , R has been simulated.

Contents :

1.	Introduction	1
2.	Buck-Boost Converter	3
2.1	Converter Topology	3
2.2	State Space Representation	12
2.3	Open Loop Domain Simulation of the Converter	13
3.	State Space Averaged Model	25
3.1	State Space Average Model	25
3.2	Characteristics of Buck-Boost Converter	27
3.2.1	Value of Duty Ratio at Boundary Operation (D_{boundary})	28
3.2.2	Duration of Mode 2 (D_{1TC})	33
3.3	Converter Simulation Using State-Space Averaged Model	39
3.4	Small Signal Approximation for Linearity	51
3.4.1	Transfer Function $\frac{\hat{V}_c(s)}{\hat{d}(s)}$ and Bode Plot	53
3.4.2	Transfer Function $\frac{\hat{V}_c(s)}{\hat{u}_c(s)}$ and Bode Plot	55

4.	Close Loop Control	63
4.1	Transient Response of a Second -order System	63
4.1.1	Pole Placement	66
4.2	Design of Servo System	68
4.3	Open-loop Damping Ratio and Undamped Natural Frequency	72
4.4	Close-loop Control of Converter	74
4.5	Simulation of Converter with Close-loop Control	77
4.5.1	Close-loop Response for Step Change in Load Resistance R and V_{REF}	78
4.5.2	Close-loop Response for Sinusoidal Variation in V_{REF}	79
4.5.3	Close-loop Response for Sinusoidal Variation in V_{dc}	80
4.5.4	Close-loop Response for Sinusoidal Variation in R	80
5.	Conclusion and Future Work	92
	REFERENCES	94
	APPENDIX -A	95
	APPENDIX -B	100
	APPENDIX -C	108

List of Figures

Fig. 2.1	Circuit topology of Buck-Boost converter	4
Fig. 2.2(a)	Mode-1 equivalent circuit	4
Fig. 2.2(b)	Mode-2 equivalent circuit	4
Fig. 2.2(c)	Mode-3 equivalent circuit	4
Fig. 2.3(a)	Approximate I_L and V_c waveforms in continuous conduction mode	6
Fig. 2.3(b)	Approximate I_L and V_c waveforms in boundary conduction mode	6
Fig. 2.3(c)	Approximate I_L and V_c waveforms in discontinuous conduction mode	7
Fig. 2.4	Open-loop time domain simulation using state-space differential equation model.	14
Fig. 2.5 (a) & (b)	System response for change in R from 10 to 5 Ohms for D=0.1	16
Fig. 2.6 (a) & (b)	System response for change in R from 10 to 20 Ohms for D=0.1	17
Fig. 2.7 (a) & (b)	System response for change in R from 10 to 30 Ohms for D=0.5	18
Fig. 2.8(a) & (b)	System response for change in D from 0.1 to 0.3 for R=30 Ohms	19
Fig. 2.9 (a) & (b)	System response for change in D from 0.1 to 0.01 for R=5 Ohms	20
Fig. 2.10(a) & (b)	System response for change in R from 10 to 30 Ohms for D=0.1	21
Fig. 2.11(a) & (b)	System response for change in R from 30 to 50 Ohms for D=0.1	22
Fig. 2.12(a) & (b)	System response for change in D from 0.1 to 0.15 for R=30 Ohms	23

Fig. 3.1	Simple r_L -L circuit	31
Fig. 3.2	D_{boundary} vs load resistance R	31
Fig. 3.3(a)	Duration of Mode-2 as given by equation (3.11)	35
Fig. 3.3(b)	Duration of Mode-2 as in actual converter	35
Fig. 3.4(a)	Average output voltage vs duty ratio	38
Fig. 3.4(b)	Average Inductor current vs duty ratio	38
Fig. 3.5(a) & (b)	System response for change in R from 10 to 5 Ohms using state space average model defined by equations 3.2 and 3.3	41
Fig. 3.5(c) &(d)	System response for change in D from 0.1 to 0.01 Ohms using state space average model defined by equations 3.2 and 3.3	41
Fig. 3.6	I_L - D_1 plane: conditions of model transition	43
Fig. 3.7(a) & (b)	System response for change in R from 10 to 20 Ohms for $D=0.1$ using conditions given by equations 3.6(b) and 3.12(A) for model transition.	43
Fig. 3.8(a) &(b)	System response for change in R from 10 to 30 Ohms for $D=0.5$ using conditions given by equations 3.6(b) and 3.12(A) for model transition.	44
Fig. 3.9(a) &(b)	System response for change in D from 0.1 to 0.3 for $R=30$ Ohms using conditions given by equations 3.6(b) and 3.12(A) for model transition.	44
Fig. 3.10(a) &(b)	System response for change in D from 0.1 to 0.01 Ohms for $R=5$ Ohms using conditions given by equations 3.6(b) and 3.12(A) for model transition.	46
Fig. 3.10(c) &(d)	System response for change in D from 0.1 to 0.01 Ohms for $R=5$ Ohms using conditions given by equations 3.6(b) and 3.12(A) for model transition, and implying it to intermediate outputs of 'ode45' subroutine.	46
Fig. 3.11(a) &(b)	System response for change in R from 10 to 30 Ohms for $D=0.1$ Ohms using conditions given by equations 3.6(b) and 3.12(A) for model transition, and implying it to intermediate outputs of 'ode45' subroutine.	47

Fig. 3.12(a) & (b)	System response for change in R from 30 to 50 Ohms for D=0.1 Ohms using conditions given by equations 3.6(b) and 3.12(A) for model transition, and implying it to intermediate outputs of 'ode45' subroutine.	47
Fig. 3.13(a) & (b)	System response for change in D from 0.1 to 0.15 for R= 30 Ohms using conditions given by equations 3.6(b) and 3.12(A) for model transition, and implying it to intermediate outputs of 'ode45' subroutine.	48
Fig. 3.14(a) & (b)	System response for change in R from 10 to 30 Ohms for D=0.1 using conditions given by equations 3.6(b) and 3.12(B) for model transition, and implying it to intermediate outputs of 'ode45' subroutine.	48
Fig. 3.15(a) & (b)	System response for change in R from 30 to 50 Ohms for D=0.1 using conditions given by equations 3.6(b) and 3.12(B) for model transition, and implying it to intermediate outputs of 'ode45' subroutine.	49
Fig. 3.16(a) & (b)	System response for change in D from 0.1 to 0.15 for R= 30 Ohms using conditions given by equations 3.6(b) and 3.12(B) for model transition, and implying it to intermediate outputs of 'ode45' subroutine.	49
Fig. 3.17(a) & (b)	System response for change in D from 0.1 to 0.01 for R= 5 Ohms using conditions given by equations 3.6(b) and 3.12(B) for model transition, and implying it to intermediate outputs of 'ode45' subroutine.	50
Fig. 3.18(a) & (b)	System response for change in R from 30 to 50 Ohms for D=0.1 and using state space average model defined by equations 3.4 and 3.5	50
Fig 3.19	Flowgraph for small signal approximation for linearity	52
Fig 3.20	Bode plot for the transfer function $\frac{\hat{V_c(s)}}{\hat{d(s)}}$ at the operating point R=5 Ohms and D=0.1	56
Fig 3.21	Bode plot for the transfer function $\frac{\hat{V_c(s)}}{\hat{d(s)}}$ at the operating point R=5 Ohms and D=0.5	56

Fig 3.22	Bode plot for the transfer function $\frac{\hat{V_c(s)}}{\hat{d(s)}}$ at the operating point R=30 Ohms and D=0.1	57
Fig 3.23	Bode plot for the transfer function $\frac{\hat{V_c(s)}}{\hat{d(s)}}$ at the operating point R=30 Ohms and D=0.5	57
Fig 3.24	Verification of Bode plot for the transfer function $\frac{\hat{V_c(s)}}{\hat{d(s)}}$	58
Fig 3.25	Bode plot for the transfer function $\frac{\hat{V_c(s)}}{\hat{V_{dc}(s)}}$ at the operating point R=5 Ohms and D=0.1	59
Fig 3.26	Bode plot for the transfer function $\frac{\hat{V_c(s)}}{\hat{V_{dc}(s)}}$ at the operating point R=5 Ohms and D=0.5	59
Fig 3.27	Bode plot for the transfer function $\frac{\hat{V_c(s)}}{\hat{V_{dc}(s)}}$ at the operating point R=30 Ohms and D=0.1	60
Fig 3.28	Bode plot for the transfer function $\frac{\hat{V_c(s)}}{\hat{V_{dc}(s)}}$ at the operating point R=30 Ohms and D=0.5	60
Fig 3.29	Verification of Bode plot for the transfer function $\frac{\hat{V_c(s)}}{\hat{V_{dc}(s)}}$	61

Fig 4.1	Relationship between $S_1, S_2, \omega_n, \omega_d, Z, \sigma$	64
Fig 4.2	Classification of the system dynamics w.r.t Z	64
Fig 4.3(a)	State Space representation of open loop system	67
Fig 4.3(b)	State Space representation of close loop regulator	67
Fig 4.4	State Space representation of Type1 servo system for Type0 plant	67
Fig 4.5 (a, b c,d,e)	Variation of (a) Z (b) ω_n w.r.t D . (c) K_1 (d) K_I (e) K_2 w.r.t D for $Z'=0.65$	73
Fig 4.6	Structure of Servo Controller using Pole Placement for the Converter	75
Fig 4.7	Algorithm to Calculate the feedback matrix K_{FB} & K_I for the servo controller using pole placement for the controller	75
Fig 4.8	System Response for change in load resistance R from 30 to 50 Ohms for $V_{ref}=5$ volts	81
Fig 4.9	System Response for change in load resistance R from 10 to 40 Ohms for $V_{ref}=3$ volts	81
Fig 4.10	System Response for change in V_{ref} = from 5 to 10 volts for $R=50$ Ohms	82
Fig 4.11	System Response for change in V_{ref} = from 15 to 10 volts for $R=5$ Ohms	82
Fig 4.12(a) & (b)	System Response for change in V_{ref} = from 7.5 to 5 volts for $R=50$ Ohms, using K_{FB} & K_I as calculated for final operating point	83
Fig 4.12(c) & (d)	System Response for change in V_{ref} = from 7.5 to 5 volts for $R=50$ Ohms, using cycle by cycle control	83
Fig 4.12(e) & (f)	System Response for change in V_{ref} = from 7.5 to 5 volts for $R=50$ Ohms, using average values of K_{FB} & K_I	84
Fig 4.12(g) & (h)	System Response for change in V_{ref} = from 7.5 to 5 volts for $R=50$ Ohms, using $K_{FB}=[1 \ 1]$ & $K_I = 1$	84

Fig 4.13(a) &(b)	Regulator Response for -2,5 v perturbation in the capacitor voltage at the operating point defined by $V_{ref}=5$ v & $R=50$ Ohms using KFB & K_I as calculated for the operating point	85
Fig 4.13(c) &(d)	Regulator Response for -2,5 v perturbation in the capacitor voltage at the operating point defined by $V_{ref}=5$ v & $R=50$ Ohms cycle by cycle control	85
Fig 4.13(e) &(f)	Regulator Response for -2,5 v perturbation in the capacitor voltage at the operating point defined by $V_{ref}=5$ v & $R=50$ Ohms using average KFB & K_I for the	86
Fig 4.13(g) &(h)	Regulator Response for -2,5 v perturbation in the capacitor voltage at the operating point defined by $V_{ref}=5$ v & $R=50$ Ohms using KFB $=[1 \ 1]$ & $K_I = 1$	86
Fig 4.14(a) & (b)	System Response to the sinusoidal variation in V_{ref} at 500 Hz of magnitude 2.5 v at the operating point $R=30$ Ohms and $V_{ref} = 5$ v	87
Fig 4.14 (c) & (d)	System Response to the sinusoidal variation in V_{ref} at 500 Hz of magnitude 2.5 v at the operating point $R=30$ Ohms and $V_{ref} = 20$ v	87
Fig 4.14 (e) &(f)	System Response to the sinusoidal variation in V_{ref} at 5000Hz of magnitude 2.5 v at the operating point $R=30$ Ohms and $V_{ref} = 5$ v	88
Fig 4.14 (g) &(h)	System Response to the sinusoidal variation in V_{ref} at 500 Hz of magnitude 2.5 v at the operating point $R=30$ Ohms and $V_{ref} = 5$ v using KFB $=[1 \ 1]$ & $K_I = 1$	88
Fig 4.15 (a) & (b)	System Response to the sinusoidal variation in V_{dc} at 50 Hz of magnitude 10 v at the operating point $R=30$ Ohms and $V_{ref} = 5$ v	89
Fig 4.15 (c) & (d)	System Response to the sinusoidal variation in V_{dc} at 5000 Hz of magnitude 1 v at the operating point $R=30$ Ohms and $V_{ref} = 5$ v	89
Fig 4.15 (e) & (f)	System Response to the sinusoidal variation in V_{dc} at 50 Hz of magnitude 10 v at the operating point $R=30$ Ohms and $V_{ref}=5$ v using KFB $=[1 \ 1]$ & $K_I = 1$	90
Fig 4.16 (a) & (b)	System Response to the sinusoidal variation in R at 50 Hz of magnitude 10 Ohms at the operating point $R=30$ Ohms and $V_{ref} = 5$ v	90

Fig 4.16 (c) &(d)	System Response to the sinusoidal variation in R at 5000 Hz of magnitude 1 Ohms at the operating point $R=30$ Ohms and $V_{ref} = 5$ v	91
Fig 4.16 (e) & (f)	System Response to the sinusoidal variation in R at 50 Hz of magnitude 10 Ohms at the operating point $R=30$ Ohms and $V_{ref} = 5$ v using $K_{FB} = [1 \ 1]$ & $K_I = 1$	91
Fig A-1	State Space representation of a system defined by Non-Linear Differential Equation	98
Fig B-1 & B-2	Graphical representation of the PWM operation	105

List of Tables

Table-1	Cases considered for openloop time domain simulation of the converter	15
Table-2	Operating points considered for Bode Plots	54
Table-3	Results of verification of small signal model defined by equation (3.17)	62
Table-4	Results of verification of small signal model defined by equation (3.19)	62
Table-5	Classification of system dynamics w.r.t Z	65
Table-6	Cases for the study of the close loop step response	78

CHAPTER I

INTRODUCTION :

In the field of industrial applications DC to DC converters play a vital role. There are many processes where direct human intervention is not possible or is not sufficient to meet the response time specifications that the plant under consideration demands. To implement a stable control loop for a system, it is required that system characteristics be known for both steady-state and transient. Therefore, detailed mathematical modelling of the system needs to be done using differential equations.

The choice of the feedback variable to a great extent decides the close-loop response. However there is a method by which all the system variables that decide its state at any given time can be used to construct a control signal which constrains the system response to specifications, however the system must qualify necessary and sufficient conditions. The system under consideration may require more than one set of differential equations to model it completely, such that each set defines it during specific intervals of time. A continuous linear model for such a system has to be formed, so that either conventional or modern control techniques can then be applied to determine the close loop system parameters..

ORGANIZATION OF THE THESIS :

The objective of the thesis was to model and study the characteristic of a Buck-boost DC to DC voltage converter and to implement a close-loop voltage control. Chapter 2 presents the study of buck-boost circuit, its operation under different modes of conduction and its mathematical model, both in differential equation and state space form. The state space model is then used to simulate open loop system responses for perturbation in duty ratio D and load resistance R . Chapter 3 explains the concepts and requirement of state-space averaging and how it is applied to the discrete differential equation models formulated in Chapter II, that define the converter in various modes of conduction to achieve continuous time representation of the converter. It is examined under what conditions do these models represent the actual converter or fail to do so. Also the linearization of continuous averaged models which are non-linear around the operating points so that design methods like Bode plot, Nyquist criteria or pole placement can then be used to determine the close loop parameters. In Chapter-IV how the pole location of the system governs the system dynamics and what conditions must the system satisfy such that its poles can be located at the desired location to *modify* its dynamics, has been discussed.

CHAPTER II

BUCK BOOST CONVERTER

DC-DC voltage converters are used to obtain variable DC voltage from a fixed dc voltage source. In this chapter section 2.1 explains the buck-boost converter topology, circuit operation and how it can be represented by differential equations, Section 2.2 gives the state space representation of the converter in different modes of circuit operation and section 2.3 explains how the state space equations can be used to simulate converter operation in open loop.

2.1 CONVERTER TOPOLOGY :-

The work presented here is based on buck boost converter as shown in fig. 2.1. The switch S is turned on and off at frequency f_s . In the discussion that follows the circuit operation is explained, equivalent circuits are formulated and differential equation model of the converter for different modes of operation is defined.

MODE 1 : The switch S is on and the diode D_e is reversed biased . The inductor L stores energy from the supply voltage V_{dc} , the capacitor C discharges into load resistance R. The equivalent circuit is as shown in Fig. 2.2a.

MODE 2 : The switch S is off and diode D_e is forward biased. The equivalent circuit is as shown in Fig. 2.2b. The energy stored in inductor L in mode 1 is now transferred to capacitor C and load resistance R. In continuous mode of conduction, mode 1 of the next

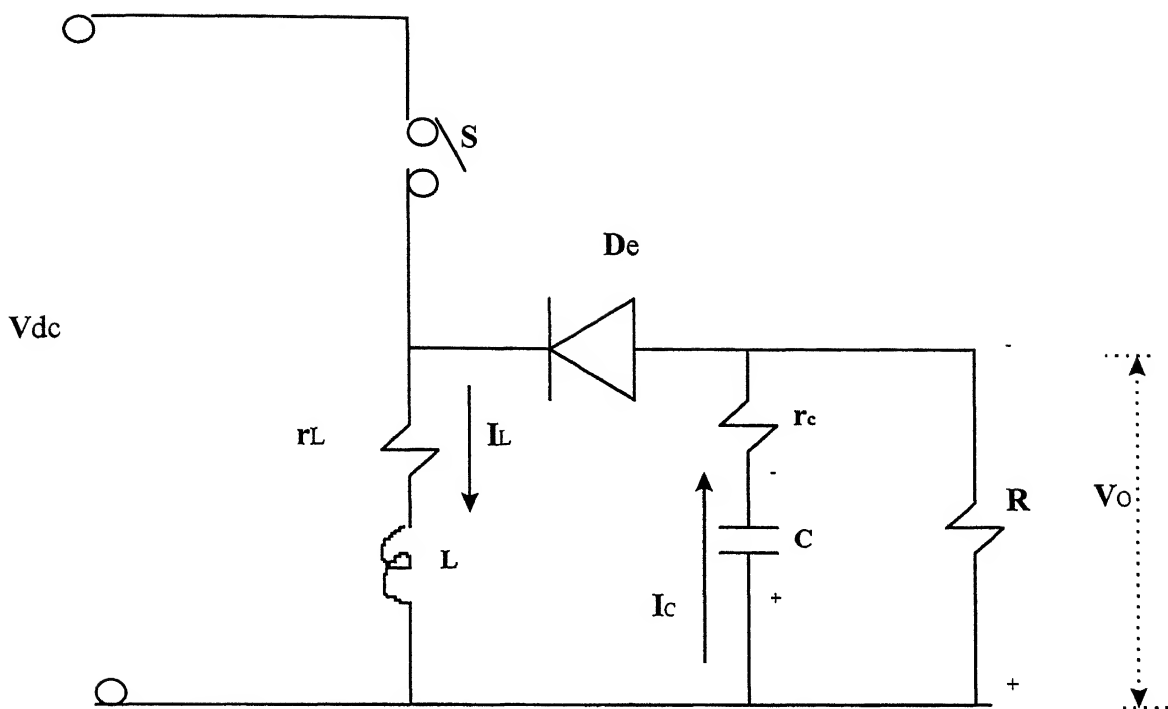


FIG 2.1:Circuit Topology of Buck - Boost Converter

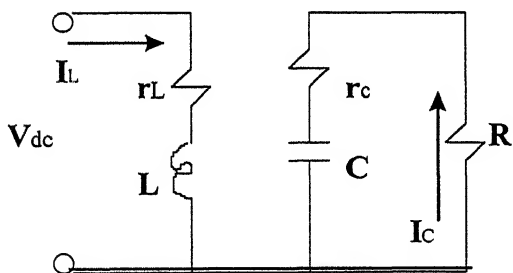


FIG 2.2(a) : Mode 1 Equivalent Circuit

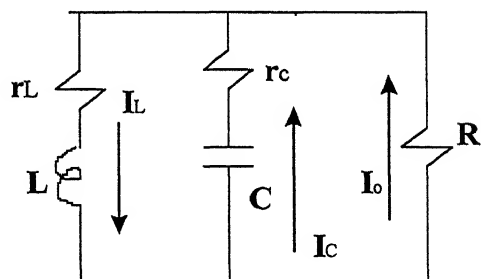


FIG 2.2(b) : Mode 2 Equivalent Circuit

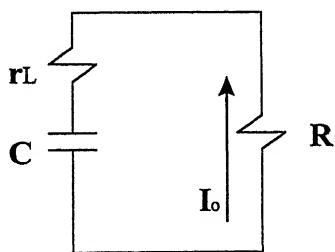


FIG 2.2(c) : Mode 3 Equivalent Circuit

MODE 2 : The switch S is off and diode D_e is forward biased. The equivalent circuit is as shown in Fig. 2.2b. The energy stored in inductor L in mode 1 is now transferred to capacitor C and load resistance R. In continuous mode of conduction, mode 1 of the next switching cycle starts before the inductor current in Mode 2 decays to zero. In discontinuous mode of conduction there is a third mode.

MODE 3 : In discontinuous mode of conduction the inductor current in mode 2 decays to zero before the next switching cycle starts. The inductor current tends to reverse but is blocked by diode D_e . The equivalent circuit is as shown in figure 2.2c. Now both switch S and diode D_e are off, inductor current remains zero till Mode 1 of next switching cycle starts and capacitor C continues to discharge in load resistance R.

A special case of 2-mode Conduction is when the converter operates in 2-mode, but at the end of mode 2 the inductor current just becomes zero. This is called Boundary conduction.

Figures 2.3 a, b, and c show the approximate waveforms of inductor current I_L and capacitor voltage V_c during a switching cycle, along with initial and final values of I_L and V_c for every mode during continuous (2-mode), boundary and discontinuous (3-mode) operation of the converter respectively.

As approximate nature of inductor current and capacitor voltage is known along with the equivalent circuits, converter operation can be represented by differential equations as follows :

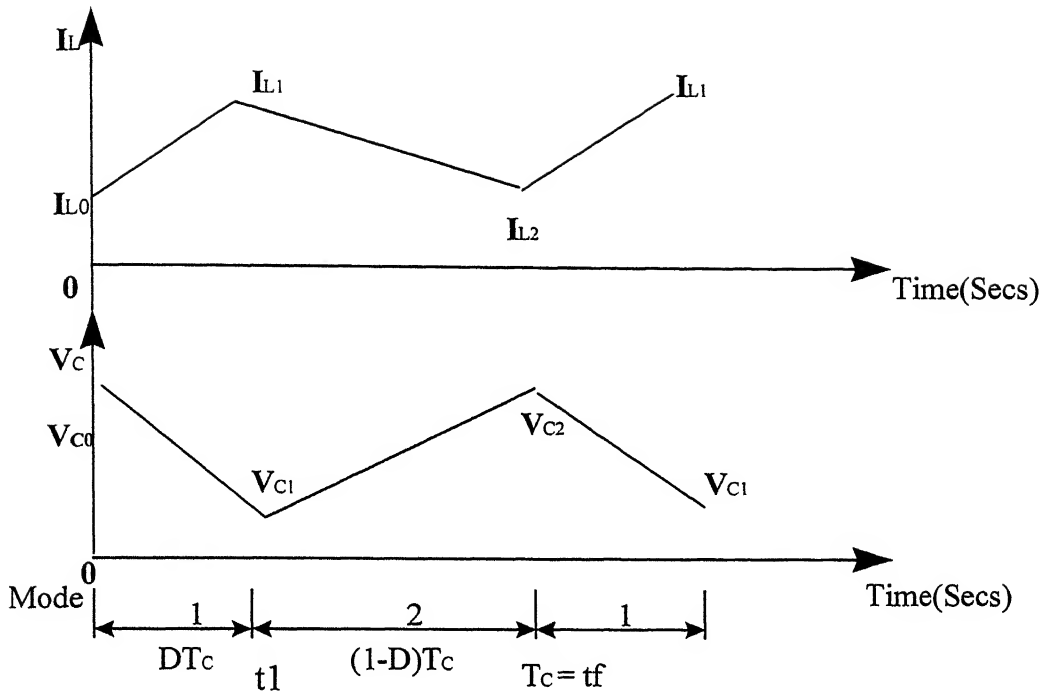


FIG 2.3(a): Approximate I_L & V_C Waveforms in Continuous Conduction Mode

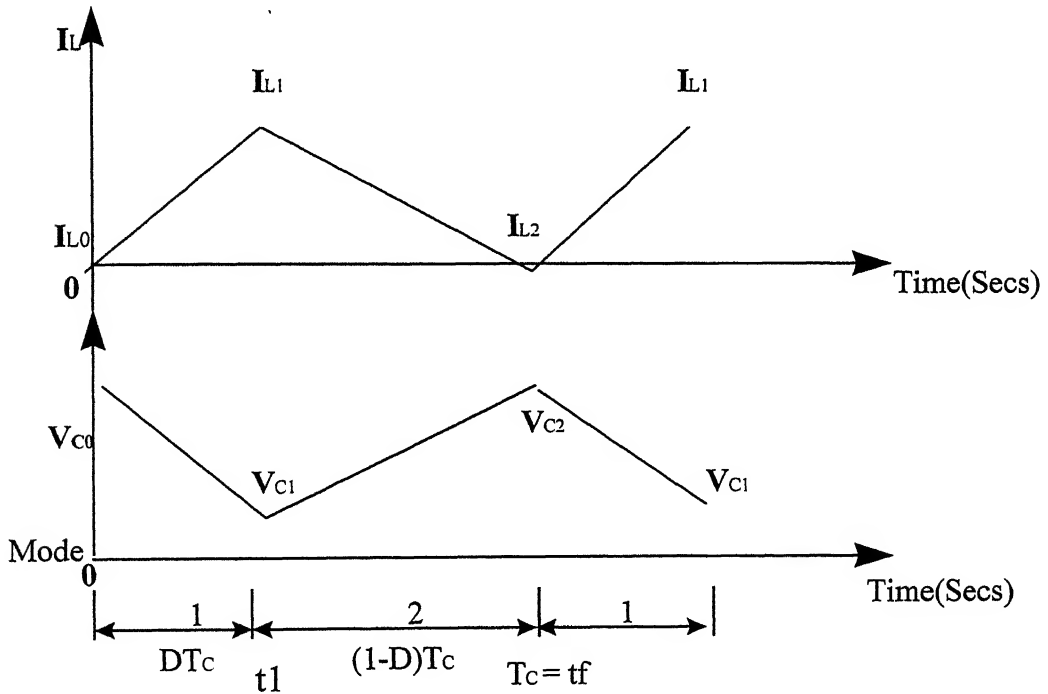


FIG 2.3(b): Approximate I_L & V_C Waveforms in Boundary Conduction Mode

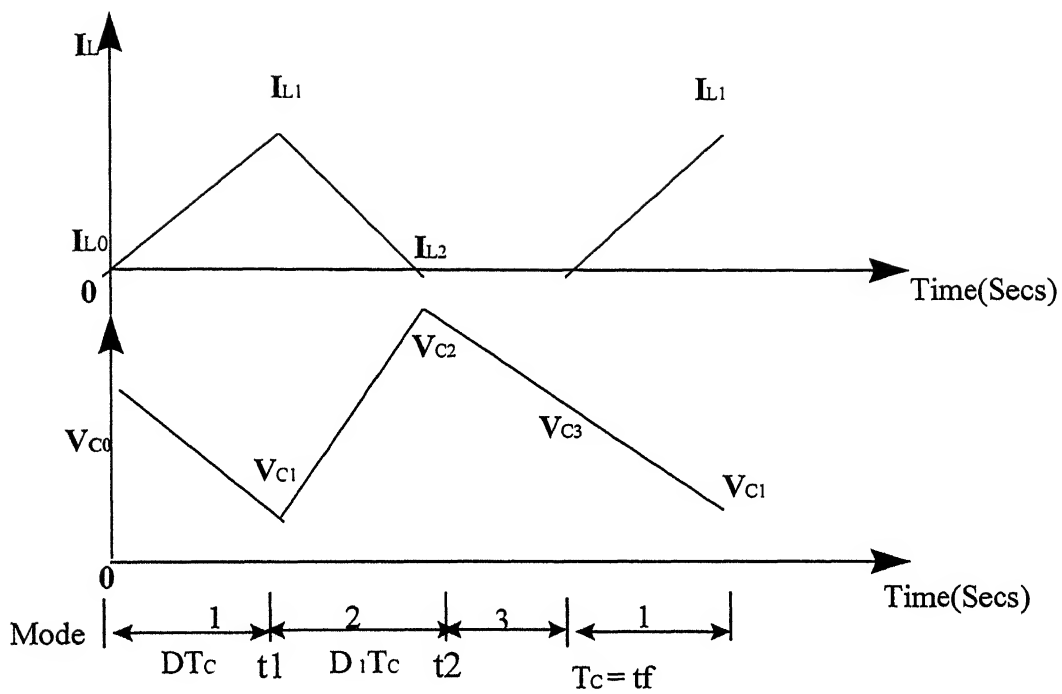


FIG 2.3(c): Approximate I_L & V_C Waveforms in Discontinuous Conduction Mode

MODE 1 : Duration of this mode is t_0 to t_1 or (DT_c)

$$\dot{V}_c = \frac{-V_c}{R_1 C} \quad (2.1)$$

Where $R_1 = R + r_c$

$$\dot{I} = \frac{V_{dc}}{L} - \frac{I_L r_L}{L} \quad (2.2)$$

Solution to above equations are

$$V_c = V_{co} e^{-t'/R_1 C} \quad (2.3)$$

$$I_L = \frac{V_{dc}}{V_L} + (I_{Lo} - \frac{V_{dc}}{r_L}) e^{-r_L t'/L} \quad (2.4)$$

Where $0 < t' \leq DT_c$.

MODE 2: Duration of this mode is t_1 to t_2 or t_f . Depending upon whether the cycle is continous/discontinuous It is assumed that load resistance is such that L-C circuit is underdamped.

$$\dot{V}_c = \frac{-V_c}{R_1 C} + \frac{R I_L}{R_1 C} \quad (2.5)$$

$$I_L = \frac{-V_c r_c / R_1}{L} - \frac{r_L I_L}{L} - \frac{R r_c I_L}{R_1} \quad (2.6)$$

Solution to above equations is

$$V_c = e^{\sigma t''} (C_1 \cos \omega t'' + C_2 \sin \omega t'') \quad (2.7)$$

$$I_L = e^{\sigma t''} (C_3 \cos \omega t'' + C_4 \sin \omega t'') \quad (2.8)$$

Where $0 < t'' \leq (1-D)T_c$ or $D_1 T_c$

$$\text{Where } C_1 = V_{C1} \quad (2.9)$$

$$C_2 = \frac{1}{\omega} \left[\frac{R I_{L1}}{R_1 C} - V_{C1} \left(\sigma + \frac{1}{R_1 C} \right) \right] \quad (2.10)$$

$$C_3 = I_{L1} \quad (2.11)$$

$$C_4 = \frac{1}{\omega} \left[\frac{V_{C1}(1 - V_c / R_1)}{L} + I_{L1} \left(\sigma + \frac{r_L}{L} + \frac{Rr_c}{R_1 L} \right) \right] \quad (2.12)$$

$$\sigma = - \frac{\frac{1}{R_1 C} + \frac{r_L}{L} + \frac{Rr_c}{R_1 L}}{2} \quad (2.13)$$

$$\omega = \frac{\sqrt{\frac{4(R + r_L)}{R_1 LC} - \left(\frac{1}{R_1 C} + \frac{r_L}{L} + \frac{Rr_c}{R_1 L} \right)^2}}{2} \quad (2.14)$$

MODE 3 : Duration of this mode is from t_2 to t_f

$$\dot{V}_c = \frac{-V_c}{R_1 C} \quad (2.15)$$

$$\dot{I}_L = 0 \quad (2.16)$$

Solution to these equations is

$$V_c = V_{c2} e^{-t'''/R_1 C} \quad (2.17)$$

$$I_L = 0 \quad (2.18)$$

$$0 < t''' \leq (1-D-D_1)T_c$$

Given the values of V_{co} and I_{lo} at beginning of the switching cycle it can be determined whether present switching cycle for given duty ratio D will be continuous / discontinuous. (refer Appendix A-1 for converter Parameters). If t_2 is the time taken by inductor current to decay to zero in mode 2 then depending upon its value the present switching cycle can be classified as a case of continuous / discontinuous/boundary conduction.

Substituting $I_{L2} = 0$ in equation 2.8 (i.e. now value of $t'' = t_2$). Results in

$$e^{\sigma t_2} [C_3 \cos \omega t_2 + C_4 \sin \omega t_2] = 0$$

since $e^{\sigma t_2}$ cannot be zero

$$[C_3 \cos \omega t_2 + C_4 \sin \omega t_2] = 0$$

Therefore $\frac{\sin \omega t_2}{\cos \omega t_2} = \frac{C_3}{-C_4}$

$$\tan \omega t_2 = \frac{C_3}{-C_4}$$

Therefore
$$t_2 = \frac{\tan^{-1}[C_3 / -C_4]}{\omega}$$

C_4 could be positive or negative, to ensure that sign of C_4 does not effect the value of t_2

$$t_2 = \frac{\Pi + \tan^{-1}\left[\frac{C_3}{-C_4}\right]}{\omega} \quad (2.19)$$

If $t_2 > (1-D)T_c$ then the present switching cycle is continous.

If $t_2 = (1-D)T_c$ then the present switching cycle is a case of Boundary conduction.

If $t_2 < (1-D)T_c$ then the switching cycle is discontinous.

2.2 STATE SPACE REPRESENTATION: *why is it required?*

A scalar differential equation can be transformed into state equations of the form

$\dot{X} = Ax + Bu$ (refer Appendix A-2). Therefore equations 2.1, 2.2, 2.5, 2.6 and 2.15 and 2.16 can be represented in the form

$$\dot{X} = A_1X + B_1u \quad (2.20)$$

$$\dot{X} = A_2X + B_2u \quad (2.21)$$

$$\dot{X} = A_3 X + B_3 u \quad (2.22)$$

$$\text{Where } \dot{X} = \begin{bmatrix} \dot{V}_c \\ \dot{I}_L \end{bmatrix} ; X = \begin{bmatrix} V_c \\ I_L \end{bmatrix} ; u = V_{dc}$$

$$A_1 = \begin{bmatrix} \frac{-1}{R_1 C} & 0 \\ 0 & \frac{-r_L}{L} \end{bmatrix} ; A_2 = \begin{bmatrix} \frac{-1}{R_1 C} & \frac{R}{R_1 C} \\ \frac{-R}{R_1 C} & \frac{-1}{L} \left[r_L + \frac{r_c R}{R_1} \right] \end{bmatrix} ; A_3 = \begin{bmatrix} \frac{-1}{R_1 C} & 0 \\ 0 & 0 \end{bmatrix}$$

$$B_1 = \begin{bmatrix} 0 \\ \frac{1}{L} \end{bmatrix} ; B_2 = \begin{bmatrix} 0 \\ 0 \end{bmatrix} ; B_3 = \begin{bmatrix} 0 \\ 0 \end{bmatrix} ;$$

Matrices A_1 , A_2 , A_3 , B_1 , B_2 , B_3 are called systems matrices.

2.3 OPEN LOOP TIME DOMAIN SIMULATION OF THE CONVERTER :

Using the equations 2.20 to 2.22 converter operation in continuous or discontinuous mode can be simulated. As seen the value of t_2 decides whether present switching cycle is continuous/discontinuous. Algorithm used for simulation is shown in figure 2.4. In open-loop converter operating point is defined by Duty Ratio D , input voltage V_{dc} and load resistance R .

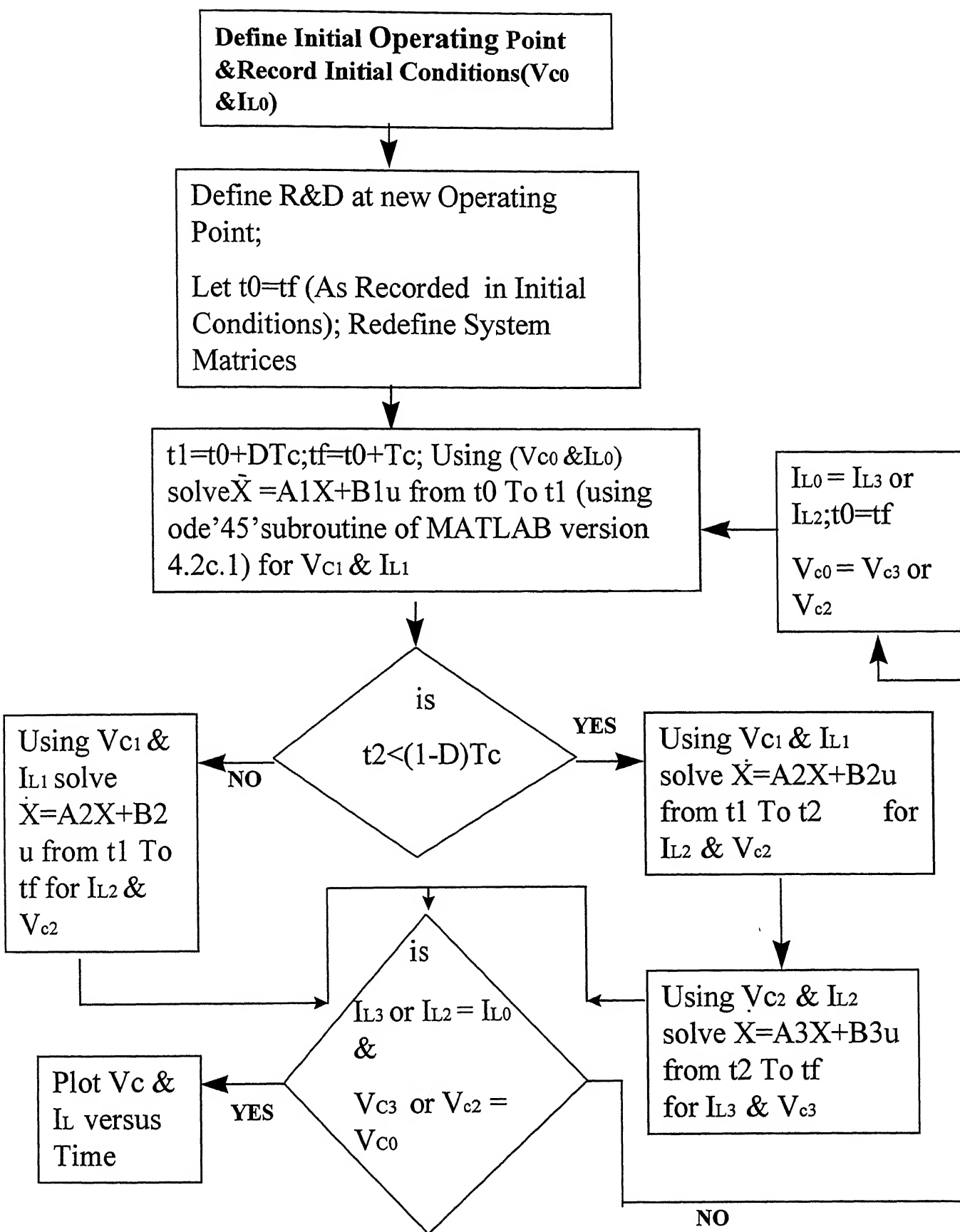


FIG 2.4 : Open - loop Time Domain Simulation Using State - Space Differential Eqn Model

Cases given in Table 1 have been considered for converter simulation in open loop.

S.No.	Initial Condition		Final condition	
	Duty Ratio	Load Resistance	Duty Ratio	Load Resistance
1	0.1	10Ω	0.1	5Ω
2	0.1	10Ω	0.1	20Ω
3	0.5	10Ω	0.5	30Ω
4	0.1	30Ω	0.3	30Ω
5	0.1	5Ω	0.01	5Ω
6	0.1	10Ω	0.1	30Ω
7	0.1	30Ω	0.1	50Ω
8	0.1	30Ω	0.15	30Ω

Table 1

Results of simulation are shown in Fig. 2.5 to Fig. 2.12. Every operating point defined by D , V_{dc} and R has a unique value of capacitor voltage and inductor current in steady state. If the ripple is neglected the average capacitor /output voltage and inductor current can determined without solving the differential equation (discussed in chapter 3). From the time domain simulation of the converter in open-loop maximum overshoot , delay time, rise time and settling time for perturbation in D and R can be observed. Also the ripple in inductor current and output voltage can be observed during transient and steady state. Result show that as the load resistance is increased the converter tends to discontinuous operation during transient and steady state, and depending upon its value as the value of duty ratio D is decreased the converter either goes into discontinuous operation or remains in continous operation, and as

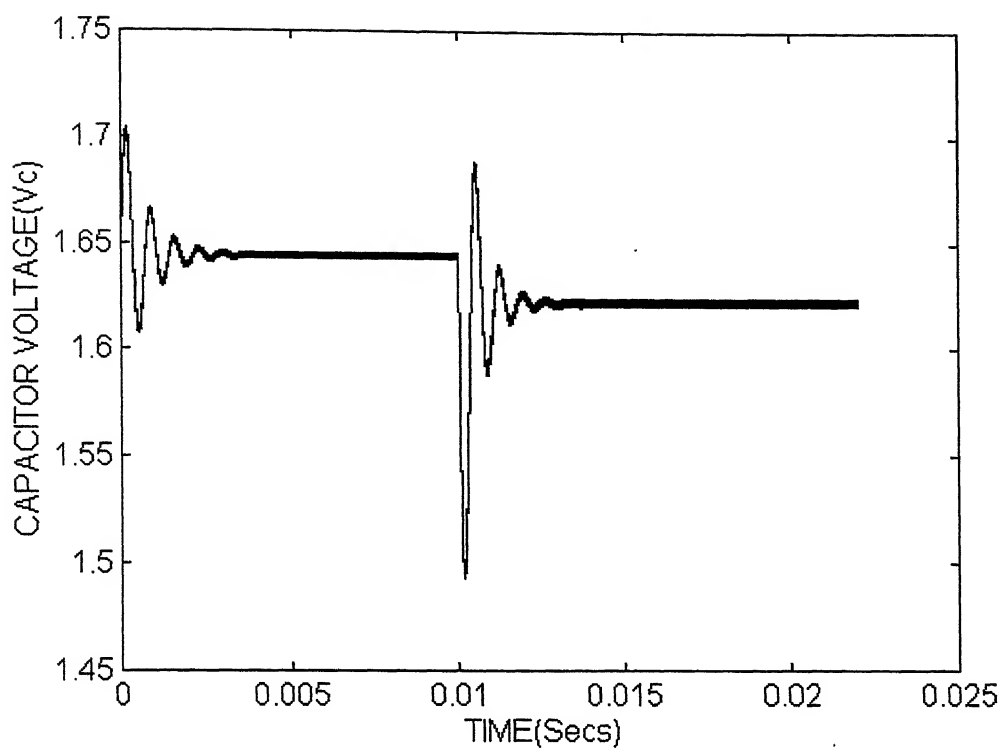


FIG 2.5(a)

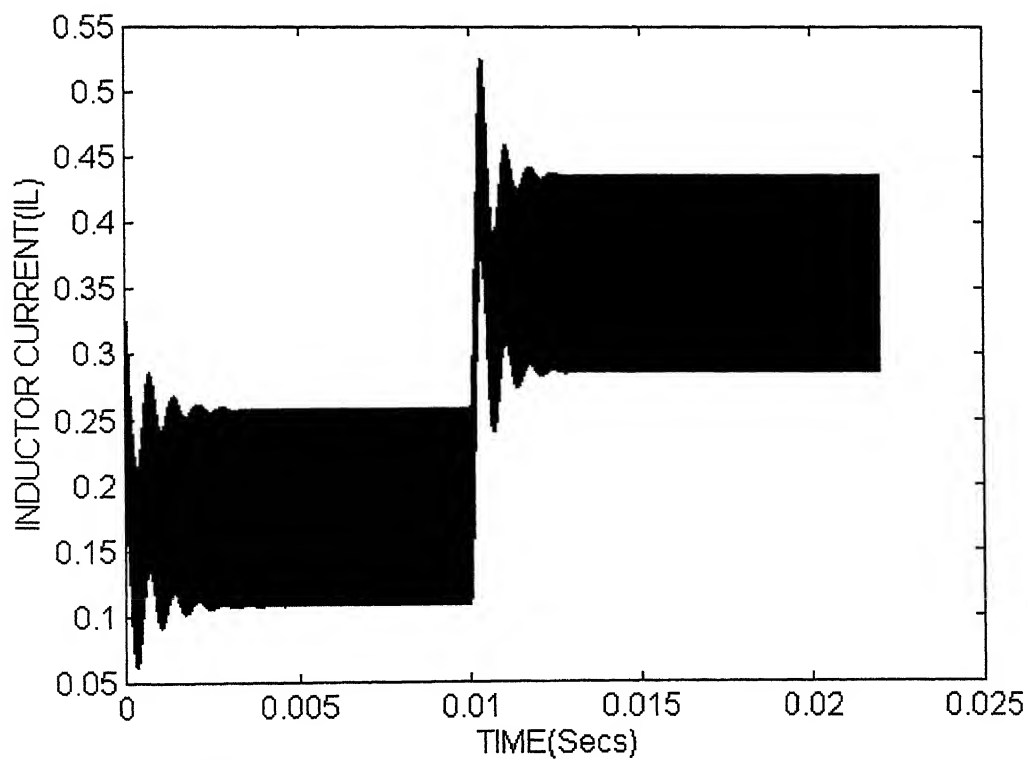


FIG 2.5(b)

FIG 2.5: System Response for Change in R from 10 to 5 Ohms for $D=0.1$

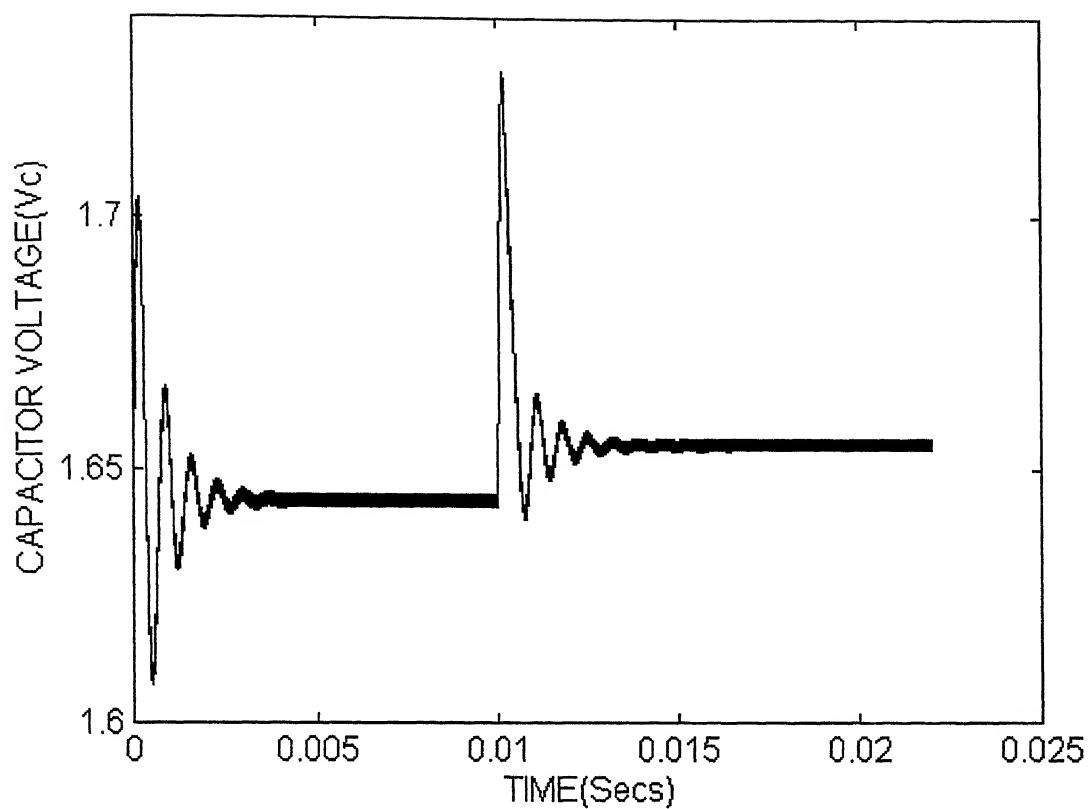


FIG 2.6(a)

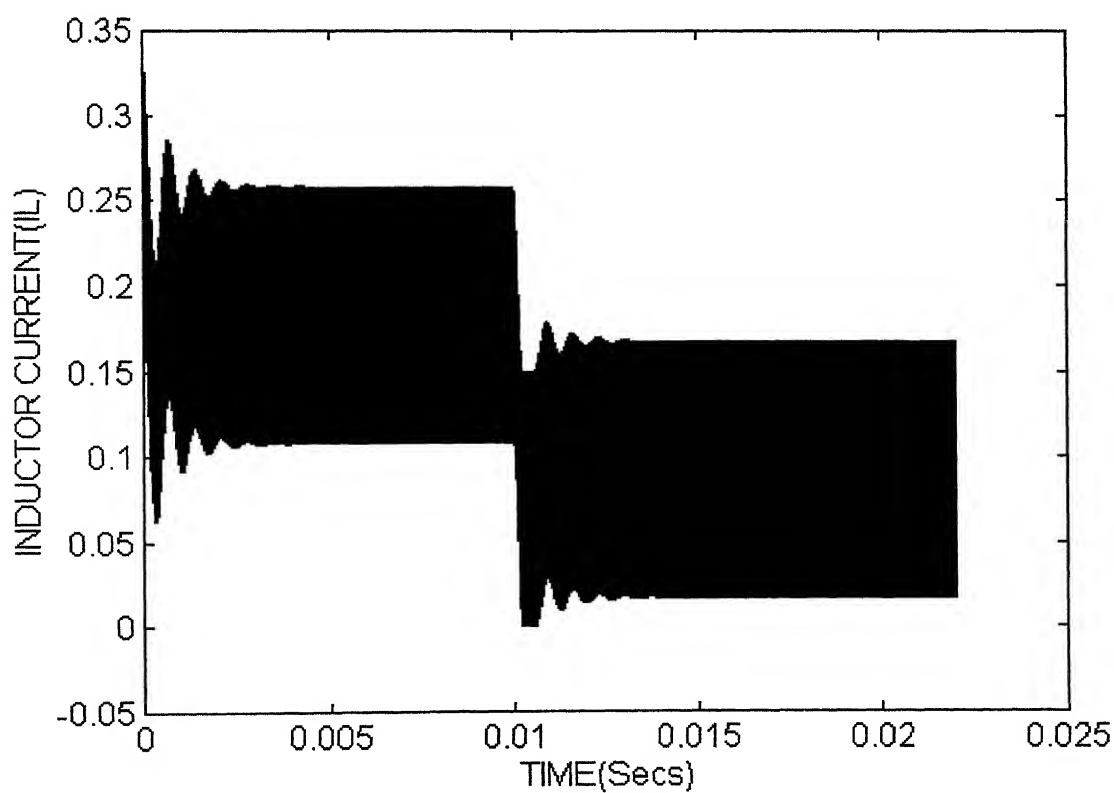


FIG 2.6(b)

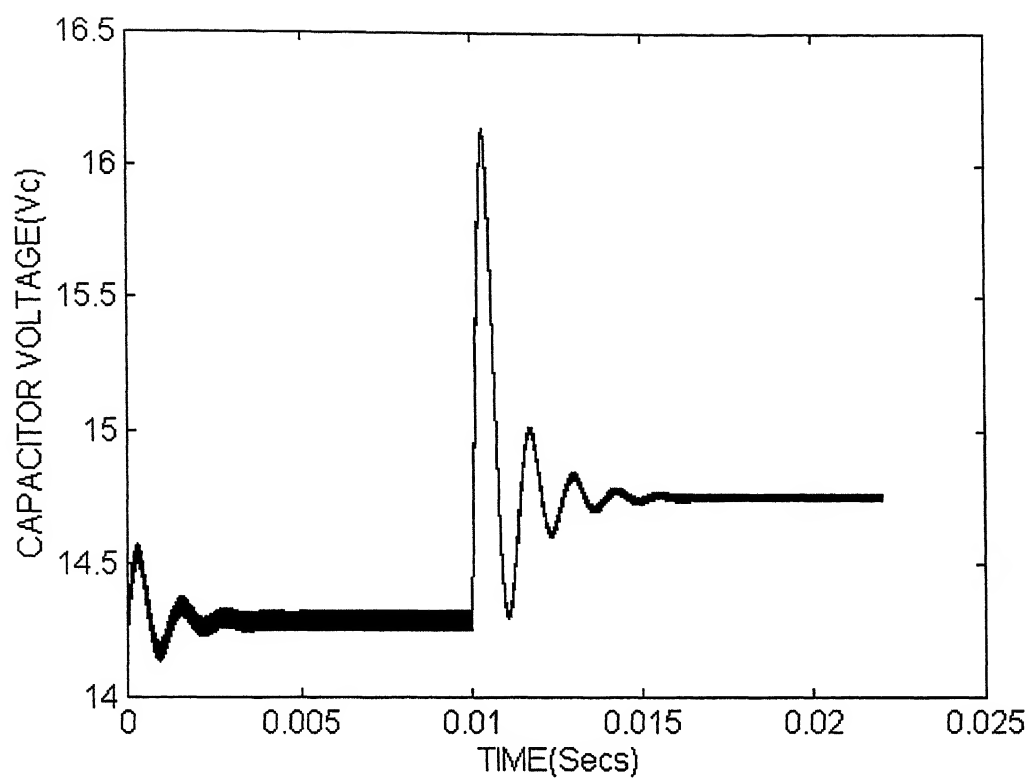


FIG 2.7(a)

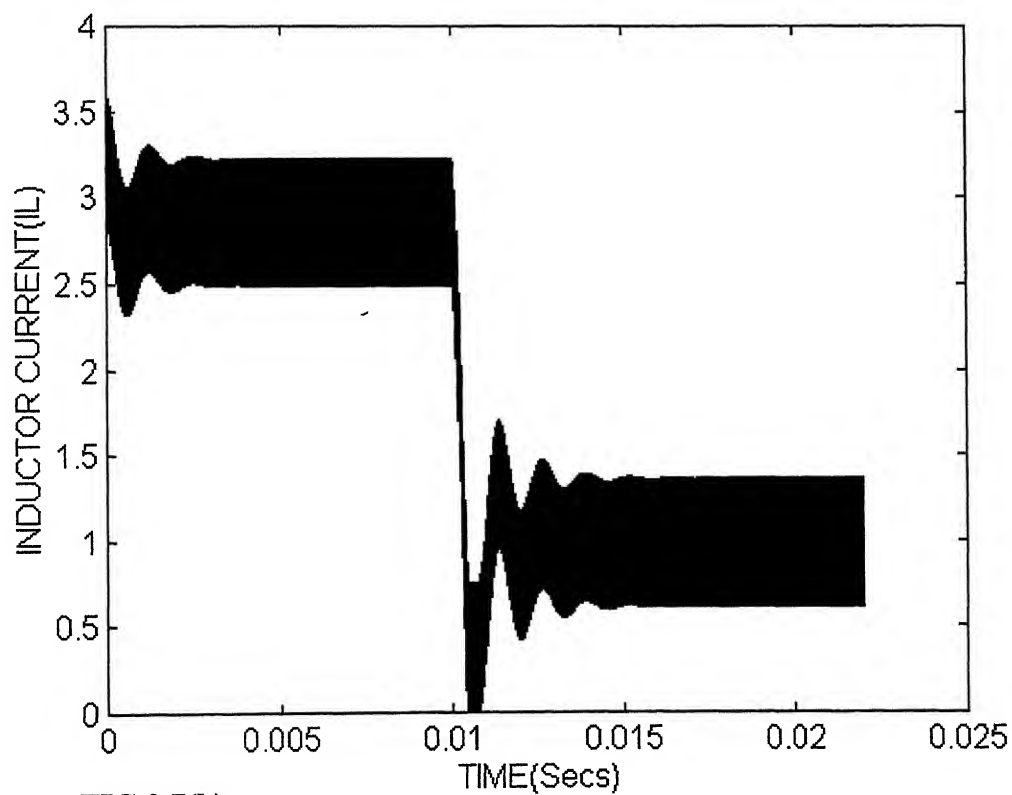
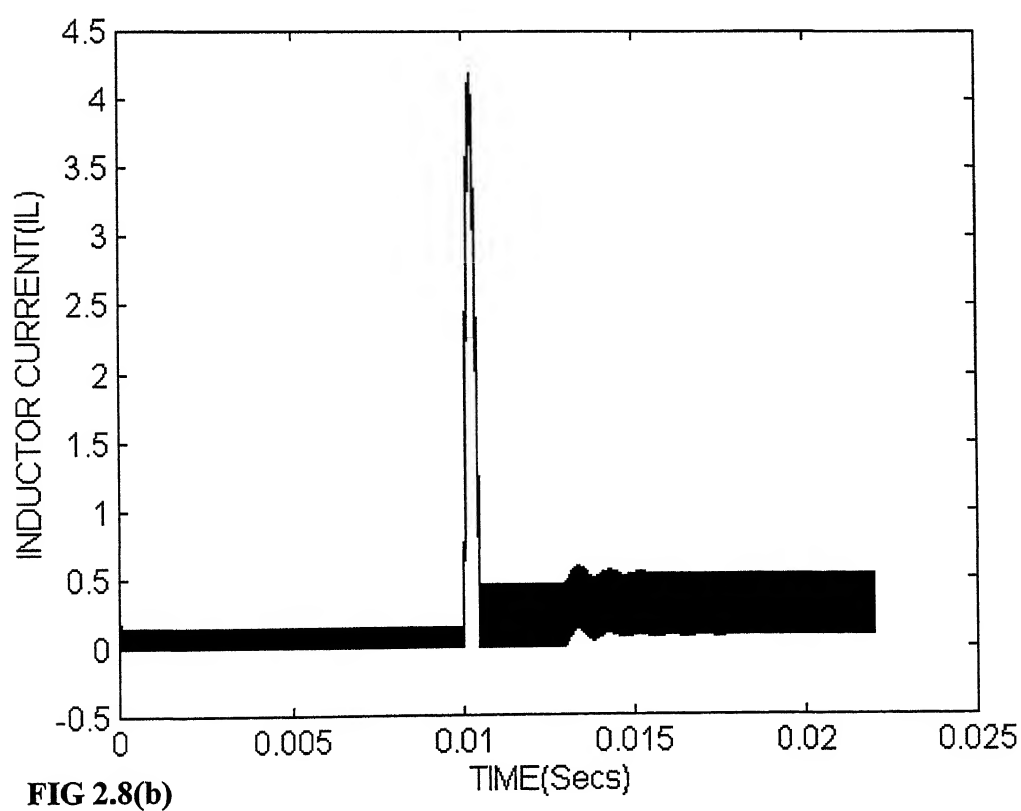
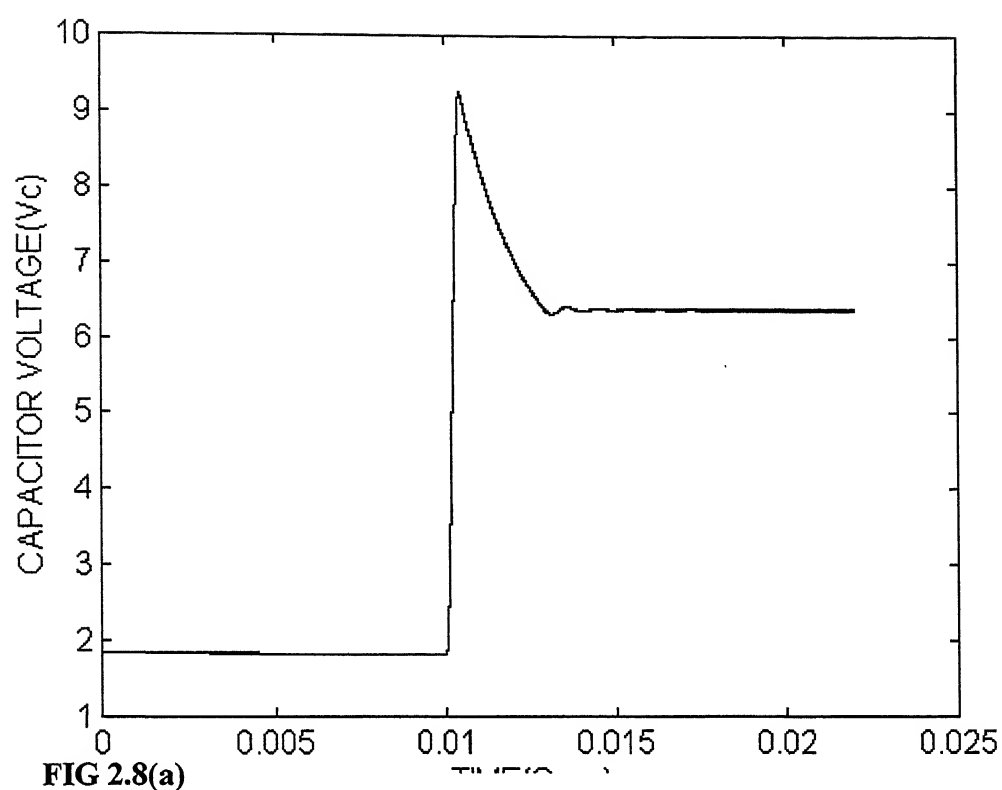


FIG 2.7(b)



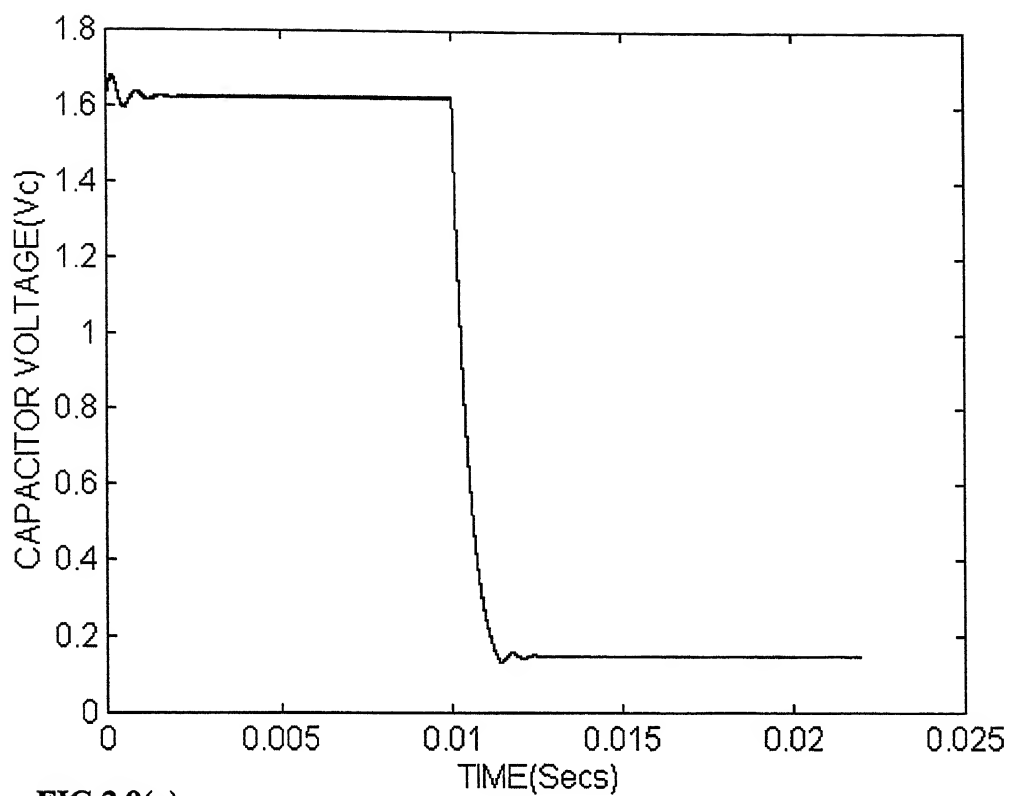


FIG 2.9(a)

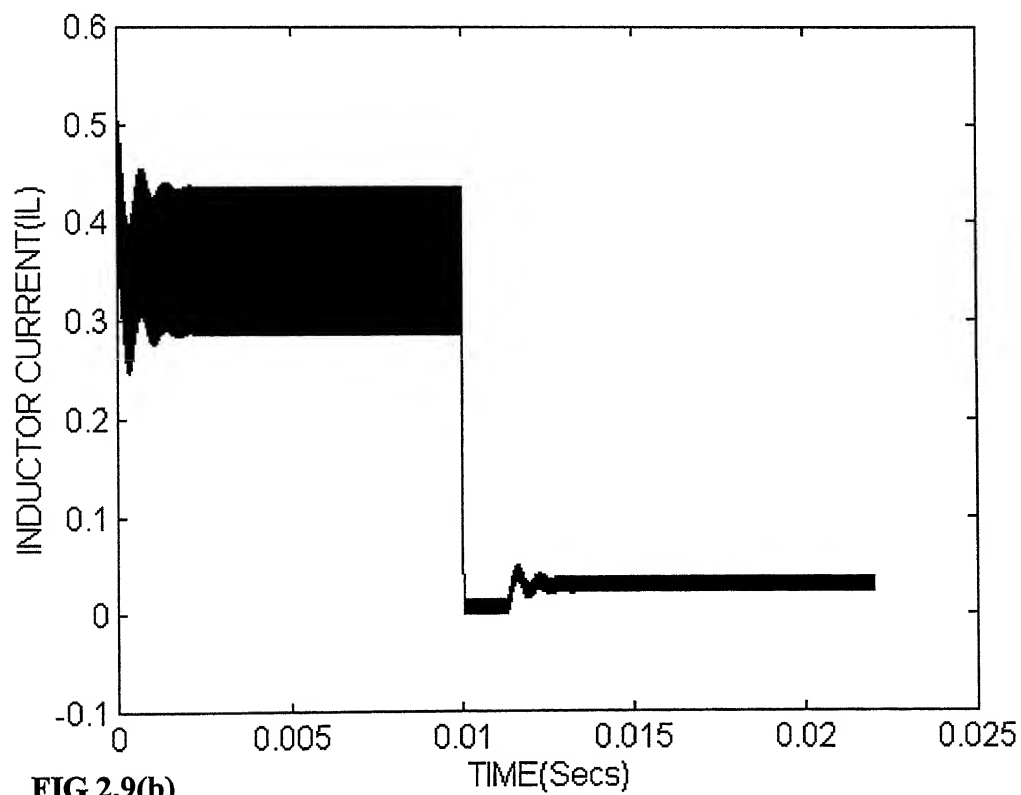


FIG 2.9(b)

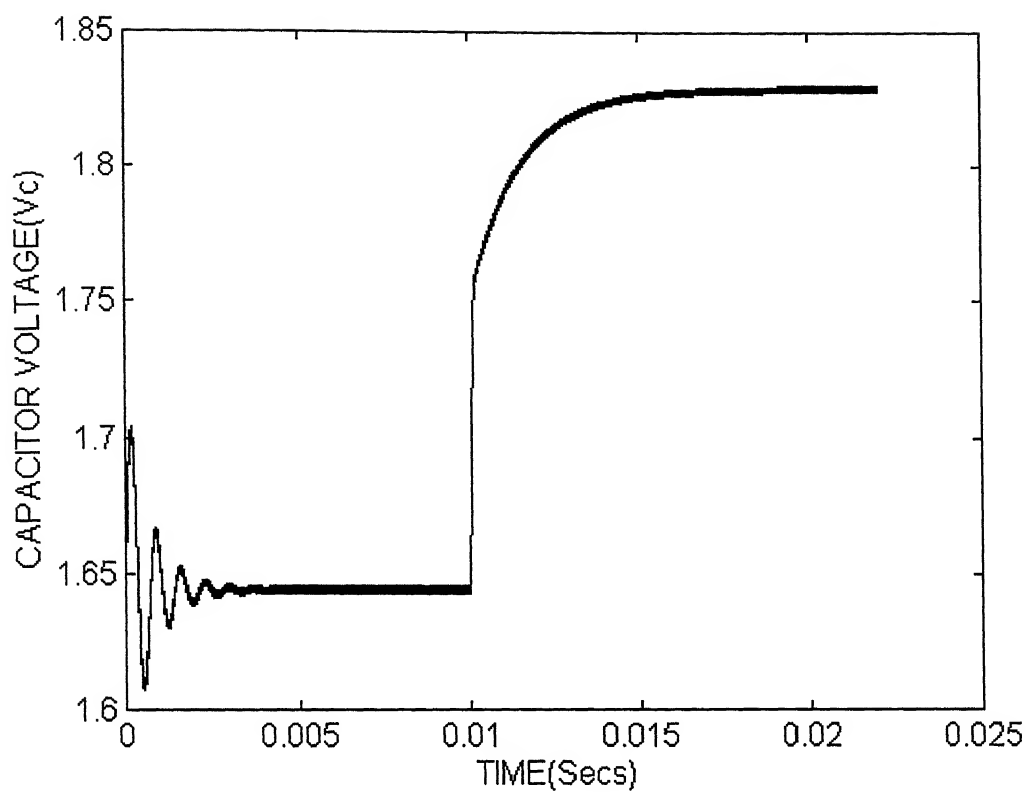


FIG 2.10(a)

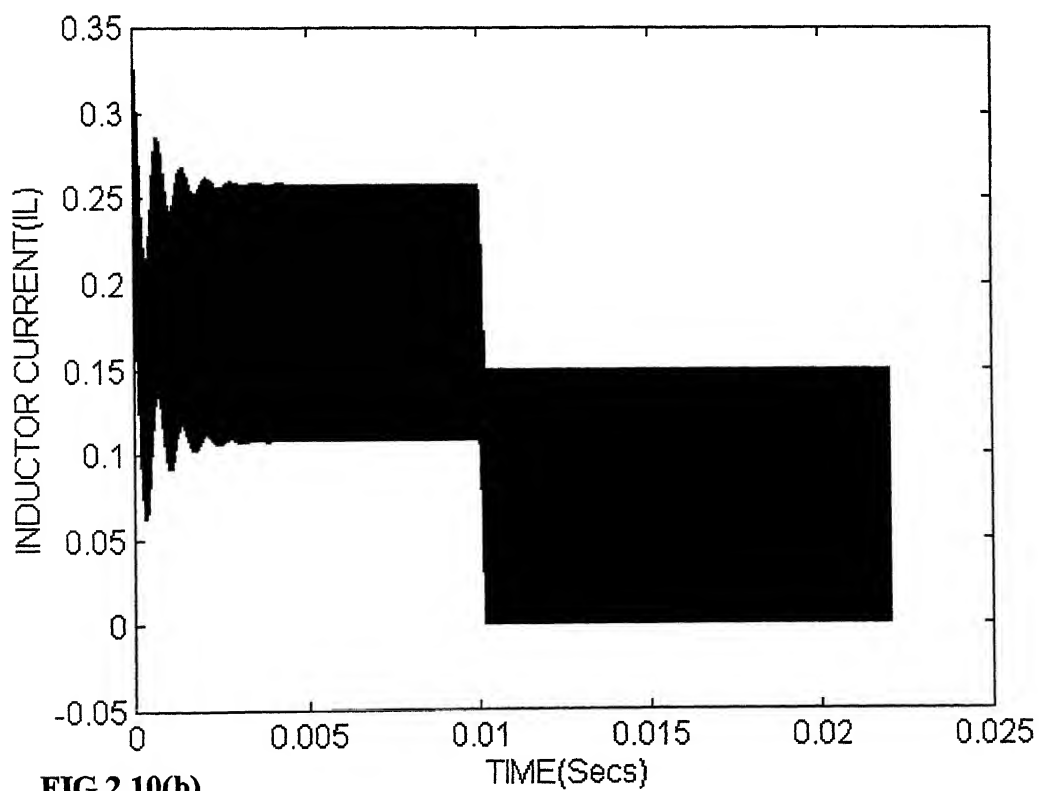


FIG 2.10(b)

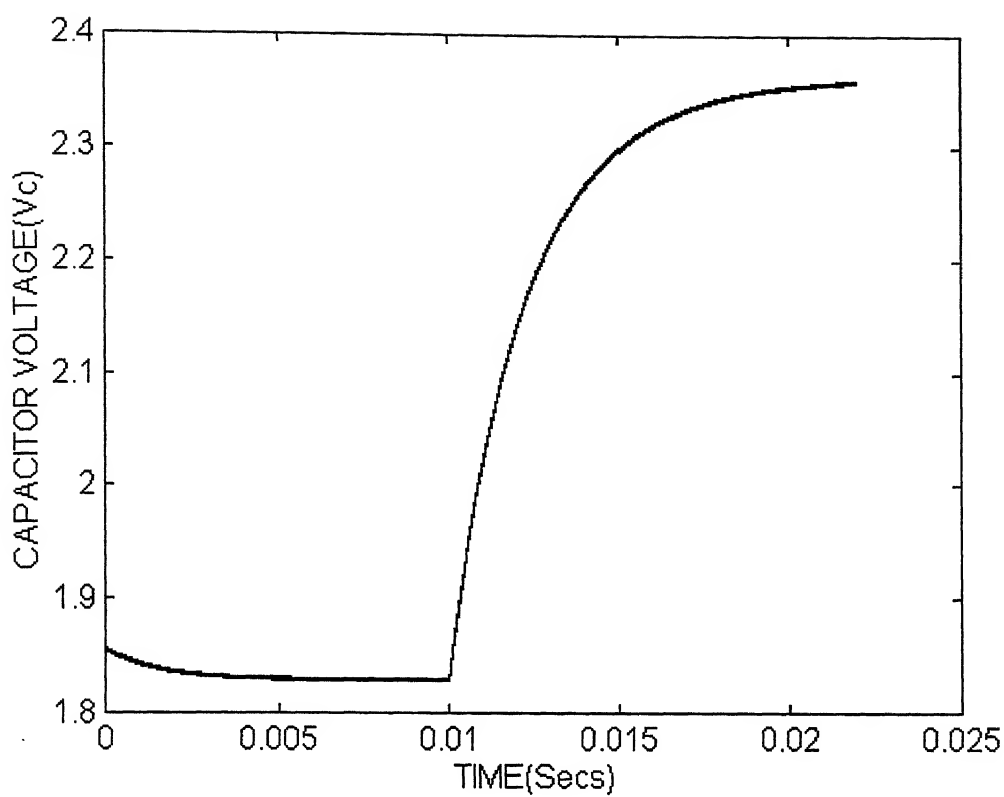


FIG 2.11(a)

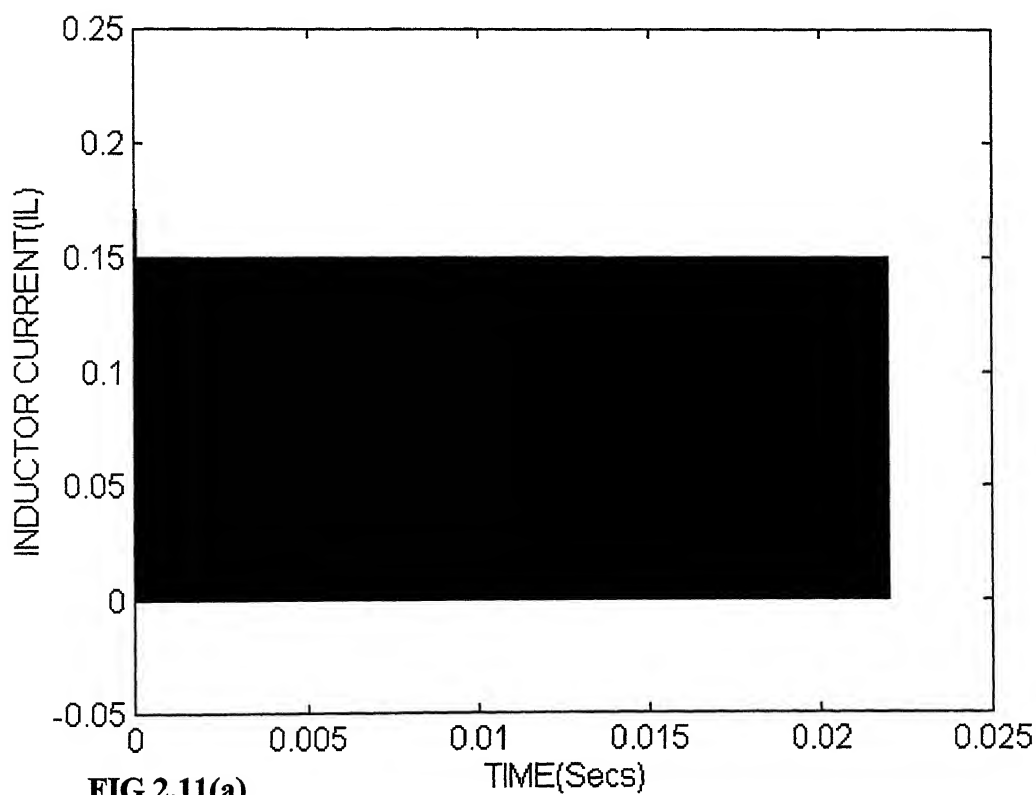


FIG 2.11(a)

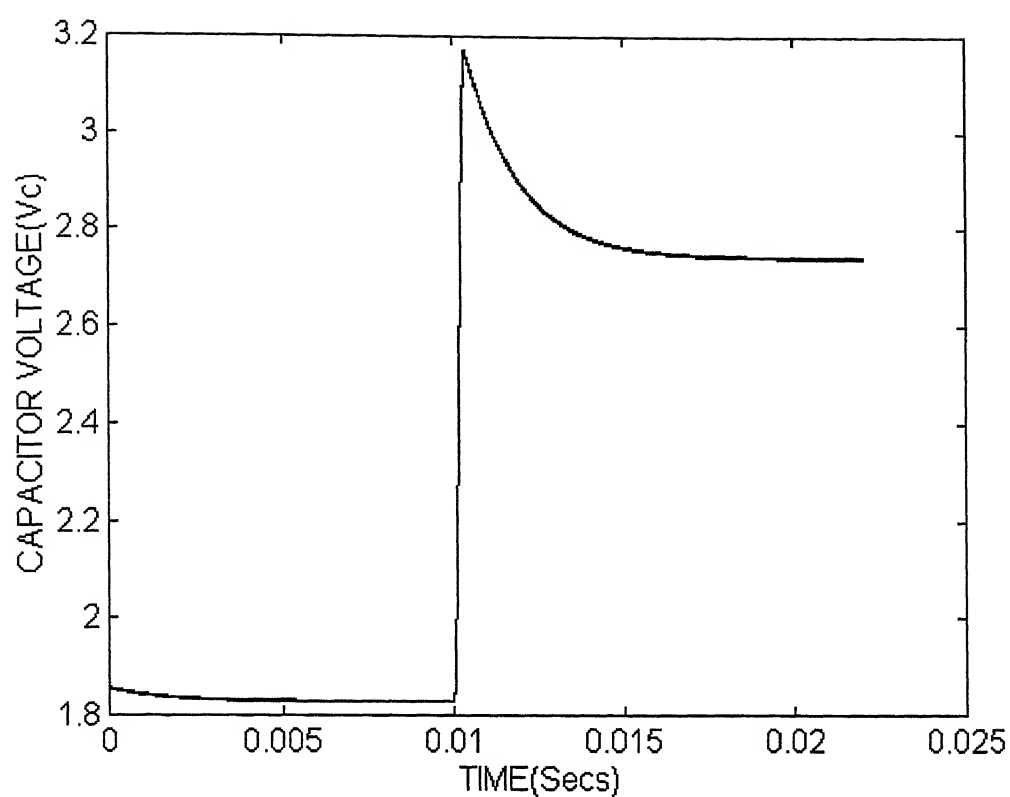


FIG 2.12(a)

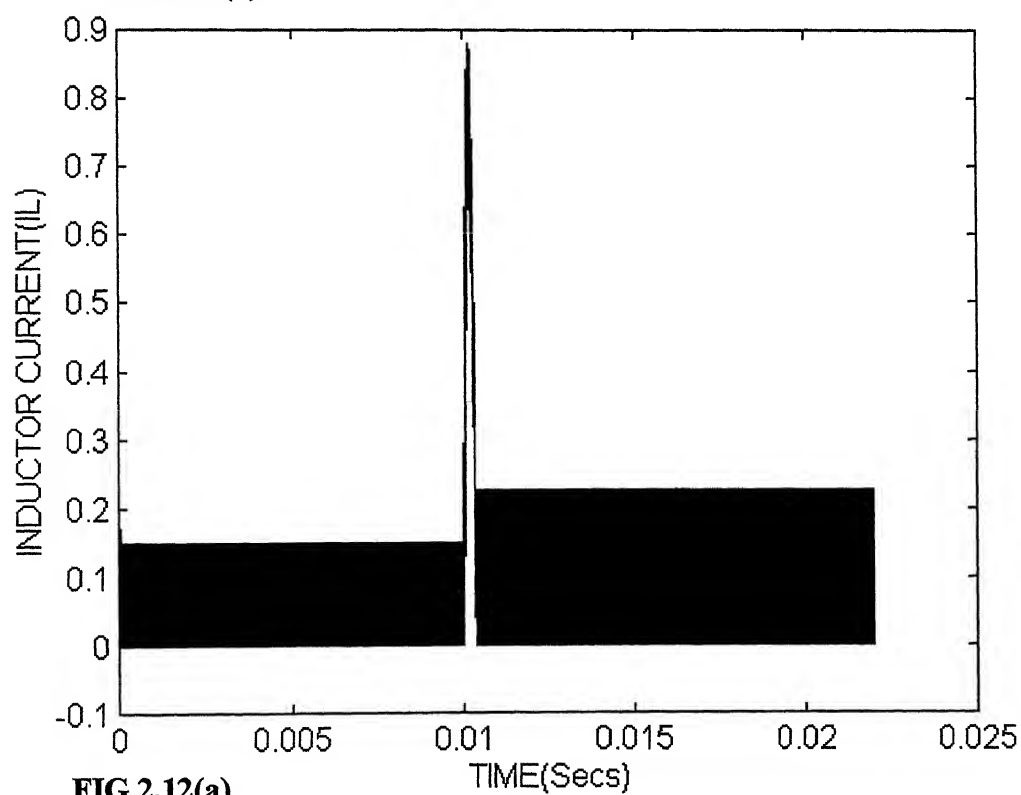


FIG 2.12(a)

the value of D is increased the converter either remains in discontinuous operation or tends to continuous operation. Hence it can be concluded that zones of continuous, discontinuous and Boundary operation can be defined, (discussed in chapter 3).

CHAPTER III

STATE SPACE AVERAGE MODEL

The characteristics of switched systems can be studied by averaged models using simpler programming techniques that give faster output compared to the linear differential equation model. However certain information is obscured by such models. Section 3.1 discusses the state space averaged model representation of the buck-boost converter in the 2-mode and 3-mode operation. Section 3.2 uses the state-space averaged model to highlight characteristics of the buck-boost converter. Section 3.3 discusses how state-space averaged models represent the converter operation for all kinds of perturbations in Duty ratio D and load resistance R . Since state-space averaged models are non-linear, they have to be linearized about a DC operating point, so that feed back design techniques can be used to provide close-loop control for the converter. Section 3.4 discusses how small signal approximation gives linearized model of the converter about a DC operating point.

3.1 STATE SPACE AVERAGED MODEL :

To design a closed-loop system for the converter for voltage regulation the linear differential equation model is of little help. Since none of the equations 2.20, 2.21 or 2.22 describe the converter for time interval long enough to include a discontinuity. State space

averaging allows discontinuous (switched) systems to be approximated as a continuous but non-linear system (refer Appendix B-1). Linearization allows the resulting non-linear system to be approximated as a continuous and a linear system and the resulting equations can then be used to determine parameters of close-loop feedback system for desired transient and steady state response (refer appendix B-2). The continuous time state space averaged representation of Buck-boost converter is given by

$$\dot{X} = A_0 X + B_0 u \quad (3.1)$$

$$\text{Where } A_0 = A_1 D + A_2 (1-D) \quad (3.2)$$

$$= \begin{bmatrix} \frac{-1}{R_1 C} & \frac{R(1-D)}{R_1 C} \\ \frac{-R(1-D)}{R_1 C} & \frac{-r_L}{L} - \frac{-r_c R(1-D)}{L R_1} \end{bmatrix}$$

$$\text{Where } B_0 = B_1 D + B_2 (1-D) \quad (3.3)$$

$$= \begin{bmatrix} 0 \\ D \\ L \end{bmatrix}$$

During two mode or continuous mode of conduction, and

$$A_0 = A_1 D + A_2 D_1 + A_3 (1-D-D_1) \quad (3.4)$$

$$= \begin{bmatrix} \frac{-1}{R_1 C} & \frac{R D_1}{R_1 C} \\ \frac{-R D_1}{R_1 L} & -\left(\frac{r_L (D + D_1)}{L} + \frac{r_c R D_1}{L R_1}\right) \end{bmatrix}$$

$$B_0 = B_1 D + B_2 D_1 + B_3 (1-D-D_1) \quad (3.5)$$

$$= \begin{bmatrix} 0 \\ D \\ \frac{L}{T_c} \end{bmatrix}$$

Where $D_1 = \frac{\text{Duration of mode 2}}{T_c}$

during three-mode or discontinuous mode of conduction.

In feed back control systems D is a function of X and u . Thus continuous approximation of two or three switched linear systems is a non-linear system. Another advantage of using continuous time state space averaged model is that behaviors of the converter in time-domain can be studied (neglecting the switching information that can be studied exclusively by using only differential equation model) by using simpler programming techniques that give faster output compared to complete time domain analysis for perturbation in duty ratio D and load resistance R . Now $X = \begin{bmatrix} V_c \\ I_L \end{bmatrix}$ represents average value of state variables.

3.2 CHARACTERISTICS OF BUCK-BOOST CONVERTER :

As observed in chapter-II the converter operation can be distinctly classified into zones of continuous, boundary and discontinuous operation, depending upon the value of load resistance R and duty ratio D . Also it was observed that if load resistance is kept constant and value of duty ratio D is increased the converter tends to boundary and then

continuous mode of conduction, or if duty ratio D is kept constant and load resistance R is increased then the converter transits from continuous mode of conduction through boundary to discontinuous operation. In this section for given load resistance R how the classification of the three zones can be done on basis of duty ratio D , also in the discontinuous zone, for given value of R and D , how is D_1 effected and how for given load resistance R the average capacitor voltage and inductor current vary with duty ratio D , is examined.

3.2.1 VALUE OF DUTY RATIO D AT BOUNDARY OPERATION (D_{boundary}) :

(As a function of load resistance R)

During the two mode operation of the converter for given load resistance R there is a unique value of duty ratio D for which the inductor current at end of mode-2 just becomes zero. In steady state.

$$\dot{X} = \begin{bmatrix} 0 \\ 0 \end{bmatrix} ;$$

therefore equation 3.1 becomes.

$$0 = A_0 X + B_0 u$$

Substituting the values of A_0 and B_0 from equations 3.2 and 3.3 since boundary conduction is a special case of two mode conduction, results in two simultaneous equations :

$$\frac{-1}{RC} V_c + \frac{R(1-D)}{R_l C} I_L = 0$$

and

$$\frac{-R(1-D)}{R_1 L} V_c - \left[\frac{r_L}{L} + \frac{r_c R(1-D)}{R_1 L} \right] I_L + \frac{D}{L} V_{dc} = 0$$

solving these equations gives

$$V_c = \frac{D R R_1 V_{dc}}{R^2(1-D) + r_c R + \frac{r_L R_1}{(1-D)}} \quad 3 \text{ (A)}$$

Where V_c = Average Capacitor Voltage

= V_o (Average output Voltage)

Consider a simple r_L -L Ckt as shown in Figure 3.1 and consider that initial value of the inductor current at $t=0$ is $i_L = 0$. This represents the equivalent circuit of the converter in Mode 1 of boundary operation at the input side.

Then value of i_L at time $t>0$ is given by

$$i_L = \frac{V_{dc}}{r_L} (1 - e^{-r_L t/L})$$

Since $\lim_{x \rightarrow 0} e^{-x} = 1 - x$

$$i_L = \lim_{r_L \rightarrow 0} \frac{V_{dc}}{r_L} (1 - (1 - \frac{r_L t}{L}))$$

Using the above relation

I_{L1} = Peak inductor current at end of Mode 1

$$\begin{aligned}
 &= \frac{V_{dc}}{r_L} * \frac{r_L DT_c}{L} \\
 &= \frac{V_{dc} DT_c}{L}
 \end{aligned} \tag{3.6a}$$

From figure 2.3 (b) it is observed that average value of inductor current during a switching cycle in Boundary conduction is

$$I_{LB} = \frac{1}{2} I_{L1}$$

Substituting value of I_{L1} gives

$$I_{LB} = \frac{1}{2} \frac{V_{dc} DT_c}{L} \tag{3.6b}$$

Equating the input-output power for Boundary conduction

$$V_{dc} I_{LB} DT_c = V_o I_o T_c$$

Where $I_o = V_o / R$

substituting the values of I_{LB} , I_o and V_o gives a fourth order quadratic equation.

$$R^2 u^4 + 2R^3 r_c u^3 + (2R^2 R_1 r_L + R^2 r_c^2 - 2L f_s R R_1^2) u^2 + 2R R_1 r_c r_L u + R_1^2 r_L^2 = 0 \tag{3.7}$$

Where $u = (1-D)$

One of the roots of above equation gives the value of ($1-D_{boundary}$) for given load resistance R , in steady state.

Therefore $D_{boundary} = 1-u$

If in equation 3.7 $r_c = r_L = 0$ then

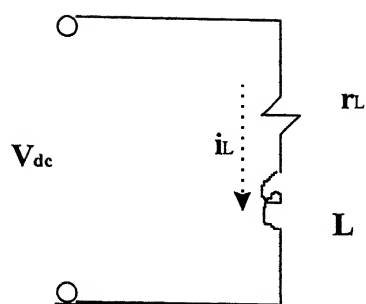


FIG 3.1: Simple r_L - L Circuit

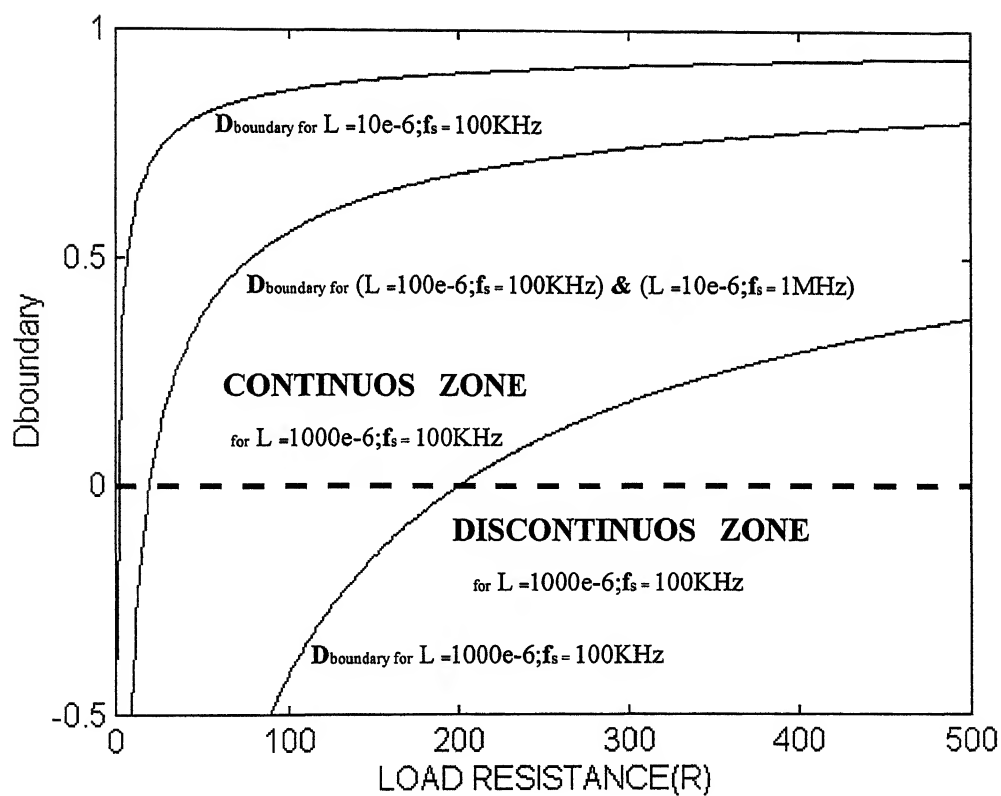


FIG 3.2: $D_{boundary}$ Versus Load Resistance R

$$R^4 u^4 + (-2L f_s R^3) u^2 = 0$$

$$\text{Therefore } D_{\text{boundary}} = 1 - \sqrt{\frac{2L}{RT_c}}$$

which implies that D_{boundary} is proportional to L/R ratio. Also if D_{boundary} is made zero (implies only continuous operation of the converter is possible for given load resistance R) then the value of load resistance R above which both continuous / discontinuous operation of the converter is possible is directly proportional to value of L and f_s .

Consider the following cases :

- (a) A plot of R versus D_{boundary} for $L=100\mu\text{H}$ and $f_s=100\text{KHZ}$
- (b) A plot of R versus D_{boundary} for $L=10\mu\text{H}$ and $f_s=100\text{KHZ}$
- (c) A plot of R versus D_{boundary} for $L=10\mu\text{H}$ and $f_s=100\text{MHZ}$
- (d) A plot of R versus D_{boundary} for $L=1000\mu\text{H}$ and $f_s=100\text{KHZ}$

As shown in Figures 3.2

It is observed that for some values of load resistance R , value of D_{boundary} is negative, it can be concluded that for these values of load resistance the converter shall never operate in discontinuous mode in steady state, however low is the value of D . Larger the values of inductance L the converter remains in continuous operation for given value of D for larger values of R in steady state. Also D_{boundary} remains same for same L/R ratio for different values of L . The value of R above which both continuous and discontinuous operation of converter is possible is proportional to L and f_s .

For given value of L and V_{dc} the area below the $D_{boundary}$ curve represents all operating points that define the discontinuous operation zone of the converter in steady state and area above the curve defines all operating points lying in the continuous operation zone of the converter in steady state.

3.2.2 DURATION OF MODE- 2 : ($D_1 T_c$)

Figure 2.3(c) shows that during discontinuous conduction the inductor current decays to zero and remains zero till the beginning of the next switching cycle, but in continuous conduction since the next switching cycle starts before the inductor current in Mode-2 decays to zero therefore duration of Mode-2 is taken as $(1-D)T_c$ and for boundary condition as $(1-D_{boundary}) T_c$. However it is to be seen that for load resistance R for which both continuous and discontinuous operation is possible, how is duration of Mode-2 and Mode-3 effected as the value of D is increased. From figure 2.3(c) the capacitor voltage at end of Mode-2, V_{c2} can be expressed as :

$$V_{c2} = V_{c1} e^{(1-D_1)T_c/T_1C} \quad (3.8)$$

Substituting this value of V_{c2} in equation 2.7 and $t'' = D_1 T_c$ results in

$$V_{c1}e^{(1-D_1)T/R_1C} = e^{\sigma D_1 T_c} [C_3 \cos \omega D_1 T_c + C_4 \sin \omega D_1 T_c] \quad (3.9)$$

In equation 2.8 if $I_{L2} = 0$ and $t'' = D_1 T_c$ then

$$e^{\sigma D_1 T_c} \{C_3 \cos \omega D_1 T_c + C_4 \sin \omega D_1 T_c\} = 0$$

since $e^{\sigma D_1 T_c}$ cannot be zero.

$$C_3 \cos \omega D_1 T_c + C_4 \sin \omega D_1 T_c = 0 \quad (3.10)$$

Substituting the values of C_3 and C_4 in equation 3.10 results in

$$I_{L1} = \frac{V_{c1}}{\omega L} \frac{(1 - r_c / R_1) \sin \omega D_1 T_c}{\left\{ \cos \omega D_1 T_c - \left(\sigma + \frac{r_L}{L} + \frac{R r_c}{R_1 L} \right) \sin \omega D_1 T_c \right\}}$$

Substituting the values of C_3 , C_4 and I_{L1} in equation 3.9 and eliminating V_{c1} results in

$$e^{(1-D_1)T_c/R_1C} - e^{\sigma T_c D_1} \left\{ \begin{aligned} & \cos(\omega D_1 T_c) + \frac{R(1 - r_c / R_1)}{R_1 C \omega^2 L} \frac{\sin^2 \omega T_c D_1}{\left\{ \cos(\omega D_1 T_c) - \frac{(\sigma + \frac{r_L}{L} + \frac{R r_c}{R_1 r_c})}{\omega} \sin(\omega D_1 T_c) \right\}} - \\ & \frac{(\sigma + \frac{1}{R_1 C})}{\omega} \sin(\omega D_1 T_c) \end{aligned} \right\} = 0$$

(3.11)

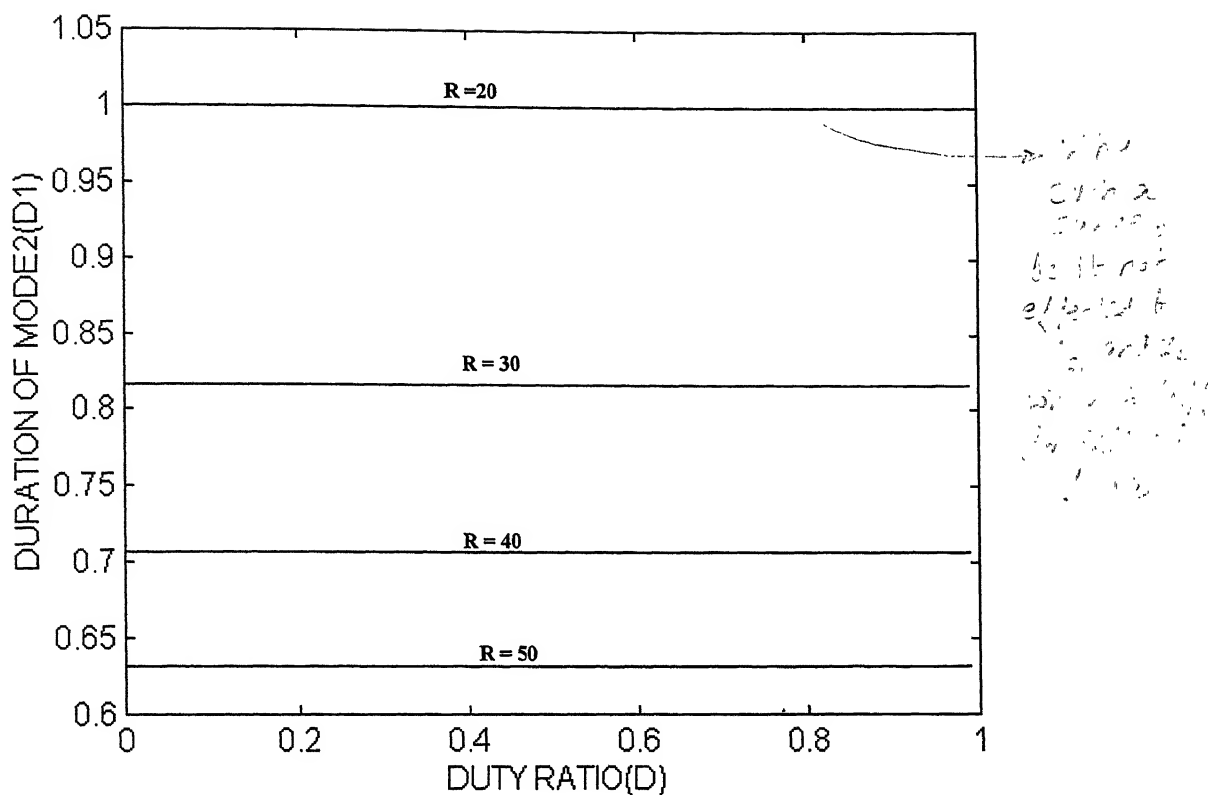
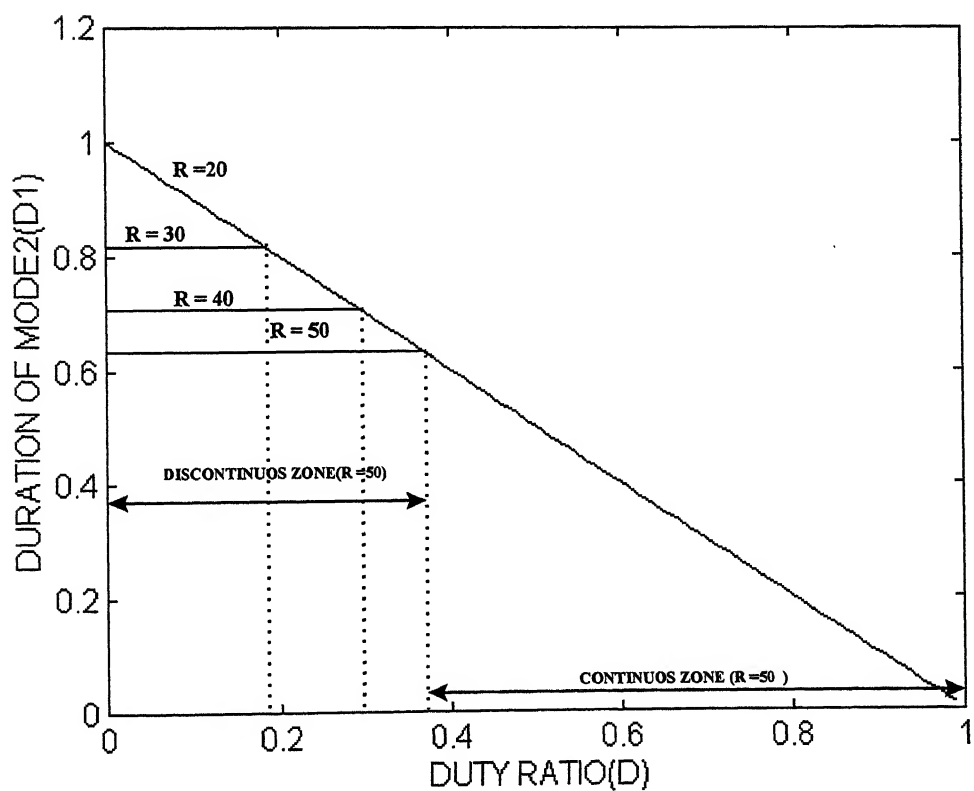


FIG 3.3:(a) Duration of Mode2 as given by eqn(3.11)



For given parameters of the converter and load resistance R solution of the transcendental equation 3.11 will give us the value of D_1 and D_1T_c (the duration of Mode-2) or the time required for inductor current in Mode-2 to decay to zero, but in continuous mode of conduction duration of Mode-2 is $(1-D)T_c$. As seen in Figures 3.3 (a & b) for the following cases.

- (a) Plot of D Vs D_1 for $R = 20 \Omega$
- (b) Plot of D Vs D_1 for $R = 30 \Omega$
- (c) Plot of D Vs D_1 for $R = 40 \Omega$
- (d) Plot of D Vs D_1 for $R = 50 \Omega$

in Figure 3.3(a) to Figure 3.3(b)

It is observed that value of D_1 remains constant for given value of R , irrespective of values of D . This is so because as seen from equivalent ckt in Figure 2.2(b) the rate of decay of inductor current is decided by the value of R and capacitor C . But in actual operation for $D \geq D_{\text{boundary}}$, $D_1 = (1-D)$. The results show that in discontinuous zone $D_1 = (1-D_{\text{boundary}})$ where D_{boundary} for given load resistance R is given by Equation 3.11. Therefore it can be concluded that in steady state during the discontinuous operation for given value of R it is only the duration of Mode-1 and Mode-3 that change while that of Mode-2 remains constant with change in value of D .

With this information given any operating point a state space averaged model of the converter can be defined, and the variation in steady state average values of Inductor current and Capacitor voltage for given load resistance and can be studied, as shown in Figures 3.4(a) and (b). Simultaneous equations in section 3.2.1 give the steady state values of V_c and I_L during continuous mode of conduction, similarly we can obtain relations for discontinuous mode of conduction by substituting in $0=A_0X+B_0u$ values of A_0 and B_0 as given by equations 3.4 and 3.5 as follows.

$$\frac{-1}{R_1C}V_c + \frac{RD_1}{R_1C}I_L = 0$$

$$\frac{-RD_1V_{dc}}{R_1L} - \left[\frac{r_L}{L}(D + D_1) + \frac{r_cRD_1}{R_1L} \right] I_L = \frac{-DV_{dc}}{L}$$

Solution to the above simultaneous equations gives

$$V_c = V_o = \frac{RR_1DV_{dc}}{R^2D_1 + R_1r_L(1 + \frac{D}{D_1}) + r_cR} \quad (3 B)$$

Else using the relation $0 = A_0X + B_0u$

the steady state value of the average capacitor/output voltage and inductor current corresponding to given D and R can be determined as

$$X_0 = \begin{bmatrix} V_c \\ I_L \end{bmatrix} = \text{inv}(A_0)B_0V_{dc}$$

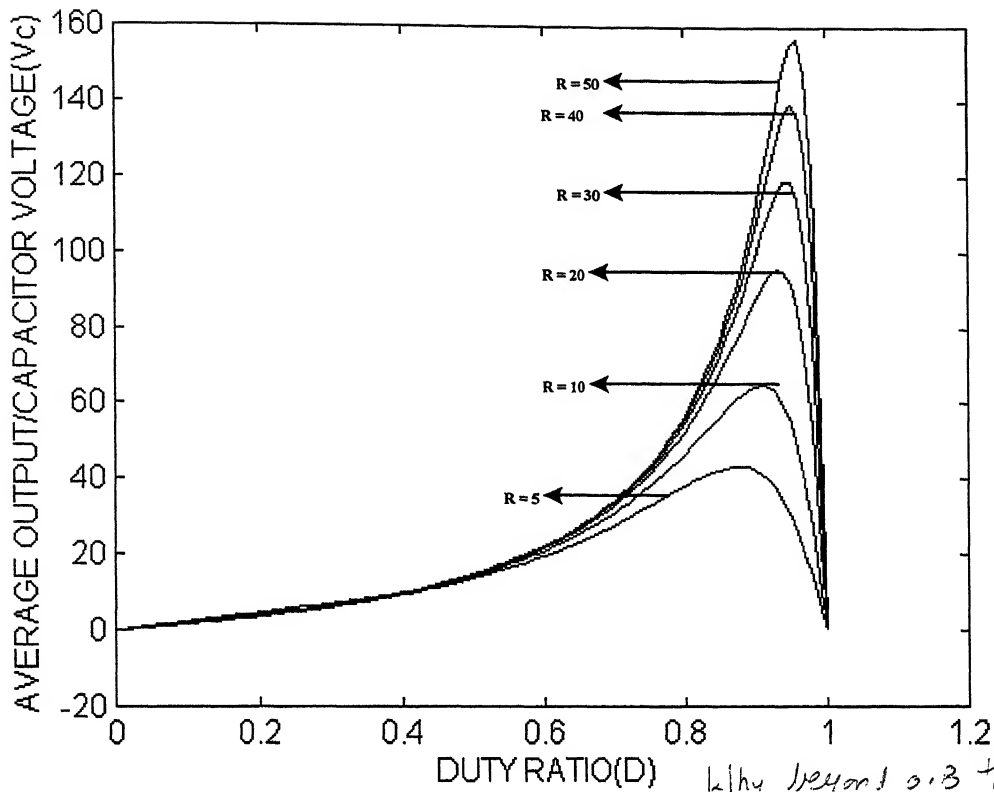
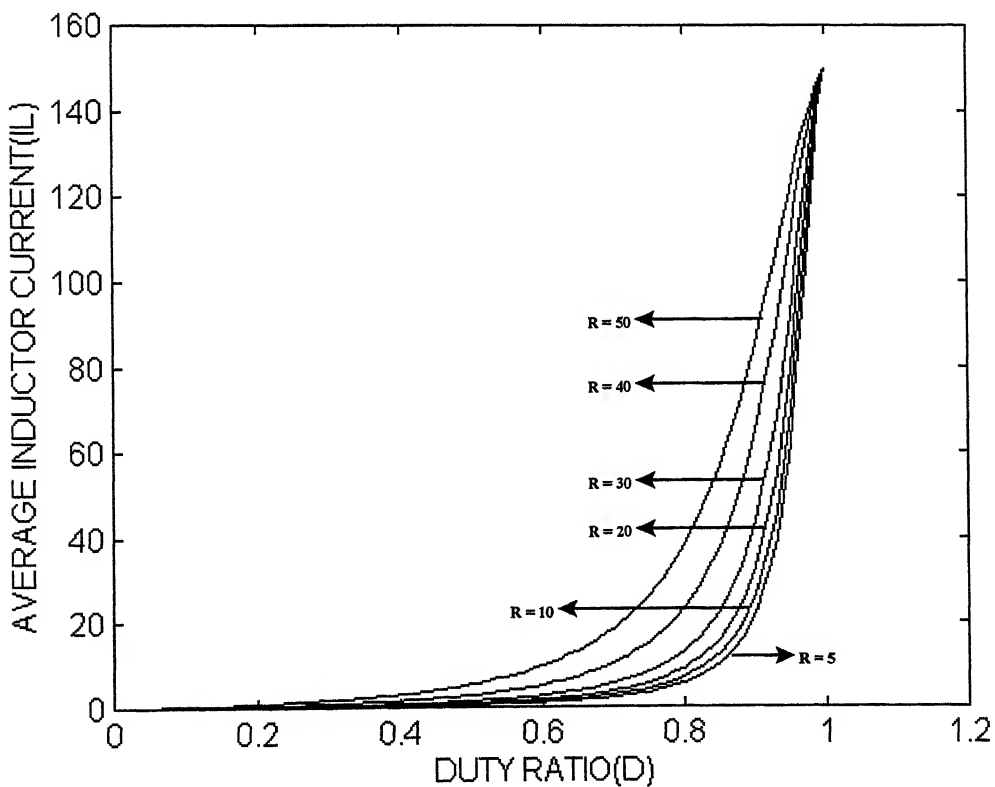


FIG 3.4:(a):Average Output Voltage versus Duty Ratio



Where A_0 and B_0 are given by equations 3.2 and 3.3 or 3.4 and 3.5 depending upon the operating point (defined by D, R and V_{dc}) lies in continuous or discontinuous operating zone respectively.

It is observed that for a given load resistance the output voltage and average inductor current increase gradually and marginally as D is increased, till $D=0.8$. Also for different values of load resistance R the output voltage V_0 is not significantly different for given value of D till $D=0.8$. The output voltage varies significantly for different values of the load resistance R in the range $D=0.8$ to 0.99 . For all values of R the slope of I_L vs D curve increases sharply beyond $D=0.8$.

3.3 CONVERTER SIMULATION USING STATE-SPACE AVERAGED MODEL :

If the converter behaviour has to be studied in time domain for perturbation in duty ratio D and load resistance R without observing the switching information then state space average model provides means of doing so by employing simpler programming techniques which also provide faster output. Consider the cases given in Table-1. As observed in Chapter-II converter operation can be classified as one of the following cases.

Sl. No.	Initial condition	Transient State	Final Condition
1.	Continuous Mode	Continuous Mode	Continuous Mode
2.	Continuous Mode	Discontinuous Mode	Continuous Mode
3.	Continuous Mode	Discontinuous Mode	Discontinuous Mode
4.	Discontinuous Mode	Discontinuous Mode	Discontinuous Mode
5.	Discontinuous Mode	Continuous Mode	Discontinuous Mode
6.	Discontinuous Mode	Continuous Mode	Continuous Mode

Consider case 1 of Table-1, if we use only the continuous mode state space averaged model to simulate the perturbation, we observe that if the ripple is neglected the results match those of the differential equation model very accurately, as shown in the Fig. 3.5 (a & b) . However, if the same model is used to simulate the case 5 we observe that the results are incorrect as shown in Fig. 3.5 (c & d). In the differential equation model the value of t_2 decides whether the present switching cycle is continuous or discontinuous, but in state space averaged model t_2 holds no validity. Therefore, the conditions that are to be examined while using state space averaged model to effect the model transition, so that the model accurately represents the process for all cases of perturbations in load and duty ratio are the value of I_L and D_1 . Equation 3.6(b) gives the value of average inductor current I_{LB} for a given value of duty ratio D when the converter is operating at the boundary condition. A value of average inductor current I_L below this value at any instant for given D implies the converter may be in discontinuous conduction. The converter operation while using averaged model can be defined in I_L - D_1 plane as shown in Fig. 3.6.

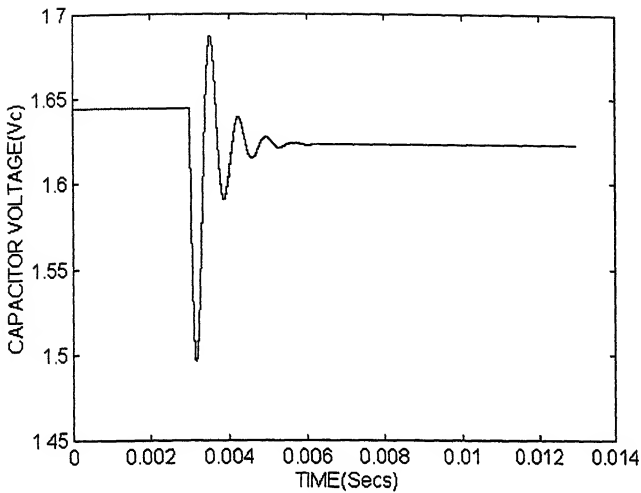


FIG 3.5(a): System Response for change in R from 10 to 5 Ohms for $D = 0.1$; using state - space averaged model defined by eqns (3.2) & (3.3)

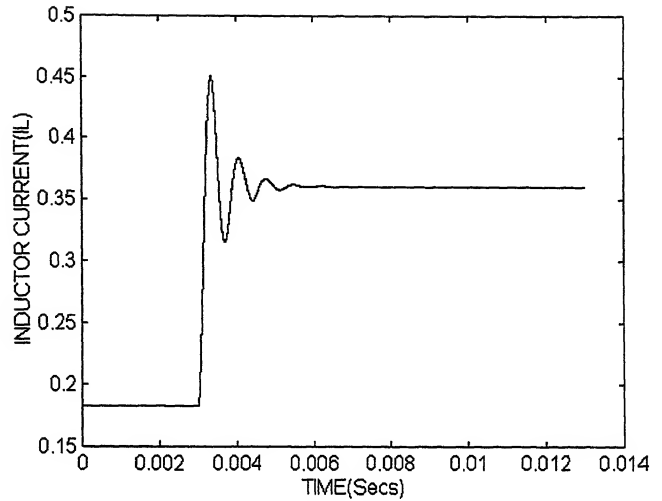


FIG 3.5(b): System Response for change in R from 10 to 5 Ohms for $D = 0.1$; using state - space averaged model defined by eqns (3.2) & (3.3)

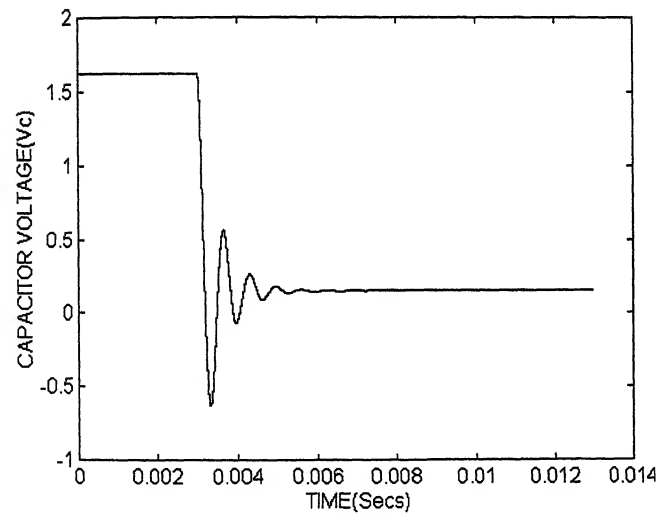


FIG 3.5(c): System Response for change in D from 0.1 to 0.01 for $R = 5$ Ohms ; using state - space averaged model defined by eqns (3.2) & (3.3) ; results show Model failure

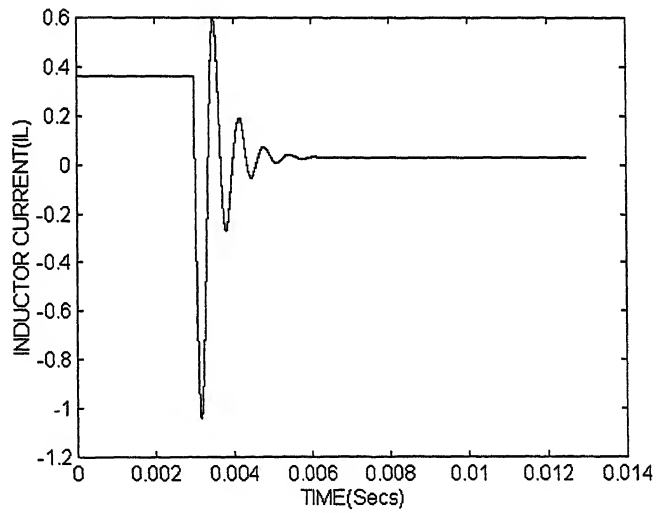


FIG 3.5(d): System Response for change in D from 0.1 to 0.01 for $R = 5$ Ohms ; using state - space averaged model defined by eqns (3.2) & (3.3) ; results show Model failure

if in equation (3 B), $r_c = r_L = 0$ then

$$V_c = \frac{V_{dc}D}{D_1}$$

Therefore

$$D_1 = \frac{V_{dc}D}{V_c} \quad (3.12A)$$

If the output of an averaged model at any instant satisfies the conditions :

$$I_L < I_{LB}$$

$$D_1 < (1-D)$$

then for further solution averaged model as defined by equations 3.4 and 3.5 is used till the above conditions are satisfied.

Case 2 to 5 given in Table 1 are simulated, using the above logic for Model transition.

The results are shown in figures 3.7 to 3.10 respectively.

It is observed from Fig. 3.10 (b) that despite implying model transition conditions the model fails because the above conditions of Model transition are not applied to the intermediate output of ode`45' subroutine. Fig. 3.10 (c & d) shows the response for case 5 of Table 1 when conditions of model transition are checked at every intermediate output of

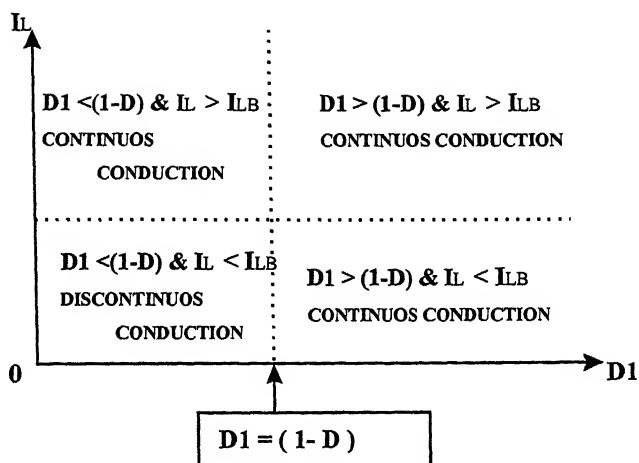


FIG 3.6: L - D1 Plane: Conditions of Model transition fromCM ↔ DCM
for given value of R & D

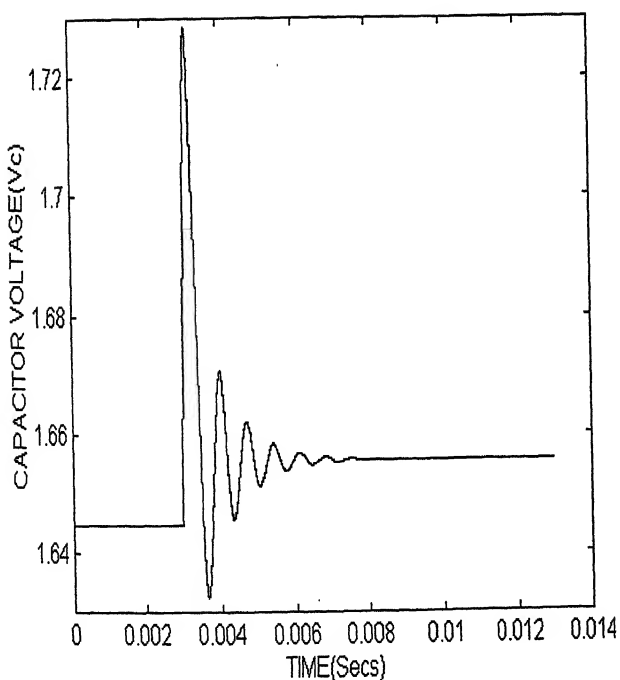


FIG 3.7(a): System Response for change in R from 10 to 20 Ohms for D = 0.1 ; using conditions given by eqns(3.6 b) and (3.12 A)for model transition.

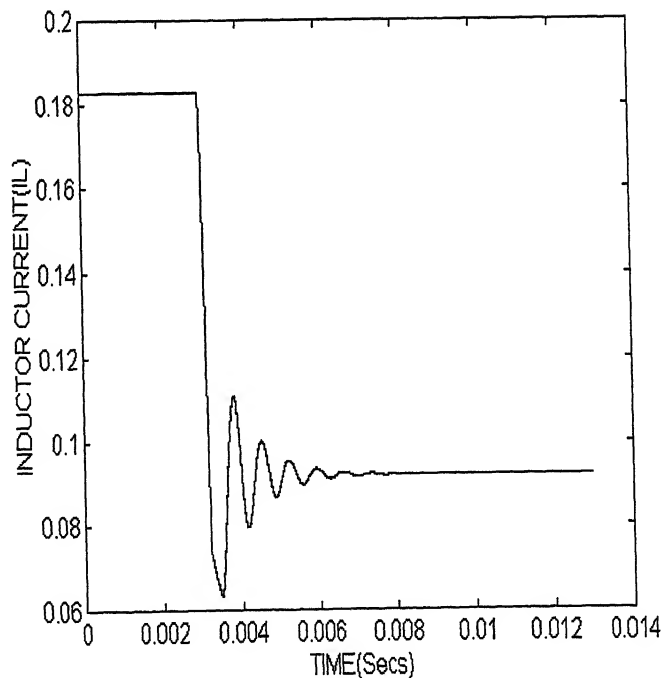


FIG 3.7(b): System Response for change in R from 10 to 20 Ohms for D = 0.1 ; using conditions given by eqns(3.6 b) and (3.12 A)for model transition.

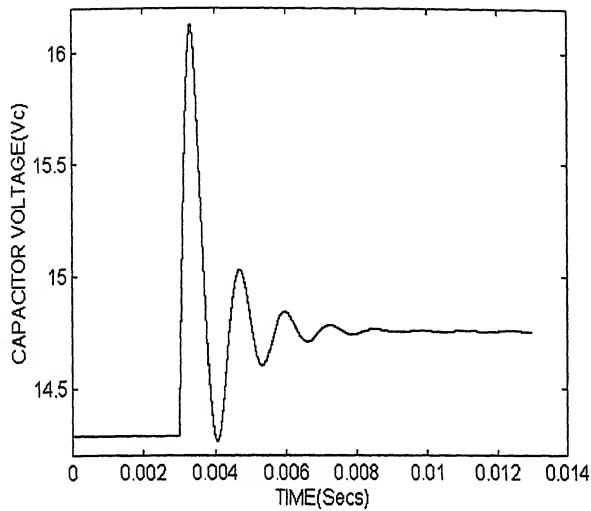


FIG 3.8(a): System Response for change in R from 10 to 30 Ohms for $D = 0.5$; using conditions given by eqns(3.6 b) and (3.12 A)for model transition.

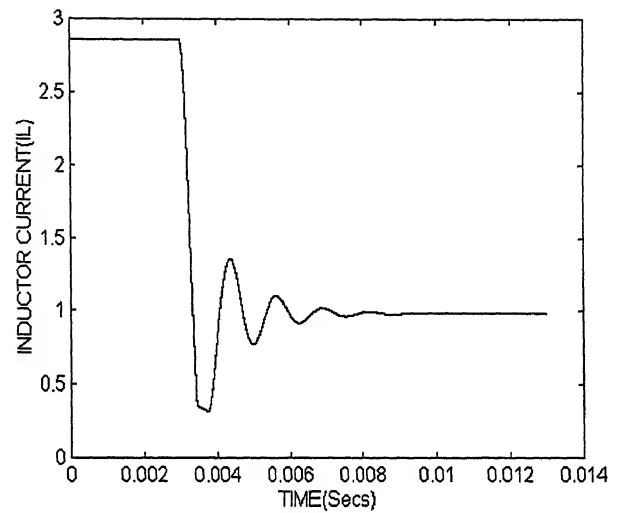


FIG 3.8(b): System Response for change in R from 10 to 30 Ohms for $D = 0.5$; using conditions given by eqns(3.6 b) and (3.12 A)for model transition.

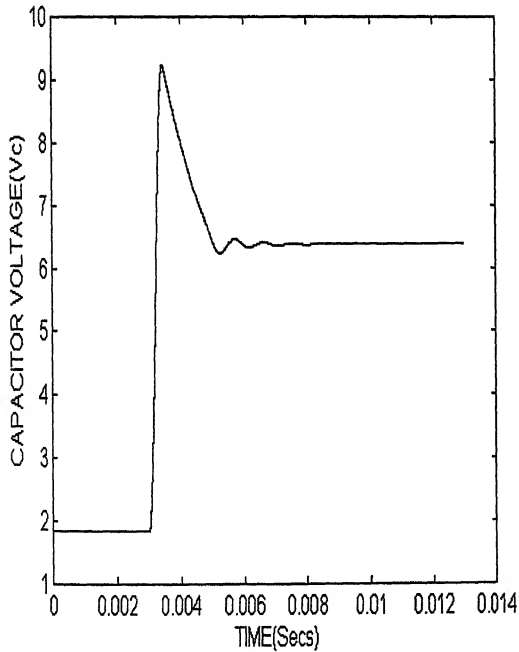


FIG 3.9(a): System Response for change in D from 0.1 to 0.3 for $R = 30$; using conditions given by eqns(3.6 b) and (3.12 A)for model transition.

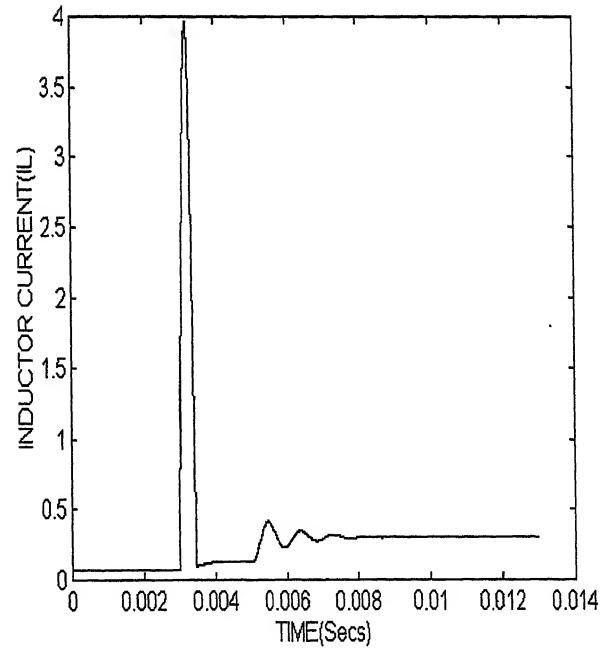


FIG 3.9(b): System Response for change in D from 0.1 to 0.3 for $R = 30$; using conditions given by eqns(3.6 b) and (3.12 A)for model transition.

'ode45' subroutine. Figures 3.11 to 3.13 show the results for cases 6, 7 and 8 given in Table 1, when the model transition conditions are implied to every intermediate output of the 'ode45' subroutine. It is observed that the state space average model fails to represents the transient process, when the results are compared with those of differential equation model.

Consider the relation given by equation (3B)

$$V_c = \frac{RR_1DV_{dc}}{R^2D_1 + R_1r_L(1 + \frac{D}{D_1}) + r_cR}$$

Solving for D_1 from the above relation results in a quadratic equation.

$$R^2D_1 - \left\{ \left(\frac{RR_1DV_{dc}}{V_c} \right) + R_1r_L + Rr_c \right\} D_1 + R_1r_LD = 0 \quad (3.12B)$$

One of the roots of the equation (3.12B) gives the value of D_1 for given R and D and Capacitor voltage V_c . Figure 3.14 to 3.16 show the result for cases 6, 7 and 8 of Table 1 when model transition condition are implied using the values of I_{LB} and D_1 as given by equations (3.6b) and (3.12B) to the intermediate output of 'ode45' subroutine. The results show that the state space average model is very sensitive to conditions implied for model transition. Figure 3.17 shows that for case 5 in Table 1 while the value of D_1 given by equation 3.6 (a) gives successful results, the value of D_1 given by equation 3.6 (b) represents the current transient incorrectly. Therefore apart from the value of D_1 what are the other

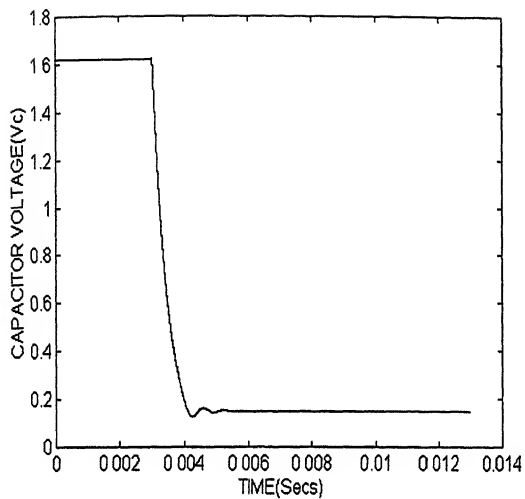


FIG 3.10 (a)

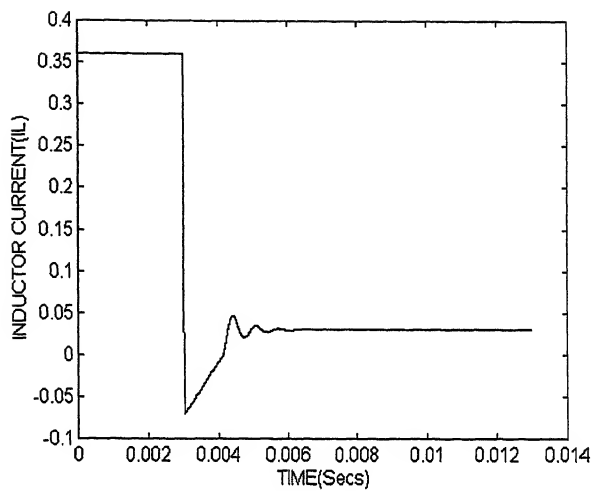


FIG 3.10 (b)

FIG 3.10:System Response for change in Duty Ratio D from 0.1 to 0.01 for $R = 5$ Ohms using Model transition criteion defined by eqns(3.6b & 3.12A)

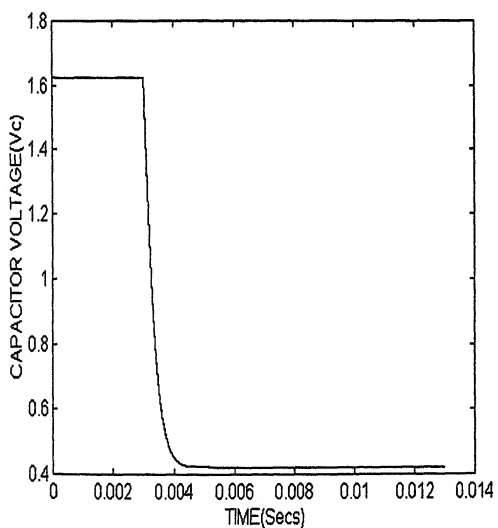


FIG 3.10 (c)

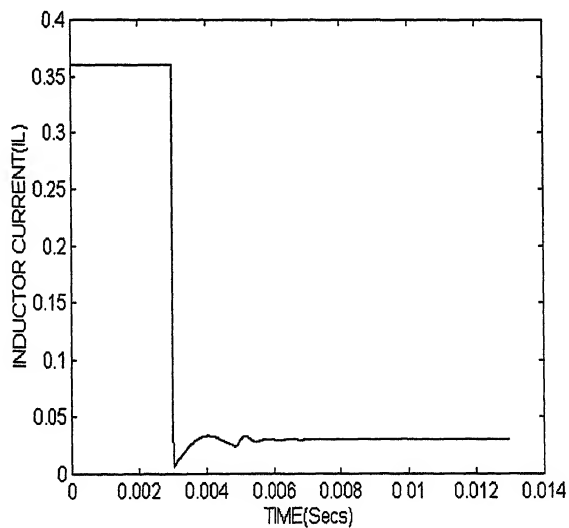


FIG 3.10 (d)

FIG 3.10:System Response for change in Duty Ratio D from 0.1 to 0.01 for $R = 5$ Ohms using Model transition conditions defined by eqns(3.6b & 3.12A) and implying it to intermediate output of 'ode45' subroutine

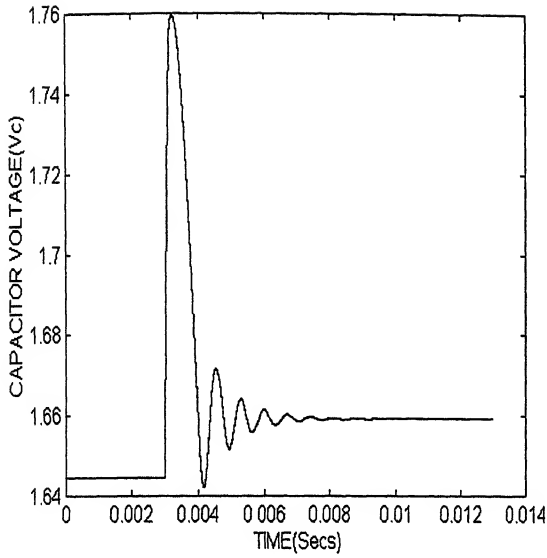


FIG 3.11(a)

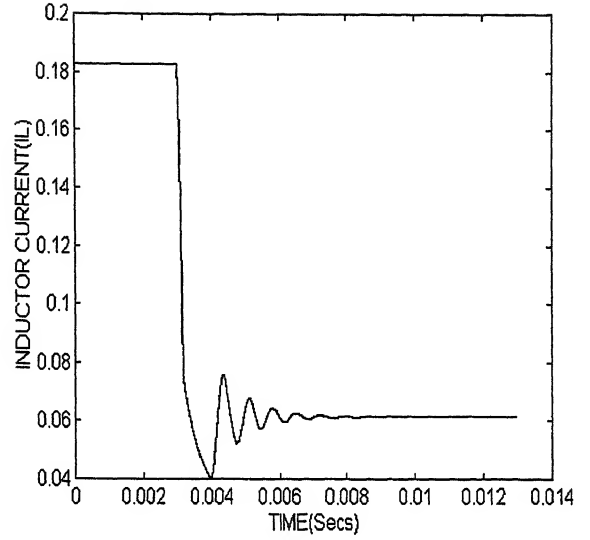


FIG 3.11(b)

FIG 3.11 :System Response for Change in R from 10 to 30 for $D = 0.1$;using Model transition conditions as defined by eqns(3.6b) & (3.12A) and implying to intermediate output of 'ode45' subroutine.

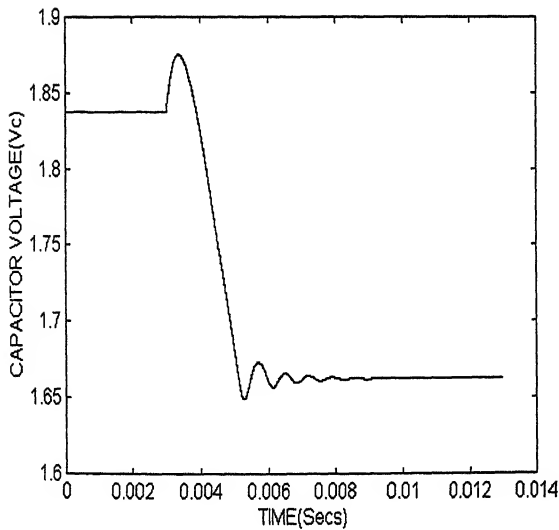


FIG 3.12(a)

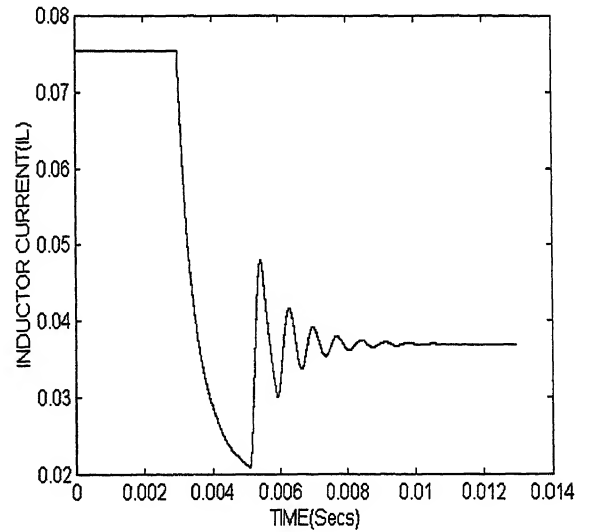


FIG 3.12(b)

FIG 3.12 :System Response for Change in R from 30 to 50 Ohms for $D = 0.1$;using Model transition conditions as defined by eqns(3.6b) & (3.12A) and implying to intermediate output of 'ode45' subroutine.

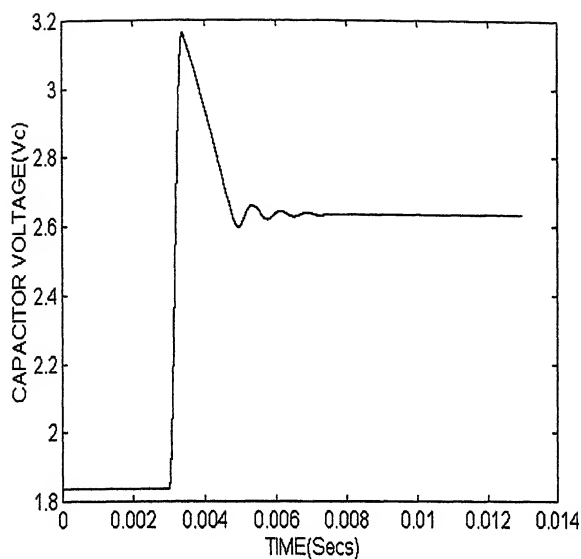


FIG 3.13(a)

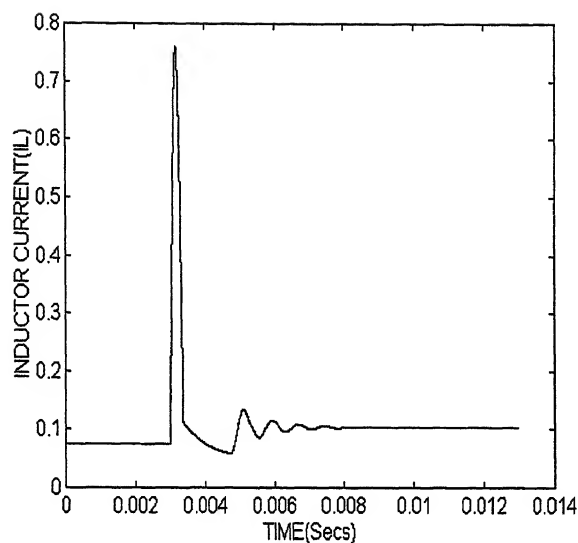


FIG 3.13(b)

FIG 3.13 :System Response for Change in D from 0.1 to 0.15 for $R = 30\Omega$;using Model transition conditions as defined by eqns(3.6b) & (3.12A) and implying to intermediate output of 'ode45' subroutine.

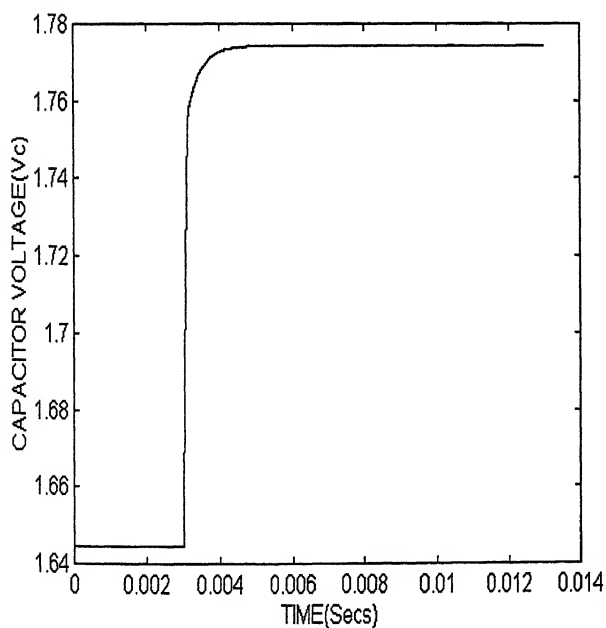


FIG 3.14(a)

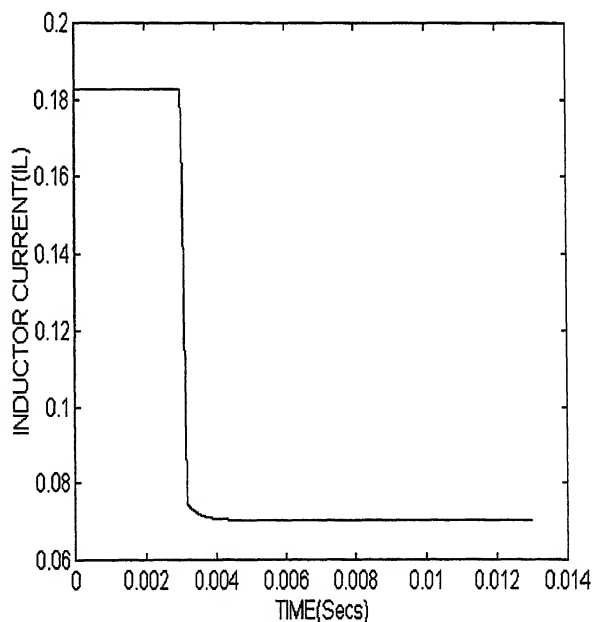


FIG 3.14(b)

FIG 3.14 :System Response for Change in R from 10 to 30 for $D = 0.1$;using Model transition conditions as defined by eqns(3.6b) & (3.12B) and implying to intermediate output of 'ode45' subroutine.

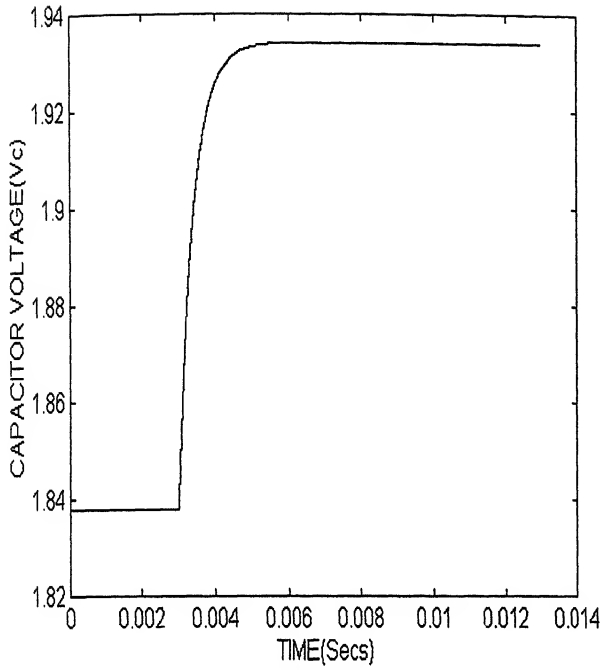


FIG 3.15(a)

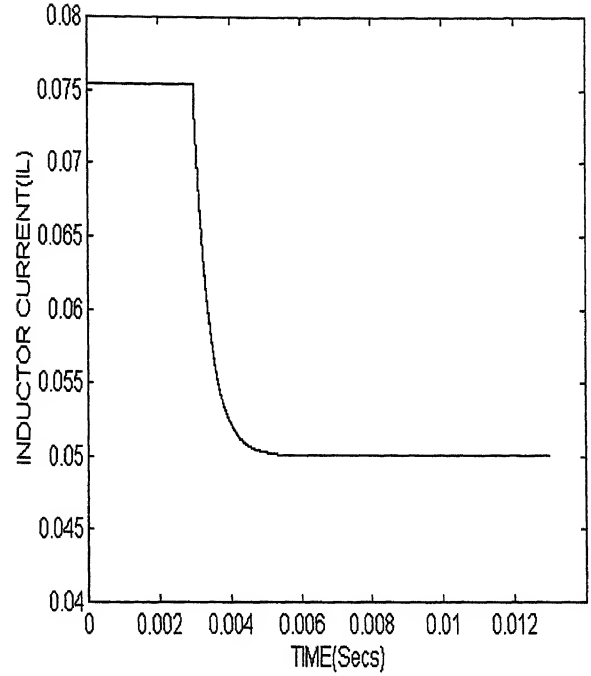


FIG 3.15(b)

FIG 3.15 :System Response for Change in R from 30 to 50 for D = 0.1 ;using Model transition conditions as defined by eqns(3.6b) & (3.12B) and implying to intermediate output of 'ode45' subroutine.

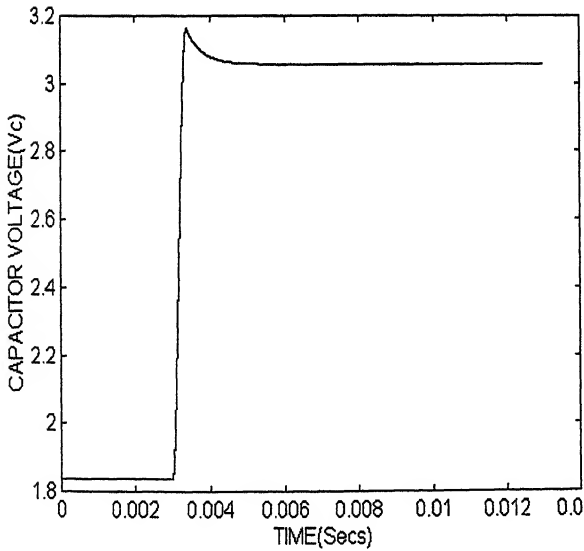


FIG 3.16(a)

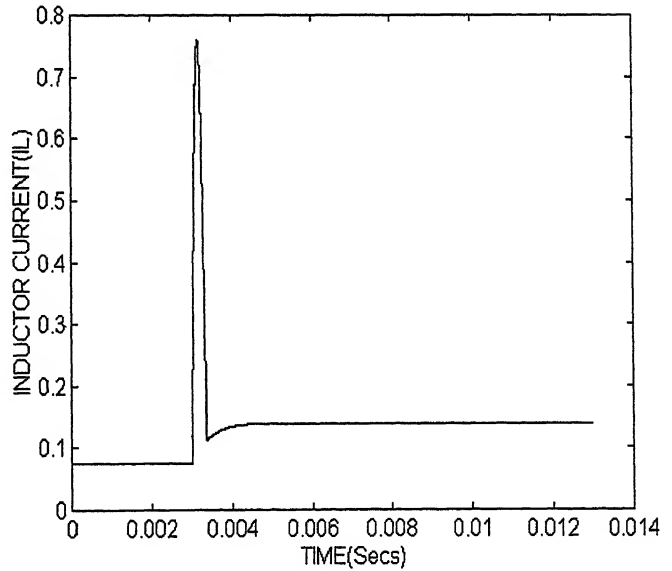


FIG 3.16(b)

FIG 3.16 :System Response for Change in D from 0.1 to 0.15 for R = 30 Ohms using Model transition conditions as defined by eqns(3.6b) & (3.12B) and implying to intermediate output of 'ode45' subroutine.

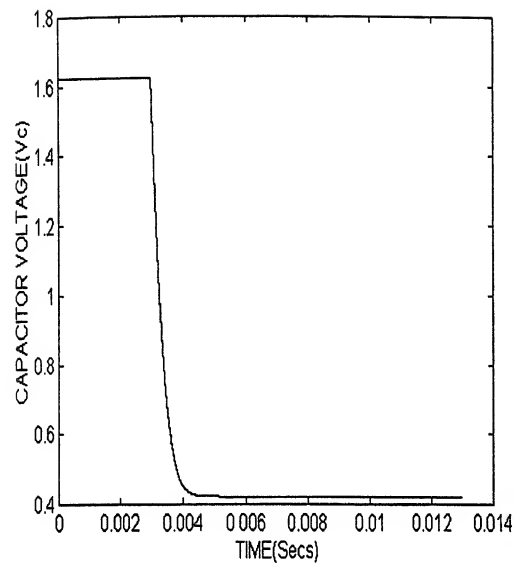


FIG 3.17(a)

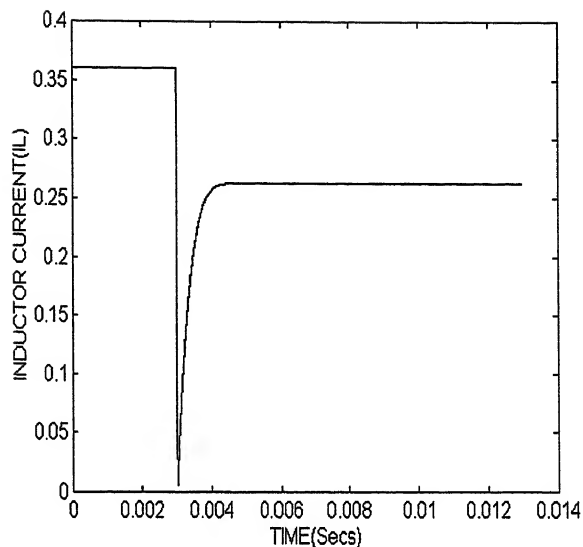


FIG 3.17(b)

FIG 3.17 :System Response for Change in D from 0.1 to 0.01 for $R = 5$ Ohms ;using Model transition conditions as defined by eqns(3.6b) & (3.12B) and implying to intermediate output of 'ode45' subroutine.

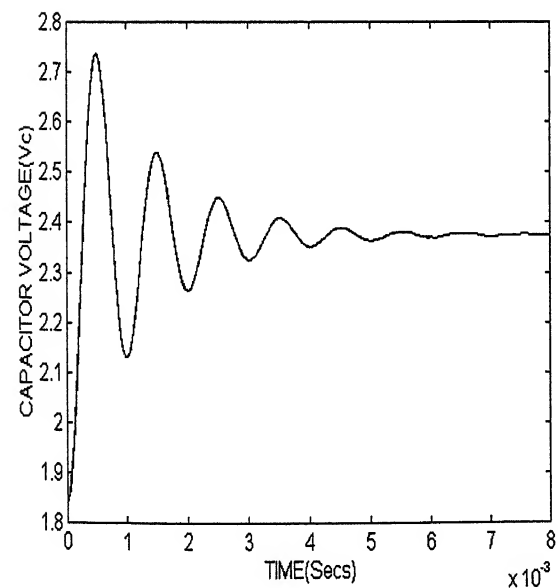


FIG 3.18(a)

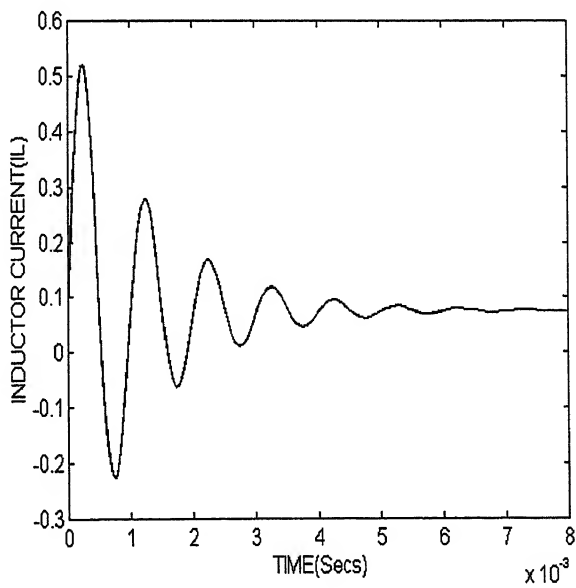


FIG 3.18(b)

FIG 3.18 :System Response for Change in R from 30 to 50 Ohms for $D = 0.1$;using State - Space Averaged Model defined by eqns(3.4) & (3.5) .

factors influencing the accuracy of state space averaged model are not apparent. For transition where the converter remains in discontinuous conduction during the initial state, the transient state and the final state it is quite logical to use average model defined by equations 3.4 and 3.5 to study the transient, where the value of D_1 is taken to be $(1 - D_{\text{boundary}})$, where D_{boundary} corresponds to the value of R at final operating point. Figure 3.18 shows the results for case 7 in Table 1. Though the final steady state value is correct this method does not represent the transient correctly.

3.4 SMALL SIGNAL APPROXIMATION FOR LINEARITY :

If the power stage of the buck-boost converter can be linearized than bode plots and stability criterion can be used to determine the appropriate compensation in feedback loop for the desired steady state and transient response. Flow graph for linear analysis of switched regulators is shown in Fig. 3.19 .

$$\hat{\dot{X}} = A_0 X + B_0 u + E \hat{d} \quad (3.13)$$

represents the converter in linearized form about a DC operating point.

Where A_0 and B_0 are given by equations 3.2 and 3.3 or 3.4 and 3.5 and matrix E is given as

$$E = (A_1 - A_2) X_0 + (B_1 - B_2) V_{dc} \quad (3.14)$$

$$E = (A_1 - A_2 - A_3) X_0 + (B_1 - B_2 - B_3) V_{dc} \quad (3.15)$$

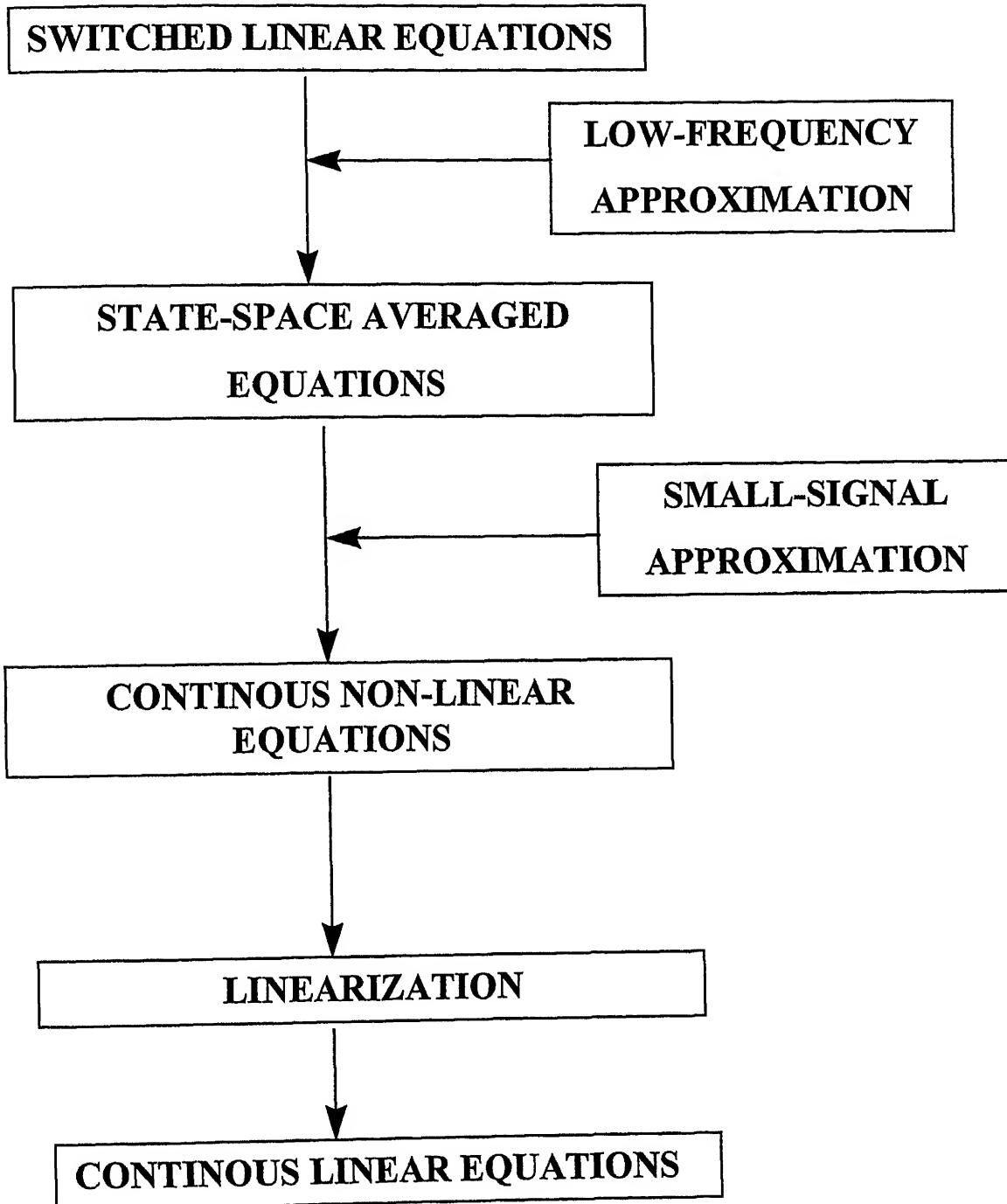


FIG 3.19: Flowgraph for Small Signal Approximation for Linearity

depending upon the operating point lies in continuous or discontinuous zone of operation.

$$X_o = -\text{inv}(A_0) B_0 V_{dc}$$

3.4.1 TRANSFER FUNCTION $\frac{\hat{V}_c}{\hat{d}(s)}$ AND BODE PLOT :

Taking the laplace transform of equation 13 in appendix B-2 results in

$$s \hat{X}(s) = A_0 \hat{X}(s) + B_0 \hat{u}(s) + E \hat{d}(s) \quad (3.16)$$

if the input voltage V_{dc} is fixed then $\hat{u}(s) = 0$

Substituting this value of $\hat{u}(s) = 0$ in equation 3.16 results in

$$\hat{X}(s) = (sI - A_0)^{-1} E \hat{d}(s) \quad (3.17)$$

Substituting the desired values of A_0 and E for an operating point in continuous zone and equating only the first row of the matrices on LHS and RHS results in

$$\frac{\hat{V}_c(s)}{\hat{d}(s)} = \frac{1}{\Delta} \left[\left(s + \frac{r_L}{L} + \frac{(1-D)Rr_c}{R_1 L} \right) \frac{(-RI_{Lo})}{R_1 C} + \frac{(1-D)R}{R_1 C} \left(\frac{V_{dc}}{L} + \frac{Rr_c I_{Lo}}{R_1 L} + \frac{(1-r_c)}{R_1} \frac{V_{co}}{L} \right) \right]$$

$$\text{Where } \Delta = \left(s + \frac{r_L}{L} + \frac{(1-D)Rr_c}{R_1 L} \right) \left(s + \frac{1}{R_1 C} \right) + \frac{(1-D)^2 R(1-V_c / R_1)}{R_1 LC} \quad (3.18)$$

Similarly transfer function for an operating point in discontinuous operating zone can be derived. The transfer function shows that the power stage of the converter is of type 0.

Fig. 3.20 to Fig. 3.23 gives the Bode plot for the operating points given in Table 2 for the above transfer function.

Sl. No.	Load Resistance	Duty Ratio
1.	5	0.1
2.	5	0.5
3.	30	0.1
4.	30	0.5

Table-2

The bode plots are verified by giving a small disturbance to duty ratio d in the small signal model defined by equation 3.17 at the frequencies given in Table-3 Figure 3.24 shows the result of verification simulation at corner frequency for each case of Table 2.

3.4.2 TRANSFER FUNCTION $\frac{\hat{V}_c(s)}{\hat{u}(s)}$ AND BODE PLOT :

If in equation 3.16 if $\hat{d}(s) = 0$ then

$$\hat{X}(s) = (sI - A0)^{-1} B0 \hat{u}(s) \quad (3.19)$$

substituting the values of A0 and B0 for an operating point in continuous zone and equating only the first row of RHS and LHS, results in

$$\frac{\hat{V}_c(s)}{\hat{u}(s)} = \frac{(1 - D)RD}{\Delta R_1 LC}$$

Where Δ is given by equation 3.18.

Similarly transfer function for an operating point in discontinuous operating zone can be derived. Figure 3.25 to 3.28 give the bode plot for the operating points given in Table 2 for the above transfer function. The bode plots are verified by giving a small disturbance to input voltage V_{dc} in the small signal model defined by equation 3.19 at the frequencies given in Table-4 Figure 3.28 shows the result of verification simulation at corner frequency for each case of Table 2.

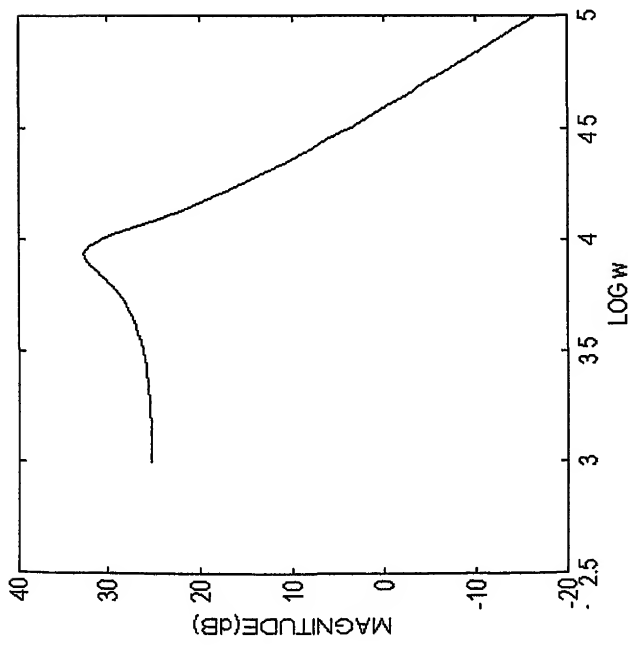


FIG 3.20 (a): For the Operating Point $R = 5$ Ohms & $D = 0.1$

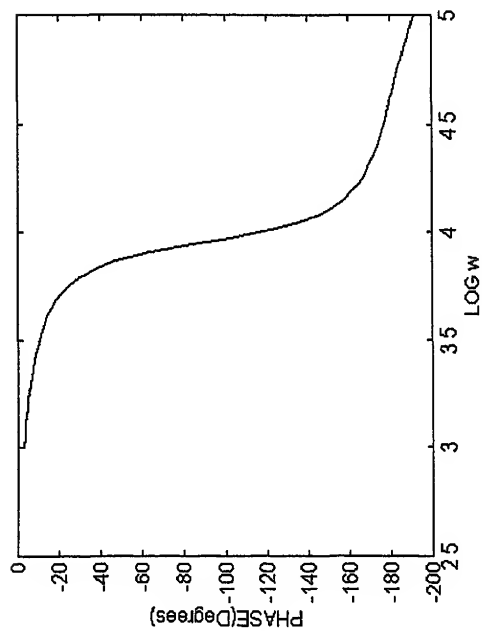


FIG 3.20 (b): For the Operating Point $R = 5$ Ohms & $D = 0.1$

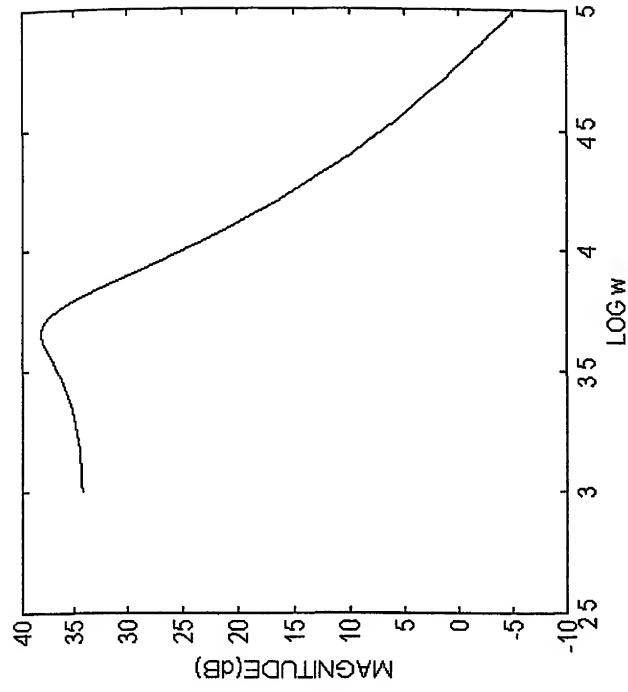


FIG 3.21 (a): For the Operating Point $R = 5$ Ohms & $D = 0.5$

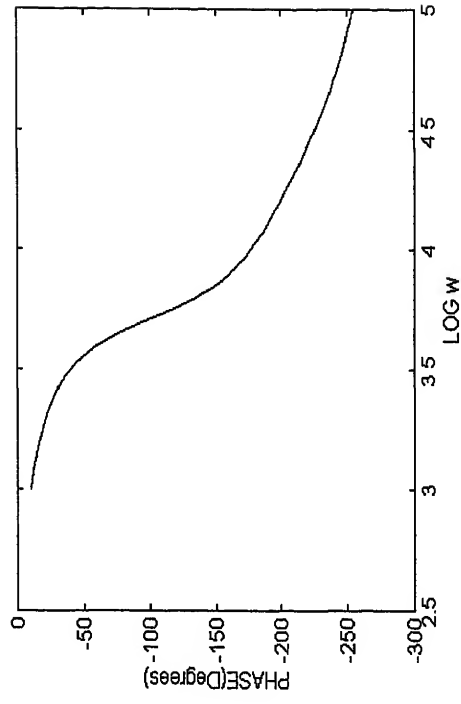


FIG 3.21 (b): For the Operating Point $R = 5$ Ohms & $D = 0.5$

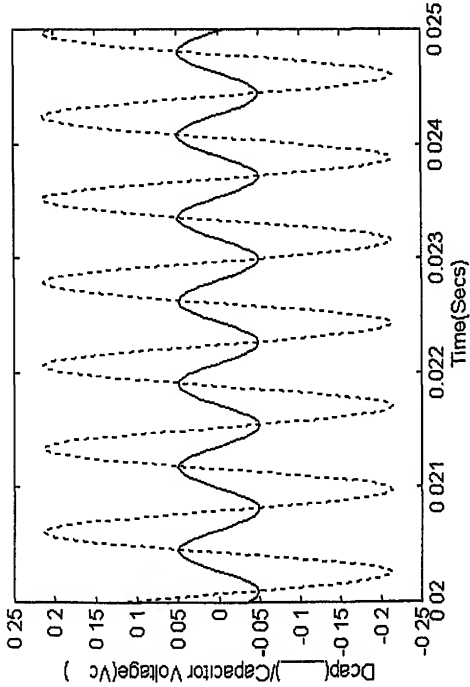


FIG 3.24(a): Verification of Bode plot for the operating point

$R = 5$ & $D = 0.1$ at the corner frequency (1381.0841 Hz)

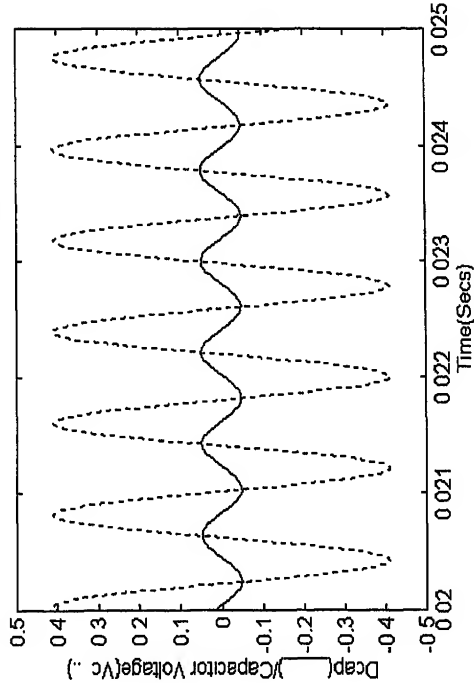


FIG 3.24(c): Verification of Bode plot for the operating point

$R = 30$ & $D = 0.1$ at the corner frequency (1271.8038 Hz)

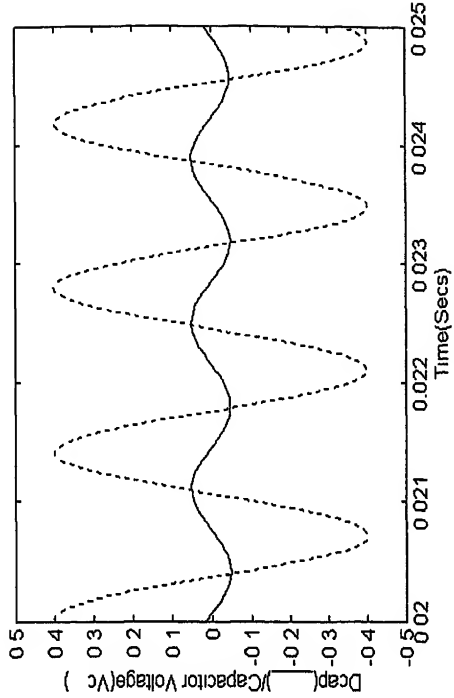


FIG 3.24(b): Verification of Bode plot for the operating point

$R = 5$ & $D = 0.5$ at the corner frequency (722.4705 Hz)

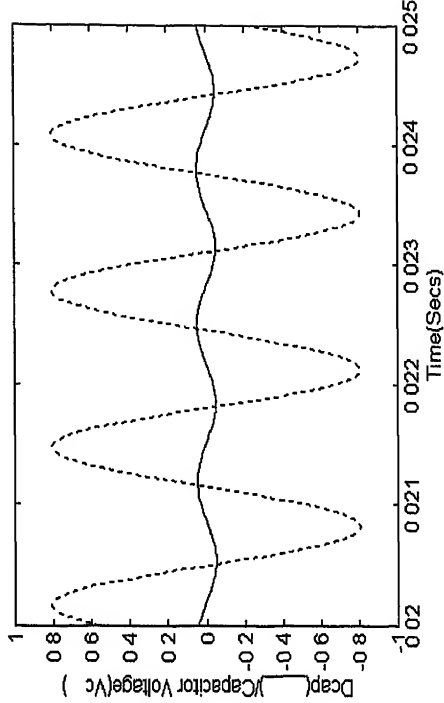


FIG 3.24(d): Verification of Bode plot for the operating point

$R = 30$ & $D = 0.5$ at the corner frequency (766.8671 Hz)

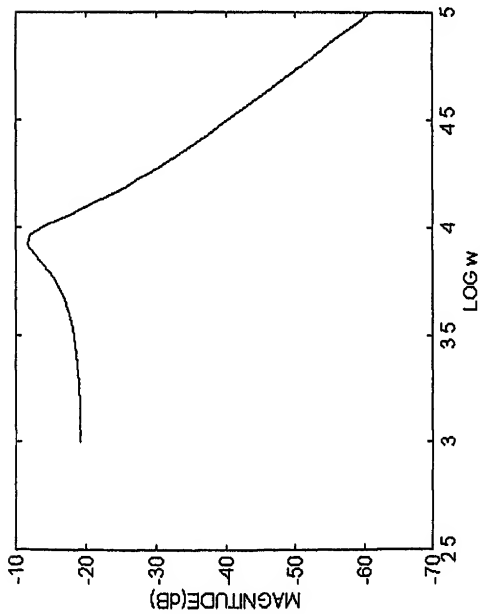


FIG 3.25(a): For the Operating Point R = 5 Ohms & D = 0.1

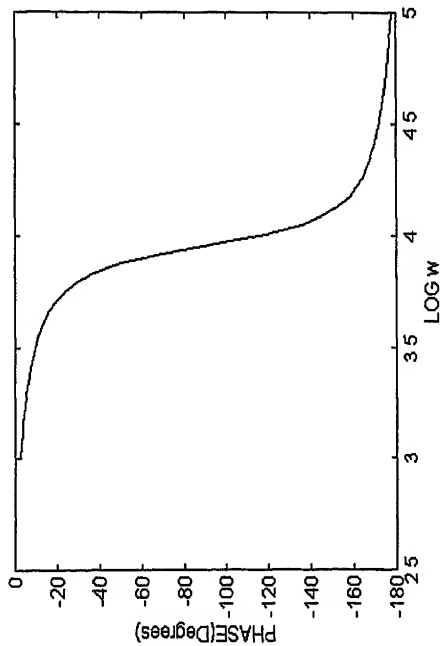


FIG 3.25(b): For the Operating Point R = 5 Ohms & D = 0.1

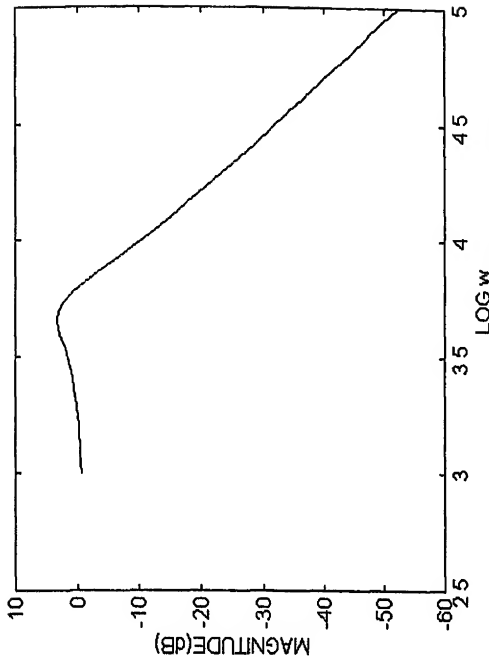


FIG 3.26(a): For the Operating Point R = 5 Ohms & D = 0.5

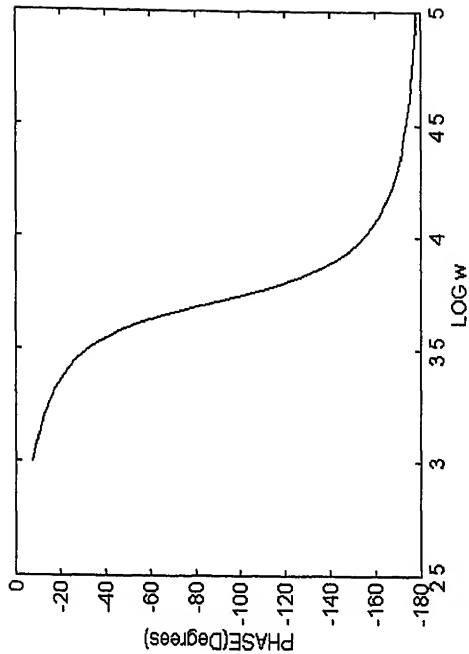


FIG 3.26(b): For the Operating Point R = 5 Ohms & D = 0.5

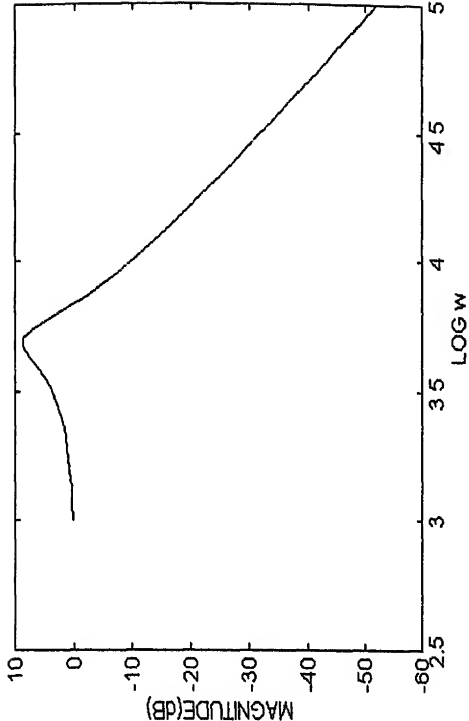


FIG 3.28(a): For the Operating Point R = 30 Ohms & D = 0.5

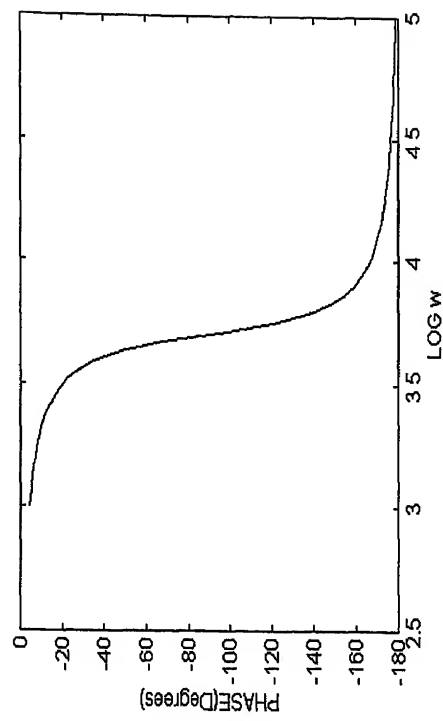


FIG 3.28(b): For the Operating Point R = 30 Ohms & D = 0.5

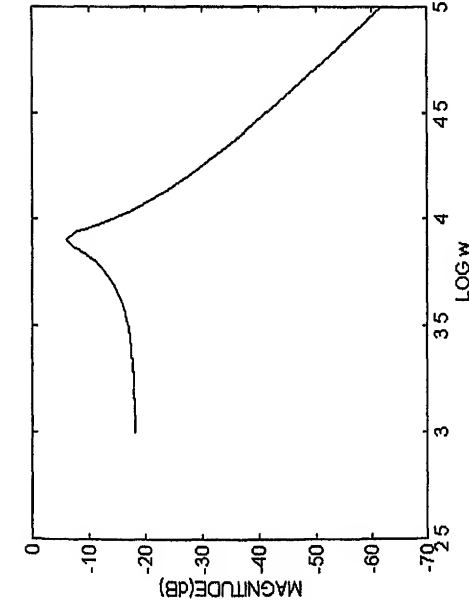


FIG 3.27(a): For the Operating Point R = 30 Ohms & D = 0.1

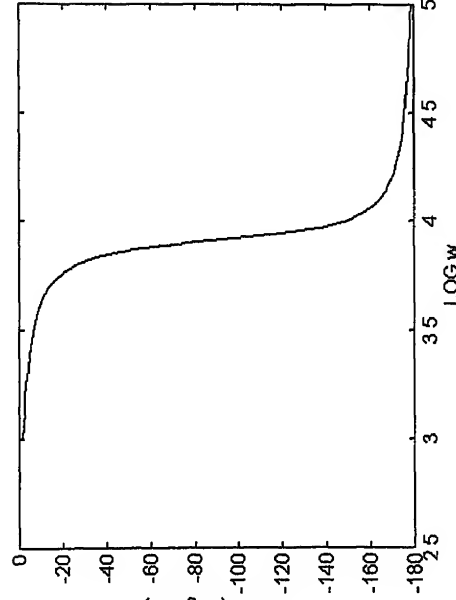


FIG 3.27(b): For the Operating Point R = 30 Ohms & D = 0.1

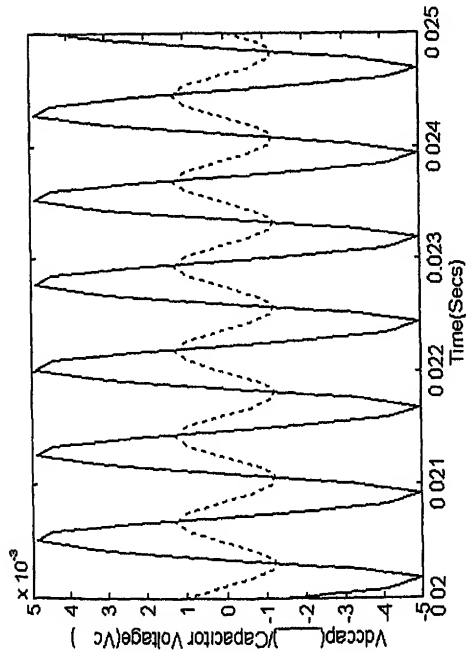


FIG 3.29(a):For the Operating Point defined by $R = 5$ Ohms and $D = 0.1$ at the corner frequency(1327.1503Hz)

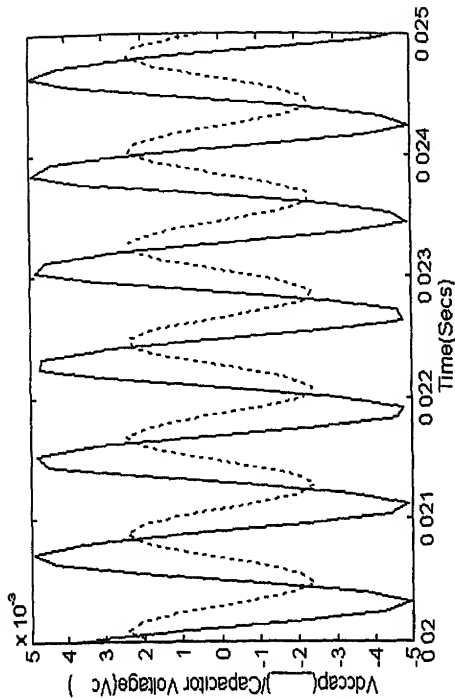


FIG 3.29(c):For the Operating Point defined by $R = 30$ Ohms and $D = 0.1$ at the corner frequency(1327.15 Hz)

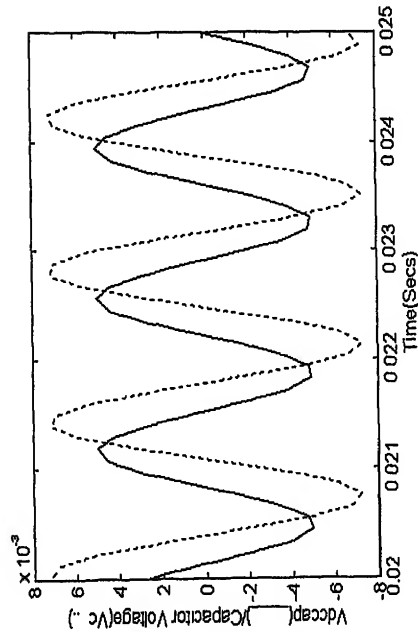


FIG 3.29(b):For the Operating Point defined by $R = 5$ Ohms and $D = 0.5$ at the corner frequency(3220.3114 Hz)

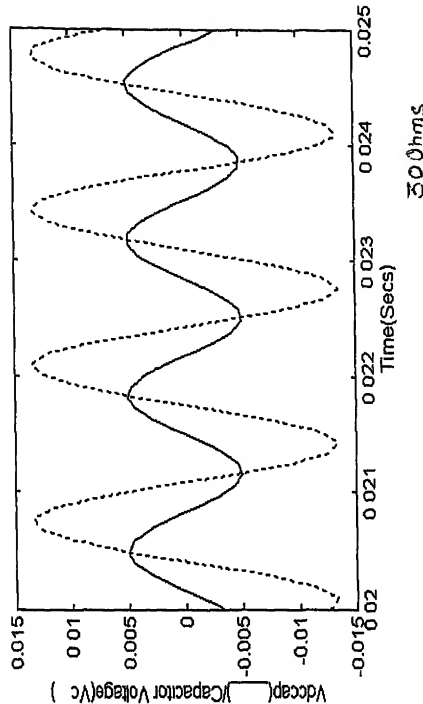


FIG 3.29(d):For the Operating Point defined by $R = 30$ Ohms and $D = 0.5$ at the corner frequency(3220.3 Hz)

FIG 3.29: Verification of BODE PLOTS for $\hat{V}_c(s) / \hat{V}_{dc}(s)$ Transfer function

Operating Point : R = 5 Ohms ; D = 0.1					Operating Point : R = 5 Ohms ; D = 0.5				
Freq	Magnitude Bode (dB)	Magnitude Verification(dB)	Phase Bode (Degrees)	Phase Verification	Freq	Magnitude Bode	Magnitude Verification	Phase Bode	Phase Verification
500 Hz	26.0635	26.0205	-10.17	-10.17	500 Hz	36.4765	36.3908	-39.6745	-40.5
1000 Hz	29.5813	29.5424	-30.8289	-31.32	1000 Hz	34.8122	34.6478	-134.0442	-135
1381.0841Hz	32.6798	32.4649	-80.614	-84.522	722.4705	38.1073	38.0617	-78.2250	-80.6277
5000 Hz	4.1043	3.52	-176.7494	-180	5000 Hz	6.9425	6.0205	-225.0361	-215
10000 Hz	-8.3746	-9.37	-185.0780	-180	10000 Hz	-0.7128	-0.9151	-245.1346	-225

Table 3 : Results of verification of the Small - Signal Model defined by Equation 3.17

Operating Point : R = 30 Ohms ; D = 0.1					Operating Point : R = 30 Ohms ; D = 0.5				
Freq	Magnitude Bode (dB)	Magnitude Verification(dB)	Phase Bode (Degrees)	Phase Verification	Freq	Magnitude Bode	Magnitude Verification	Phase Bode	Phase Verification
500 Hz	-16.8715	-16.9212	-6.5877	-6.84	500 Hz	3.6026	3.5218	-20.5442	-19.98
1000 Hz	-11.2365	-11.0568	-25.9597	-25.2	1000 Hz	2.7287	2.5421	-140.3692	-141.12
1268 Hz	-6.2190	-6.3751	-81.1526	-79.5645	744.08	8.6204	8.2995	-67.9316	-69.9316
5000 Hz	-41.1428	-41.9382	-175.9831	-180	5000 Hz	-31.7412	-32.04	-176.5698	-180
10000 Hz	-53.6243	-53.979	-178.0938	-180	10000 Hz	-43.9441	-44.1522	-178.3181	-180

Table 4 : Results of verification of the Small - Signal Model defined by Equation 3.19

CHAPTER IV

CLOSE LOOP CONTROL

The output voltage of DC power supplies are regulated within specified tolerance band, also the transient and steady state response of the converter must satisfy some desired specifications. Section 4.1 describes how the system pole locations determine the nature of transient and steady state response and how the system can be classified on the basis of pole location. Section 4.2 discusses how pole-placement technique can be used to design a servo system. Results obtained from sections 4.1 and 4.2 are used in section 4.3 to 4.5 to construct a servo controller for the buck-boost converter and simulate the response.

4.1 TRANSIENT RESPONSE OF A SECOND-ORDER SYSTEM :

Eigenvalues of matrix A_0 (where A_0 is defined by equation 3.2 or 3.4) are identical to the open-loop poles of the transfer function $G(s)$. (refer to Appendix C-1). Figure 4.1 illustrates the relationship between the location of the poles S_1, S_2 , damping ratio (Z), damping factor (σ), undamped natural frequency (ω_n) and damped frequency (ω_d).

$$S_1 = -\sigma + j\omega_d$$

$$S_2 = -\sigma - j\omega_d$$

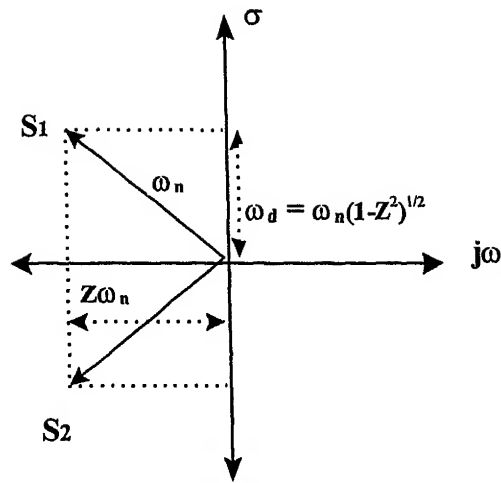


FIG 4.1: Relationship Between $S_1, S_2, \omega_n, \omega_d, Z, \sigma$

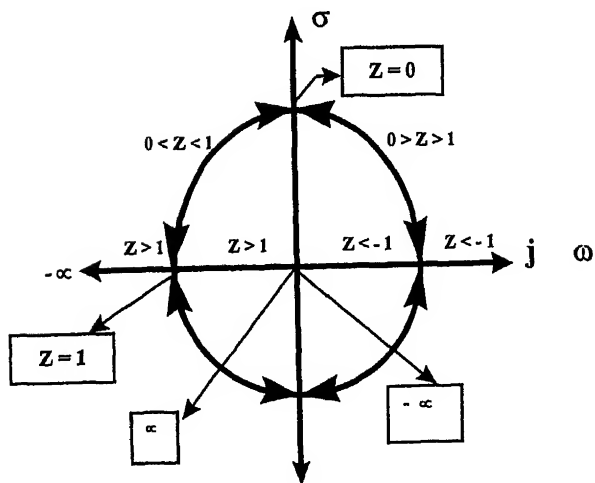


FIG 4.2: Classification of System Dynamics w.r.t Z

When the damping factor σ is positive the unit step response will settle to its constant final value. Negative damping results in a response that grows without bound with time and system is unstable. Zero damping results in a sustained sinusoidal oscillation and the system is marginally stable or unstable.

Figure 4.2 illustrates the effect of varying the damping ratio Z from $-\infty$ to ∞ on the eigenvalue location of the second order system, vice-versa the effect of eigenvalues on the damping of the second-order system.

Classification of system dynamics with respect to the value of Z is made in Table 5

Value of Z	System Classification
$0 < Z < 1$	Underdamped
$Z = 1$	Critically damped
$Z > 1$	Overdamped
$Z = 0$	Undamped
$Z < 0$	Negatively damped

Table 5 : Classification of system dynamics with respect to the value of Z

Step response of the system becomes oscillatory as Z is decreased, and if $Z \geq 1$ the step response does not exhibit any overshoot and never exceeds its final value during the transient. Maximum overshoot of the step response of second-order system is a function of damping ratio Z only, while the settling time is a function of ω_d i.e both Z and ω_n .

4.1.1 : POLE PLACEMENT

Consider a system defined by equation 4.1

$$\dot{X} = A_0 X + B_0 u \quad (4.1)$$

Where,

X = State Vector (n-vector)

u = Control signal (scalar)

A = $n \times n$ (Constant matrix)

B = $n \times 1$ (Constant matrix)

Regulator systems are feedback control systems that will bring non-zero states caused by external disturbances to the origin with sufficient speed. One approach to design regulator systems is to construct an asymptotically stable closed-loop system by specifying the desired locations for the closed loop poles. This can be accomplished by use of state feed back such that the control vector $u = -Kx$ where u is unconstrained, and x is instantaneous state.

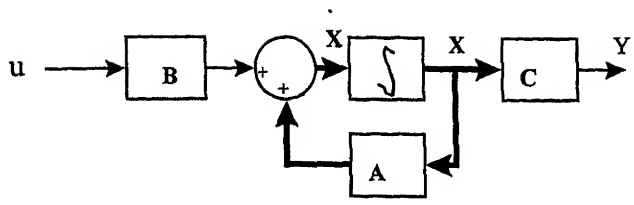


FIG4.3(a): State - Space Representation of Openloop System

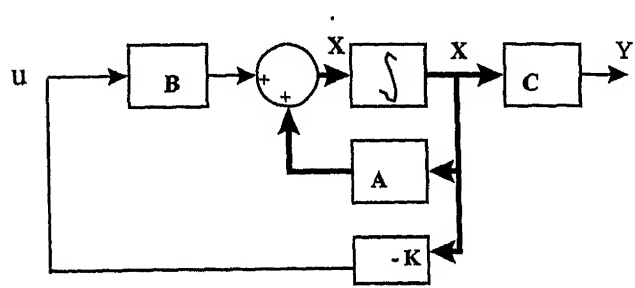


FIG4.3(b): State - Space Representation of Closeloop Regulator

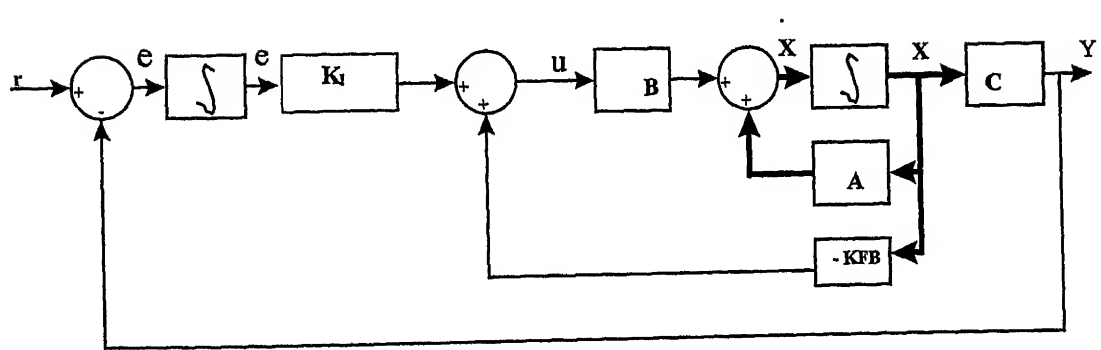


FIG4.4: State - Space Representation of Type1 Servo System
for a Type 0 Plant

Figure 4.3(a) and 4.3(b) show the open loop system and the system with state feed back respectively.

The feed back gain matrix K is so decided that the system will have a desired characteristic equation. This design scheme is referred to as pole placement. Substituting $u = -Kx$ in equation 4.1 results in

$$\dot{X}(t) = (A - BK) X(t) \quad (4.2)$$

and solution of equation 4.2 is given by

$$X(t) = e^{(A-BK)t} X(0) \quad (4.3)$$

Where $X(0)$ = initial state caused by external disturbance. If matrix K is properly chosen then matrix $(A-BK)$ can be made asymptotically stable and for all $X(0) \neq 0$, $X(t)$ approaches 0 as t approaches infinity.

4.2 DESIGN OF SERVO SYSTEMS : [When the plant has no Integrator]

Servo system is a stable regulator system that will bring the error to zero given any initial error, between the reference and the output. The basic principle of design of type 1

servo system for a type 0 plant is to insert an integrator in the feed forward path between the error comparator and the plant as shown in Fig. 4.4.

From Figure 4.4

$$X = AX + Bu \quad (4.4)$$

$$Y = CX \quad (4.5)$$

$$u = -(KFB)X + K_e e \quad (4.6)$$

$$e = r - y = r - CX \quad (4.7)$$

Where,

$$y = \text{Output signal (scalar)}$$

$$e = \text{Output of Integrator (scalar)}$$

$$r = \text{reference input signal (scalar, step function)}$$

$$C = 1 \times n \text{ (Constant matrix)}$$

It is assumed that the transfer function of the plant has no zero at the origin that has a possibility of canceling the integrator being inserted.

If r is applied at $t=0$ then for $t>0$ system dynamics can be explained by

$$\begin{bmatrix} X(t) \\ e(t) \end{bmatrix} = \begin{bmatrix} A & 0 \\ -C & 0 \end{bmatrix} \begin{bmatrix} X(t) \\ e(t) \end{bmatrix} + \begin{bmatrix} B \\ 0 \end{bmatrix} u(t) + \begin{bmatrix} 0 \\ 1 \end{bmatrix} r(t) \quad (4.8)$$

$$\begin{bmatrix} X(\infty) \\ e(\infty) \end{bmatrix} = \begin{bmatrix} A & 0 \\ -C & 0 \end{bmatrix} \begin{bmatrix} X(\infty) \\ Z(\infty) \end{bmatrix} + \begin{bmatrix} B \\ 0 \end{bmatrix} u(\infty) + \begin{bmatrix} 0 \\ 1 \end{bmatrix} r(\infty) \quad (4.9)$$

Since r is a step input

$$r(\infty) = r(t) = r \quad \text{for } t > 0$$

Therefore

$$\begin{bmatrix} X(t) - X(\infty) \\ e(t) - e(\infty) \end{bmatrix} = \begin{bmatrix} A & 0 \\ -C & 0 \end{bmatrix} \begin{bmatrix} X(t) - X(\infty) \\ e(t) - e(\infty) \end{bmatrix} + \begin{bmatrix} B \\ 0 \end{bmatrix} [u(t) - u(\infty)] \quad (4.10)$$

Define

$$X(t) - X(\infty) = X_v(t)$$

$$e(t) - e(\infty) = e_v(t)$$

$$u(t) - u(\infty) = u_v(t)$$

Where X_v , e_v , u_v are extended vectors

Then equation 4.10 can be written as

$$\begin{bmatrix} X_v(t) \\ e_v(t) \end{bmatrix} = \begin{bmatrix} A & 0 \\ -C & 0 \end{bmatrix} \begin{bmatrix} X_v(t) \\ e_v(t) \end{bmatrix} + \begin{bmatrix} B \\ 0 \end{bmatrix} u_v(t) \quad (4.11)$$

Where

$$u_v(t) = -KX_v(t) + K_I e_v(t) \quad (4.12)$$

A new $(n+1)^{\text{th}}$ order vector $V(t)$ can be defined as

$$V(t) = \begin{bmatrix} X_v(t) \\ e_v(t) \end{bmatrix}$$

Then equation 4.11 can be expressed as

$$\dot{V} = \hat{A} V + \hat{B} u_v \quad (4.13)$$

Where

$$\hat{A} = \begin{bmatrix} A & 0 \\ -C & 0 \end{bmatrix}$$

$$\hat{B} = \begin{bmatrix} B \\ 0 \end{bmatrix}$$

$$\hat{K} = [-KFB - K_I]$$

$$u_v = \hat{K}V$$

The type 1 servo system results in a stable $(n+1)^{\text{th}}$ order regulator system that will bring the new error vector $V(t)$ to zero given any initial condition $V(0)$.

If the system defined by equation 4.13 is completely state controllable then by specifying the desired characteristic equation for the system matrix \hat{K} can be determined by pole placement (Refer Appendix C).

4.3 OPEN LOOP DAMPING RATIO AND UNDAMPED NATURAL FREQUENCY

Figures 4.5(a) and 4.5(b) show open loop system damping and undamped natural frequency.

It is observed that

- (a) If the load resistance R is kept constant and duty ratio D is increased the system damping ratio increases and the undamped natural frequency reduces. For values of $R > 20\Omega$ (i.e. the value of R after which both continuous and discontinuous operation is possible) the undamped natural frequency remains constant for values of D for which the converter operates in discontinuous zone for given R , after which W_n reduces as duty ratio increases. Therefore in open loop as D increases for given value of R system responses i.e. peak overshoot and settling time reduce inherently in open loop.

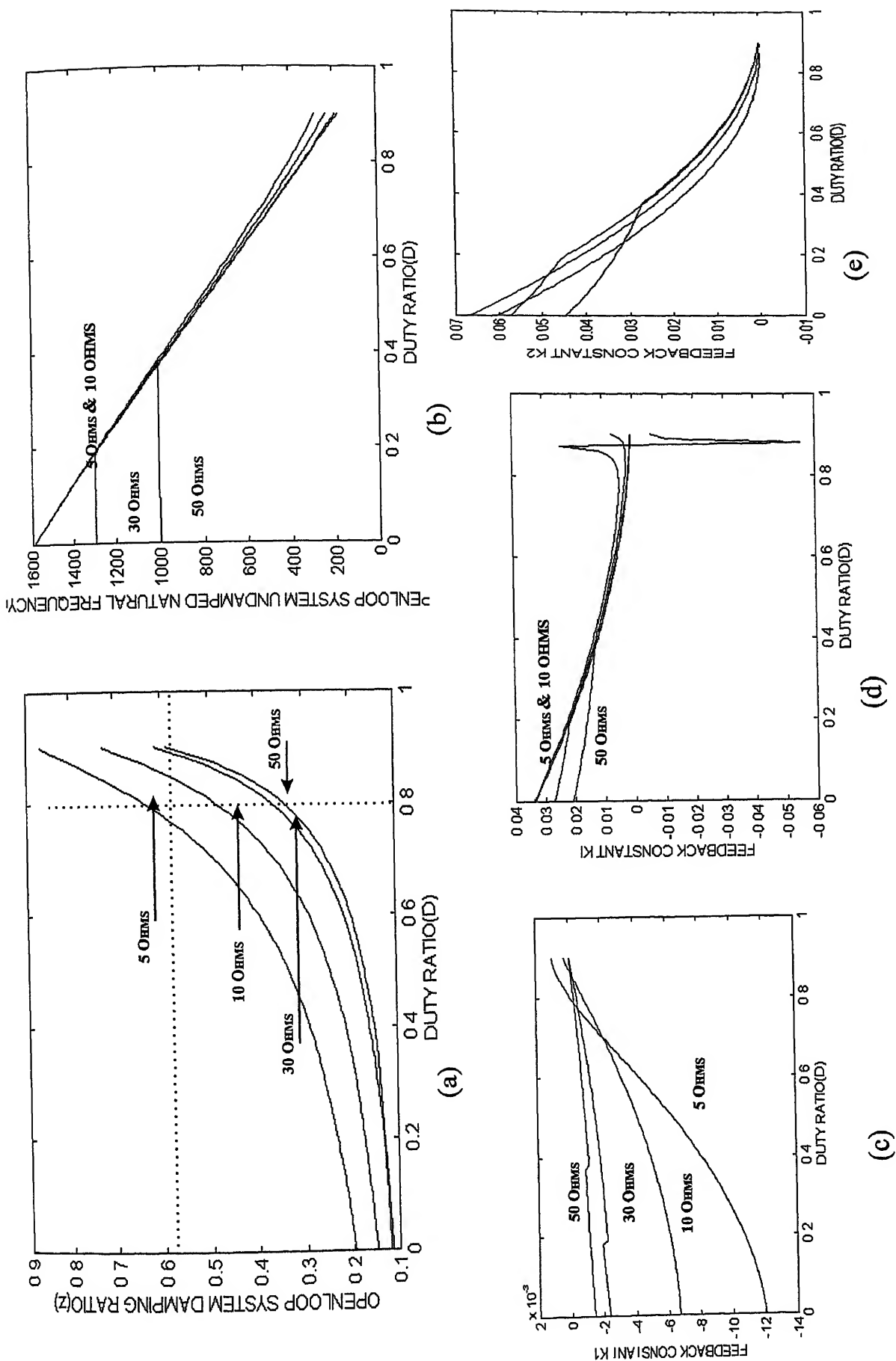


FIG 4.5 : Variation of (a) ζ (b) ω_n w.r.t Duty Ratio D (c) K_1 (d) K_1 (e) K_2 w.r.t Duty Ratio D for $Z' = 0.65$

(b) As duty ratio D is kept constant and the load resistance R is increased then for low values of duty ratio D the drop in system damping is not significant, but at higher values of D as R is increased the damping ratio decreases significantly. The undamped natural frequency in the continuous operation zone does not change as the load resistance R is increased. However if the load resistance increases to a value such that the converter operates in discontinuous zone then the undamped natural frequency reduces significantly as the load resistance R increases.

It can be concluded that for a given duty ratio D as the load resistance increases the system responses (peak overshoot and settling time) increase if the converter operating point remains in continuous zone only, and may remain same or reduce significantly if the operating point transits into discontinuous operating zone. At low values of load resistance and higher values of duty ratio the system is inherently sufficiently damped and system responses are acceptable, but at low values of load resistance and low values of duty ratio the system is not sufficiently damped inherently.

4.4 CLOSE-LOOP CONTROL OF THE CONVERTER

In section 4.2 it was discussed, how state feed back can be used to construct a stable close-loop system for a plant represented by a linear time invariant equation 4.4, when the plant is of type 0 using pole-placement. The transfer function $\hat{V}_c(s)/\hat{d}(s)$ in section 3.4.1

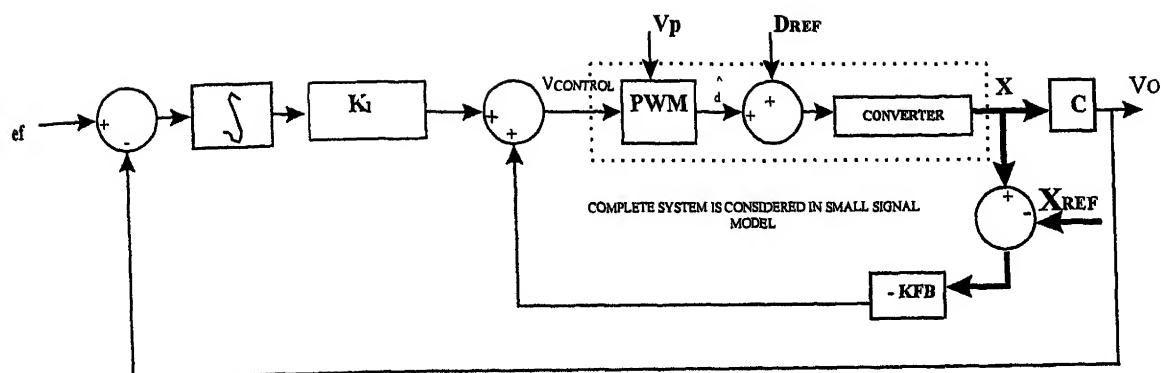


FIG 4.6 : Structure of the servo controller (using pole placement) for the converter

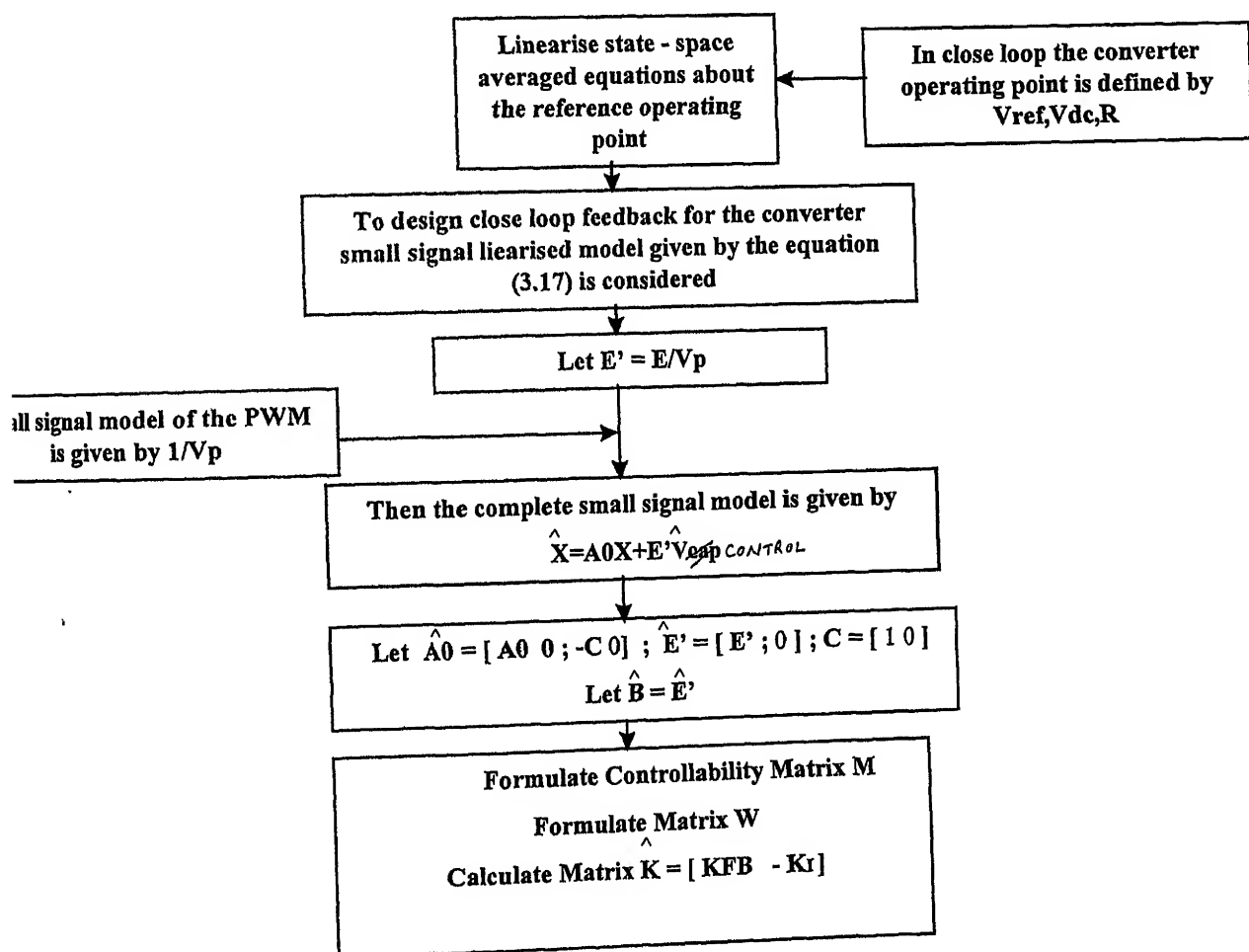


FIG 4.7 : Algorithm to calculate the feedback matrix K_{FB} & K_I of the servo controller (using pole placement) for the converter

shows that power stage of the converter is of type 0. The purpose of employing pole-placement technique to design a close-loop system is

- (a) To locate all poles of the open-loop system such that the close loop system is stable.
- (b) To locate poles of the close-loop system such that the close-loop system responses (i.e. peak overshoot, delay time, rise time and settling time) are within specified limits.

Flow graph given in Figure 4.7 shows how the state feedback pole-placement technique can be employed to construct a close loop servo system for the buck-boost converter.

To calculate \hat{K} matrix, coefficients of the desired characteristic equation need to be known. To know these coefficients, eigenvalues of new characteristic equation $|sI - (\hat{A} - \hat{B}\hat{K})|$ need to be known. Working backwards the eigenvalues of $(\hat{A} - \hat{B}\hat{K})$ (i.e. new pole locations) are specified then the corresponding coefficients of the new characteristic equation are determined and \hat{K} matrix is calculated. Since the Open loop poles of the converter are already located in the left half of the s-plane, by employing pole-placement we can modify the system response by relocating the poles, also since an integrator has been inserted, thus for the new $(n+1)^{th}$ order regulator system three eigenvalues of the new characteristic equation need to be specified.

$$(a) \quad S_1 = \text{Integrator pole location}$$

$$(b) \quad S_2 = -\sigma + j\omega_d$$

$$(c) \quad S_3 = -\sigma - j\omega_d$$

Where

$$\sigma = Z' \omega_n$$

$$\omega_n = (\sqrt{1 - Z'^2}) \omega_n$$

$$Z' = \text{Desired damping ratio of closed loop system}$$

$$\omega_n = \text{undamped natural frequency of open loop system}$$

4.5 SIMULATION OF CONVERTER WITH CLOSED-LOOP CONTROL

4.5

Fig. 4.5 shows the structure of the controller and its implementation. Fig. 3.4(a)

shows average output voltage V_0 versus duty ratio D for different values of the load resistance R . It is observed that in the range $D=0.1$ to $D=0.8$ for given D the output voltage for different values of R does not vary significantly and increases linearly with D . Therefore to operate the converter in the linear range of V_0 - D curve such that changes in load resistance R do not effect the output voltage severely V_{REF} is restricted in the range 2.5V to 35V, and load resistance R is restricted in the range 5Ω to 50Ω .

Figs. 4.5(c) (d) and (e) show how, for the complete range of V_{REF} and R the values of K_1 , K_2 and K_I vary for different operating points, if desired damping ratio is chosen to be 0.65.

4.5.1 CLOSE-LOOP RESPONSE FOR STEP CHANGE IN LOAD RESISTANCE R AND V_{REF}

Figure 4.6(a) and 4.6(b) illustrate the fact that for all values of load resistances and high values of duty ratio D the system is sufficiently damped inherently. Also it is seen that if Z' the desired value of damping ratio is made 0.65 for all operating points it sufficiently damps the system response as seen for cases in Table 6, from Figs. 4.8 to 4.11.

Sl. No.	Initial Condition		Final condition	
	R	V_{REF}	R	V_{REF}
1.	30Ω	5V	50Ω	5V
2.	10Ω	3V	40Ω	3V
3.	50Ω	5V	50Ω	10V
4.	5Ω	15V	5Ω	10V

Table 6

One option is to calculate \hat{K} (or K_{FB} and K_I)corresponding to the final operating point, other is to update the value of \hat{K} according to the value of D_p this can be referred to as cycle by cycle control, another option is to put $\hat{K}=[1 \ 1 \ 1]$ which corresponds to the case $Z'>1$ or use $\hat{K}_{average}$ where $\hat{K}_{average}$ corresponds to a feedback matrix whose elements are average

values of K_1 , K_2 , K_I as calculated for different operating points in the range $D=0$ to 1 and $R=5\Omega$ to 50Ω .

Fig. 4.12 shows the comparative results of using the different options

Fig. 4.13 illustrates, how the value of KFB as calculated by the method given in Fig. 4.6 using $Z'=0.65$ when used in a stand alone regulator as shown in Fig. 4.3(b) brings the output voltage and inductor current to reference values after they have been perturbed by an external disturbance. The operating point considered is $R=30\Omega$ and $V_{REF}=5V$.

Fig.4.14 illustrates the regulator response for the above case when $\hat{K}=[1 \ 1]$ and $\hat{K}_{average}$.

4.5.2 CLOSE-LOOP RESPONSE FOR SINUSOIDAL VARIATION IN V_{REF}

Fig. 4.14 shows the response for sinusoidal variation of V_{ref} around the operating point defined by $V_{REF}=5V$ and $R=30\Omega$.

4.5.3 CLOSED-LOOP RESPONSE FOR SINUSOIDAL VARIATION IN V_{DC} :

Fig. 4.15 shows the response for sinusoidal variation of input voltage V_{dc} around the operating point defined by $V_{ref}=5V$ and $R=30\Omega$.

4.5.4 CLOSED-LOOP RESPONSE FOR SINUSOIDAL VARIATION IN LOAD R :

4.16

Fig. 4.16 shows the response for sinusoidal variation in load resistance R of V_{ref} around the operating point defined by $V_{REF}=5V$ and $R=30\Omega$.

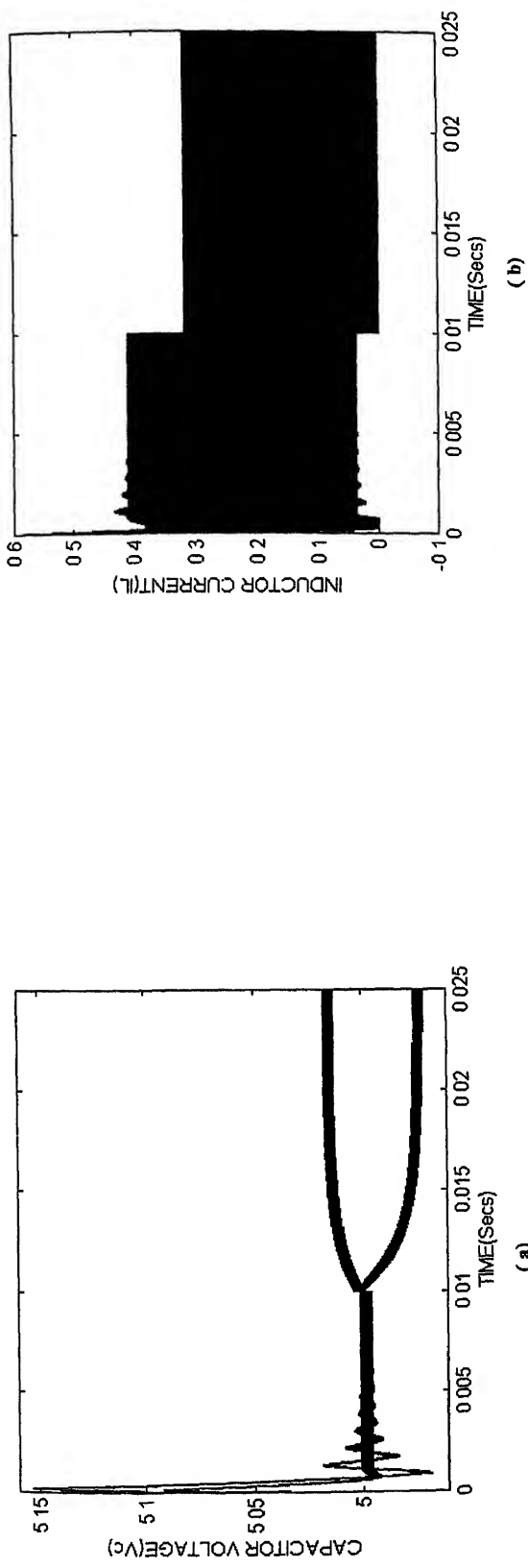


FIG 4.8: System Response to change in R from 30 to 50 Ohms for Vref = 5 volts

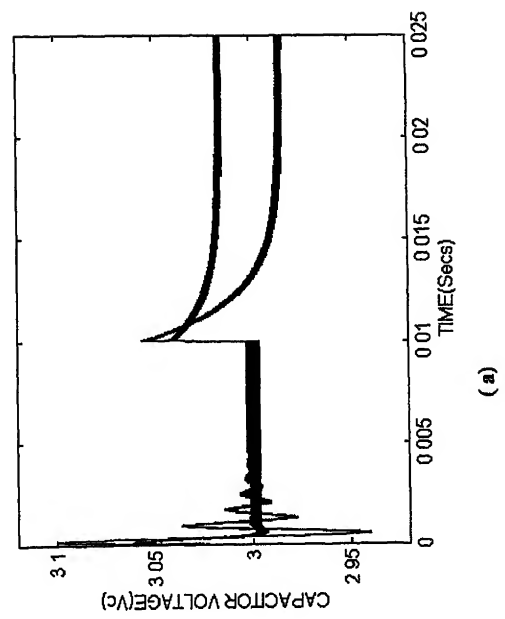
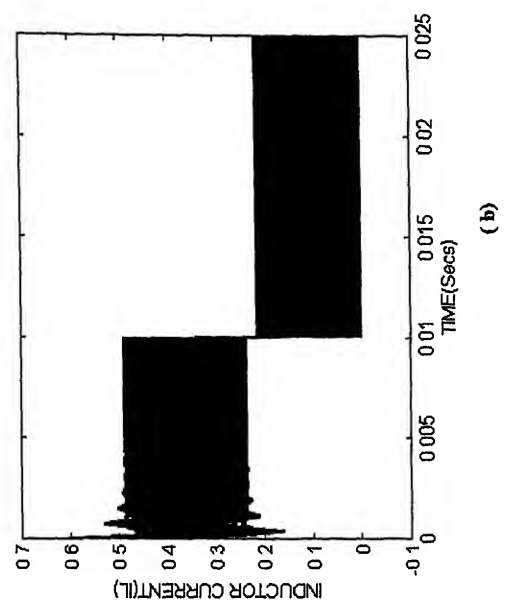


FIG 4.9: System Response to change in R from 10 to 40 Ohms for Vref = 3 volts

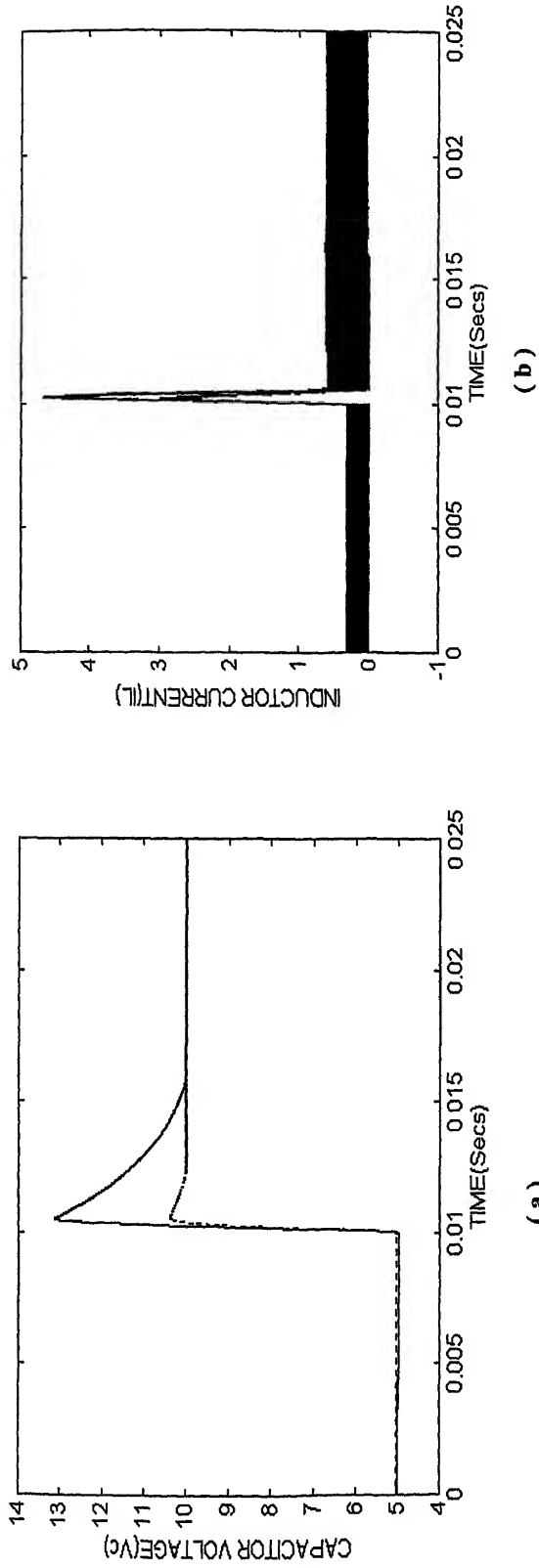


FIG 4.10 : System Response to change in V_{ref} from 5 to 10 volts for $R = 50 \text{ Ohms}$

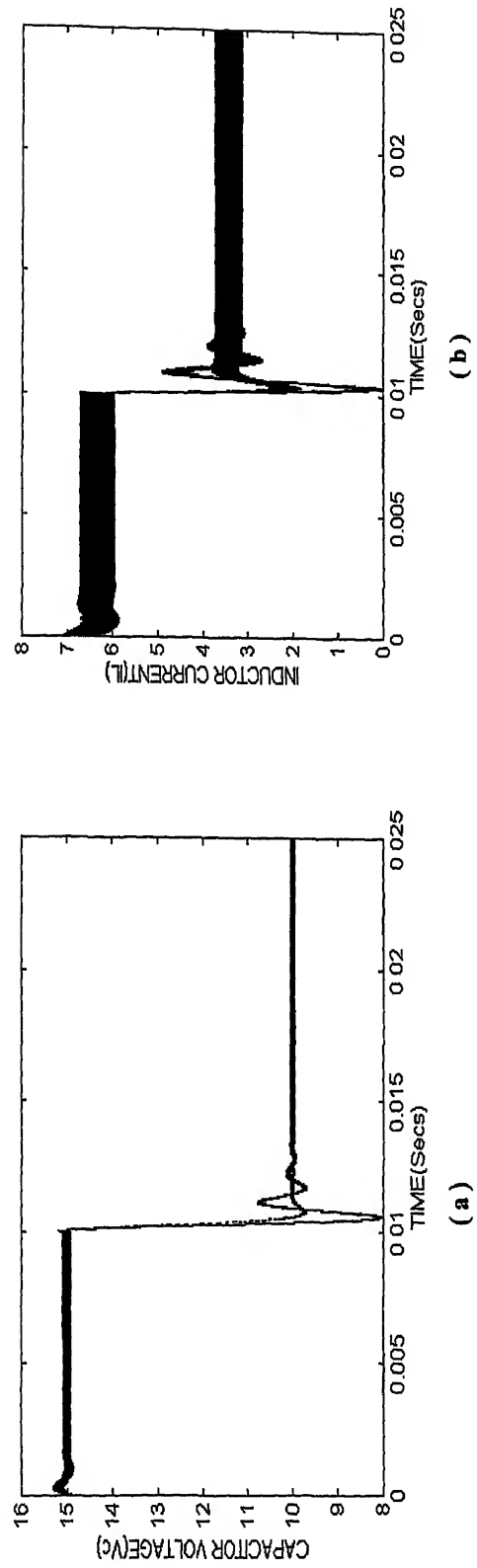


FIG 4.11 : System Response to change in V_{ref} from 15 to 10 volts for $R = 5 \text{ Ohms}$

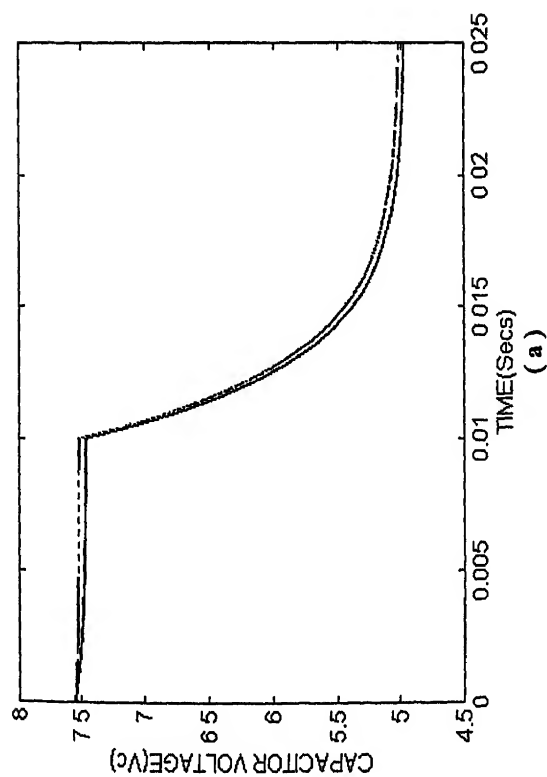


FIG 4.12 : System Response to change in V_{ref} from 7.5 to 5 volts for $R = 50$ Ohms;using KFB & K_I at final operating point

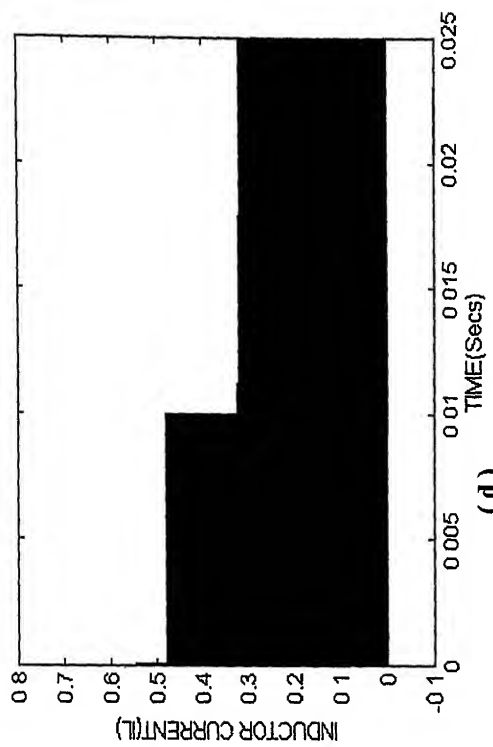
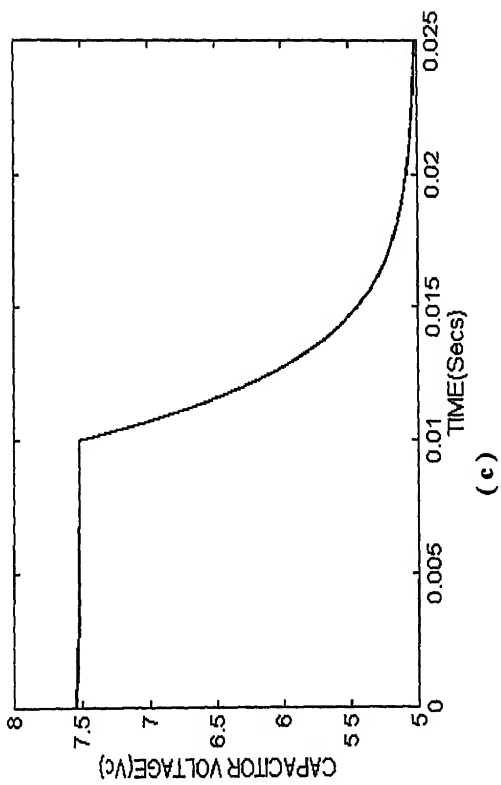
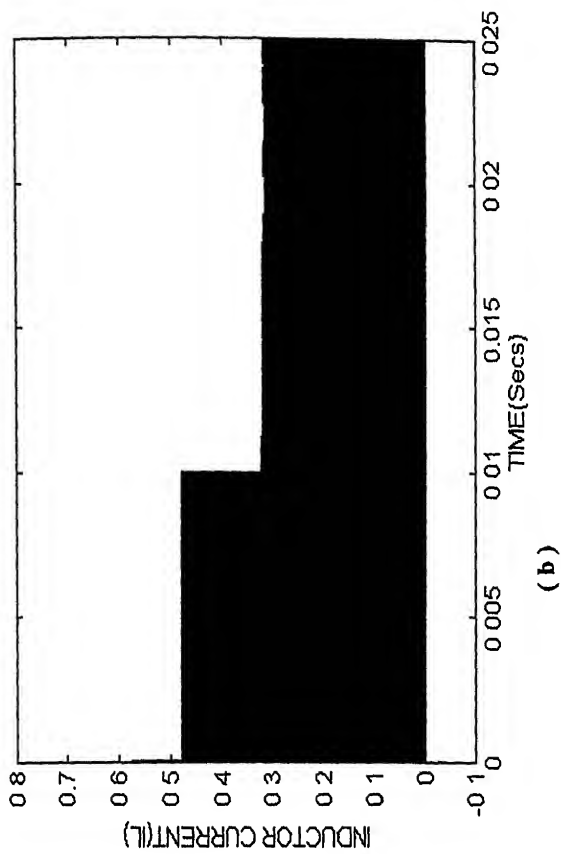


FIG 4.12 : System Response to change in V_{ref} from 7.5 to 5 volts for $R = 50$ Ohms;using CYCLE BY CYCLE CONTROL

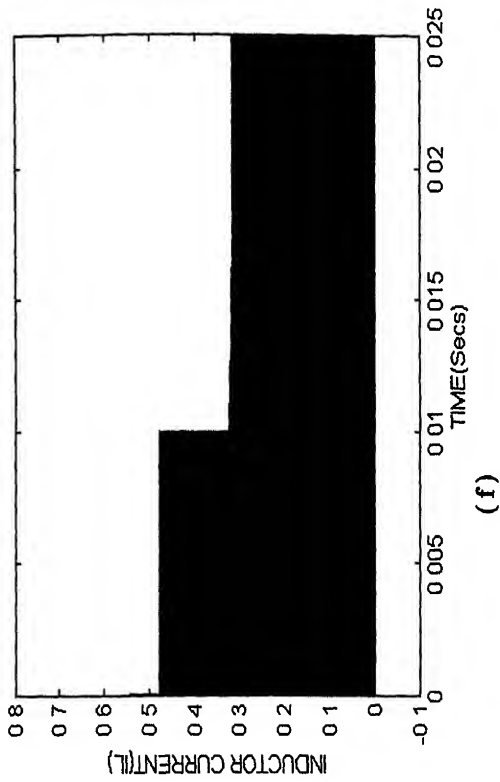
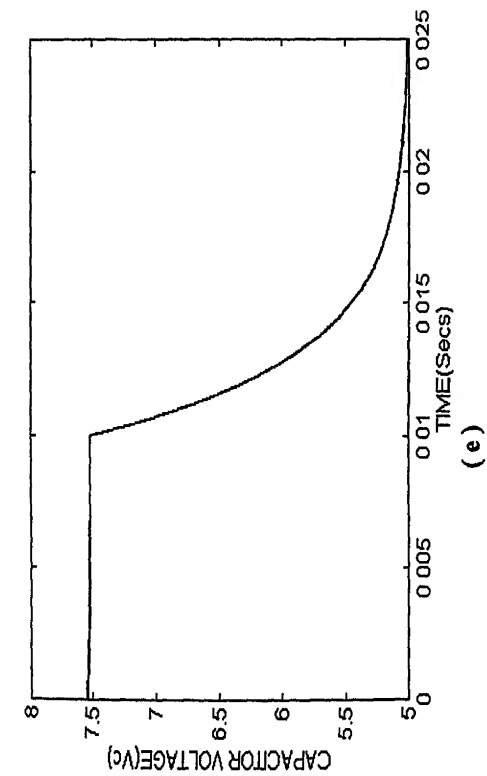


FIG 4.12 : System Response to change in V_{ref} from 7.5 to 5 volts for $R = 50$ Ohms;using average values of KFB & K_I

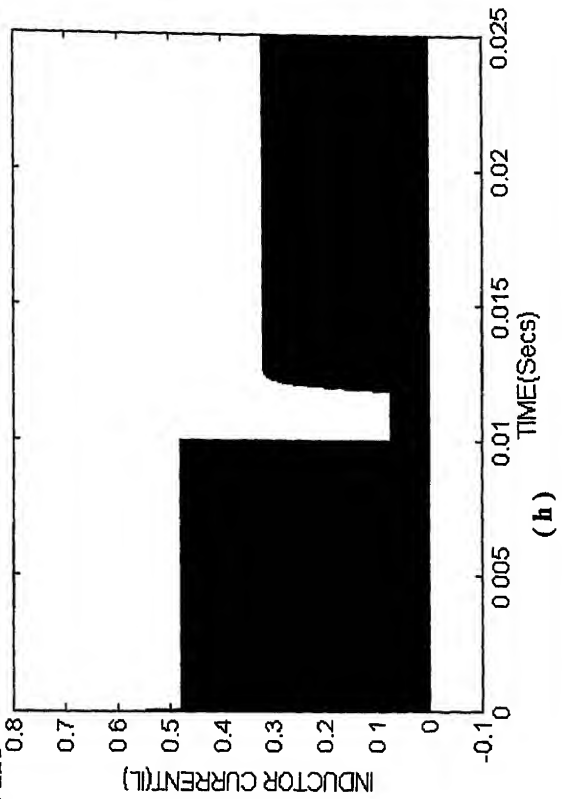
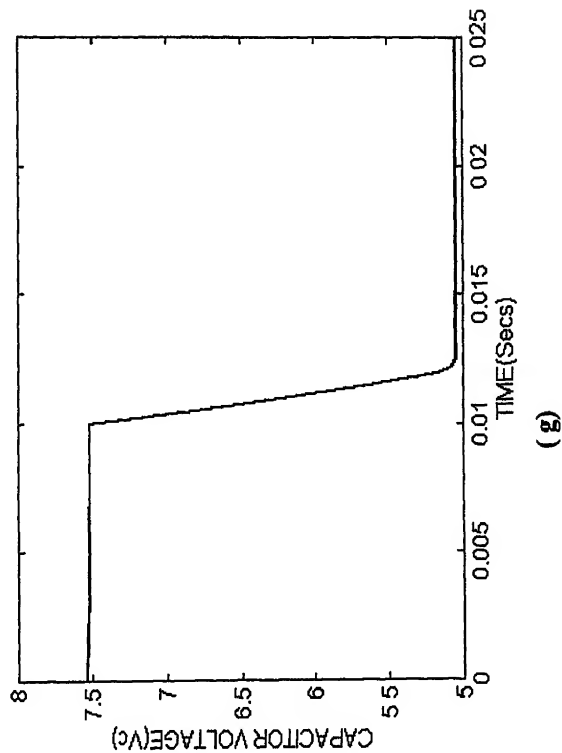


FIG 4.12 : System Response to change in V_{ref} from 7.5 to 5 volts for $R = 50$ Ohms;using KFB = [1 1] & $K_I = 1$

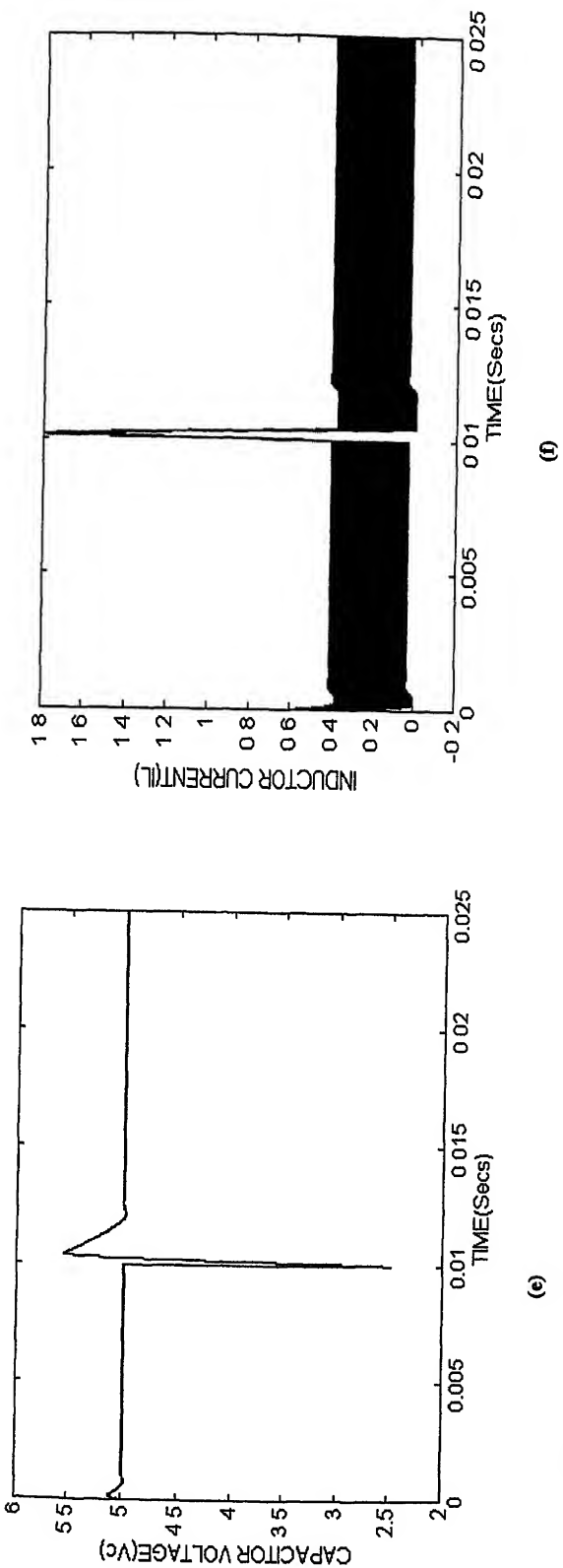


FIG 4.13: Regulator Response for -2.5V perturbation in Capacitor voltage,using average values of K_{FB} & K_I

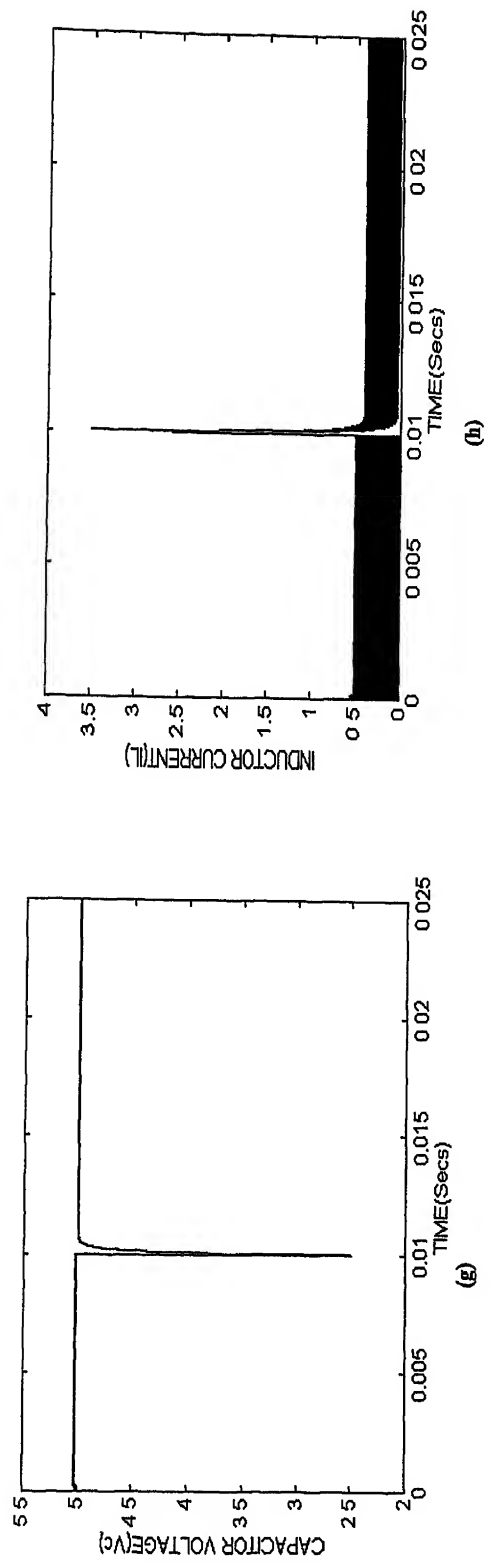


FIG 4.13: Regulator Response for -2.5V perturbation in Capacitor voltage,using $K_{FB} = [1\ 1]$ & $K_I = 1$

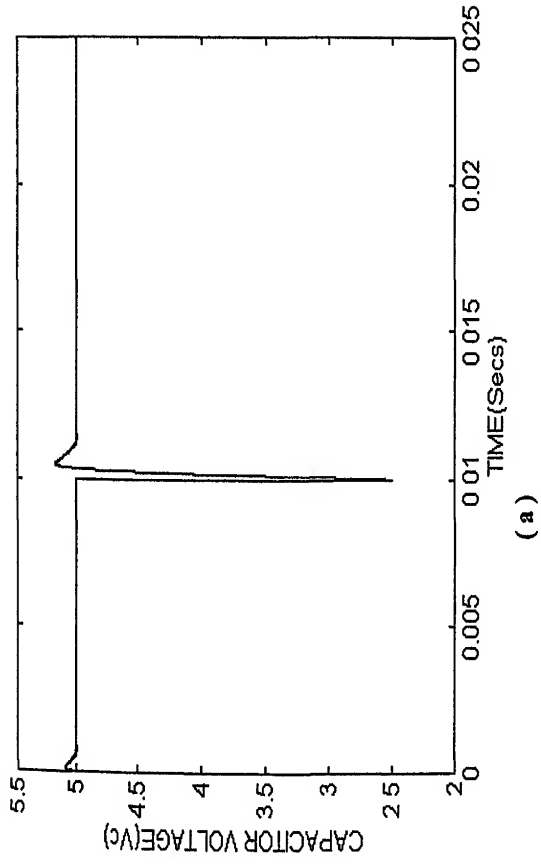


FIG 4.13 : Regulator Response to -2.5v perturbation in capacitor voltage at the operating point defined by
 $V_{ref} = 5$ volts & $R = 50$ Ohms; using KFB & K_I at operating point

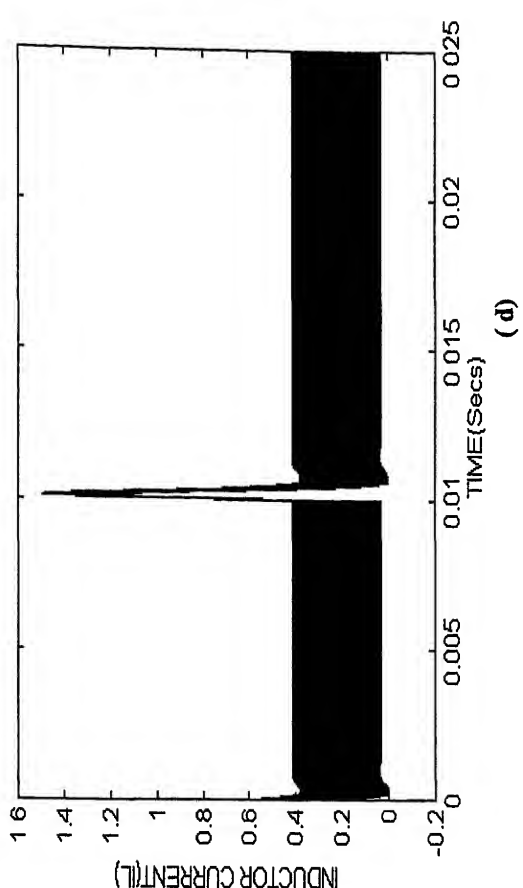
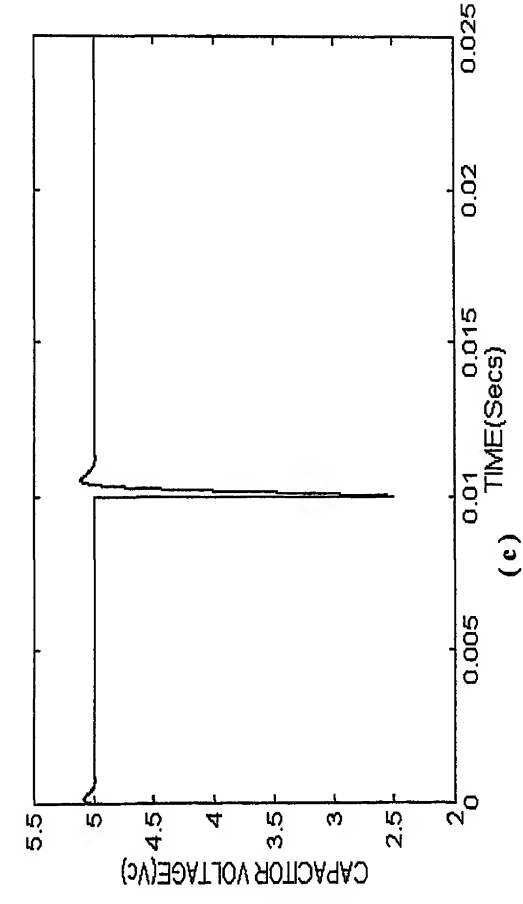
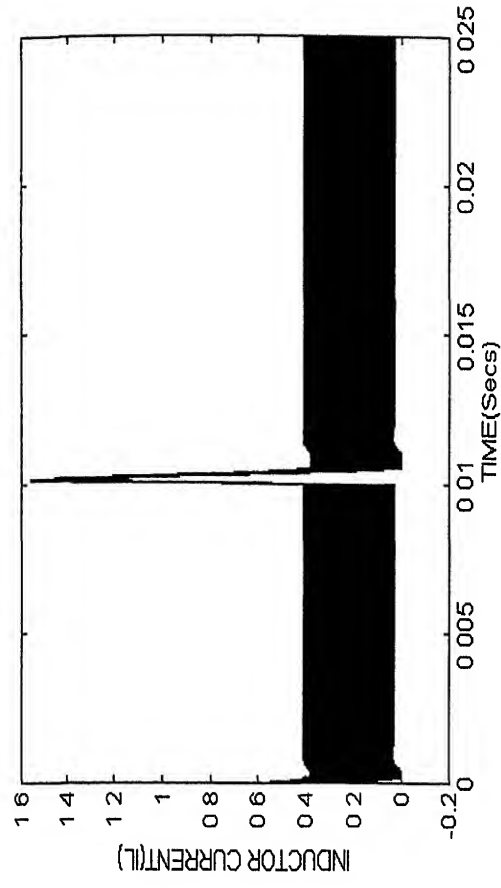
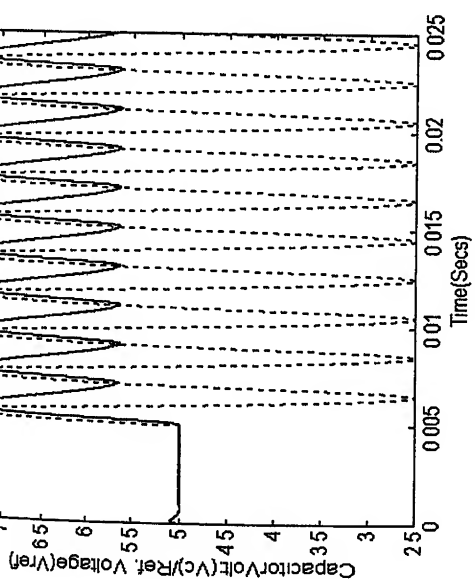
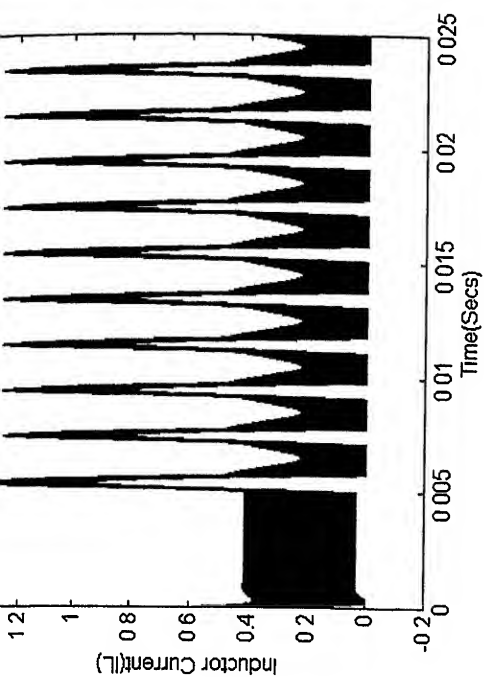


FIG 4.13 : Regulator Response to -2.5v perturbation in capacitor voltage at the operating point defined by

$V_{ref} = 5$ volts & $R = 50$ Ohms; using CYCLE BY CYCLE CONTROL

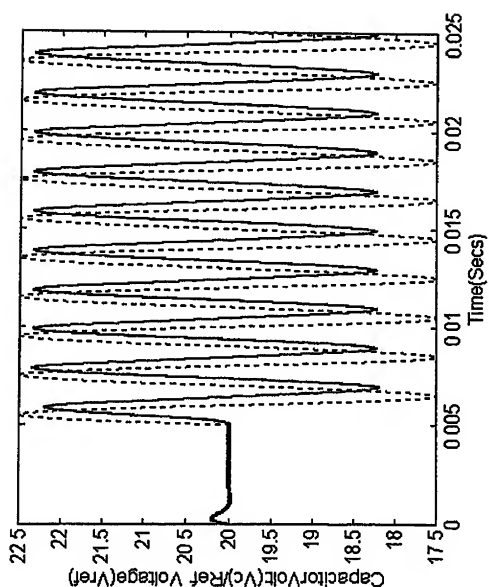


(a)

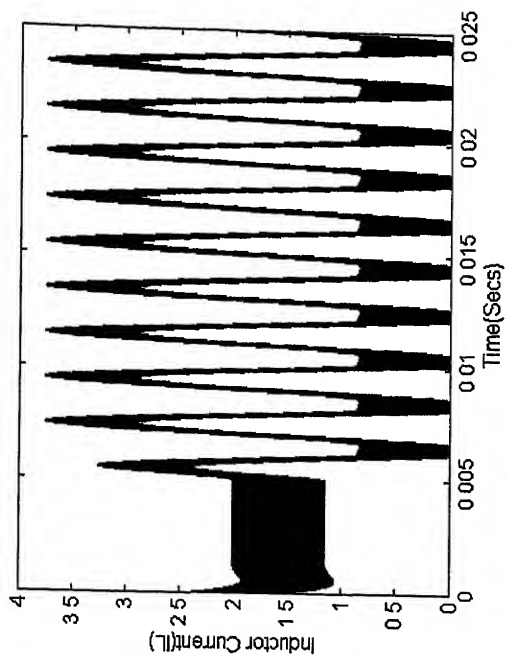


(b)

FIG 4.14 : System Response to sinusoidal variation of V_{ref} at 500 Hz of magnitude 2.5v at $R = 30$ Ohms & $V_{ref} = 5$ v.

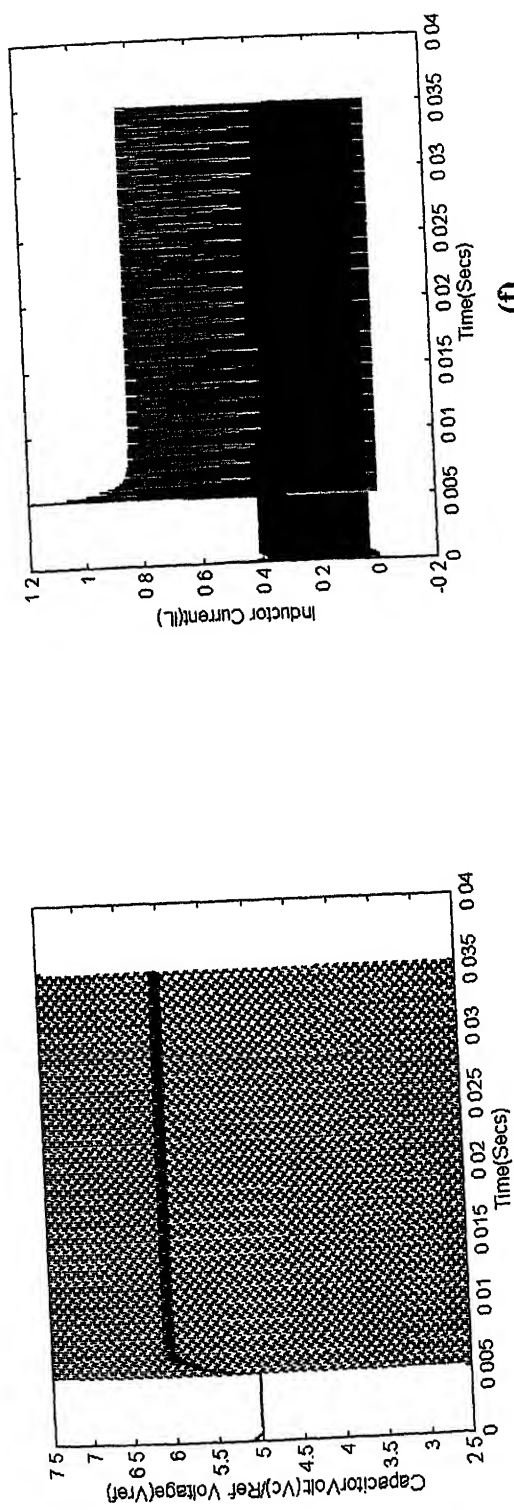


(c)



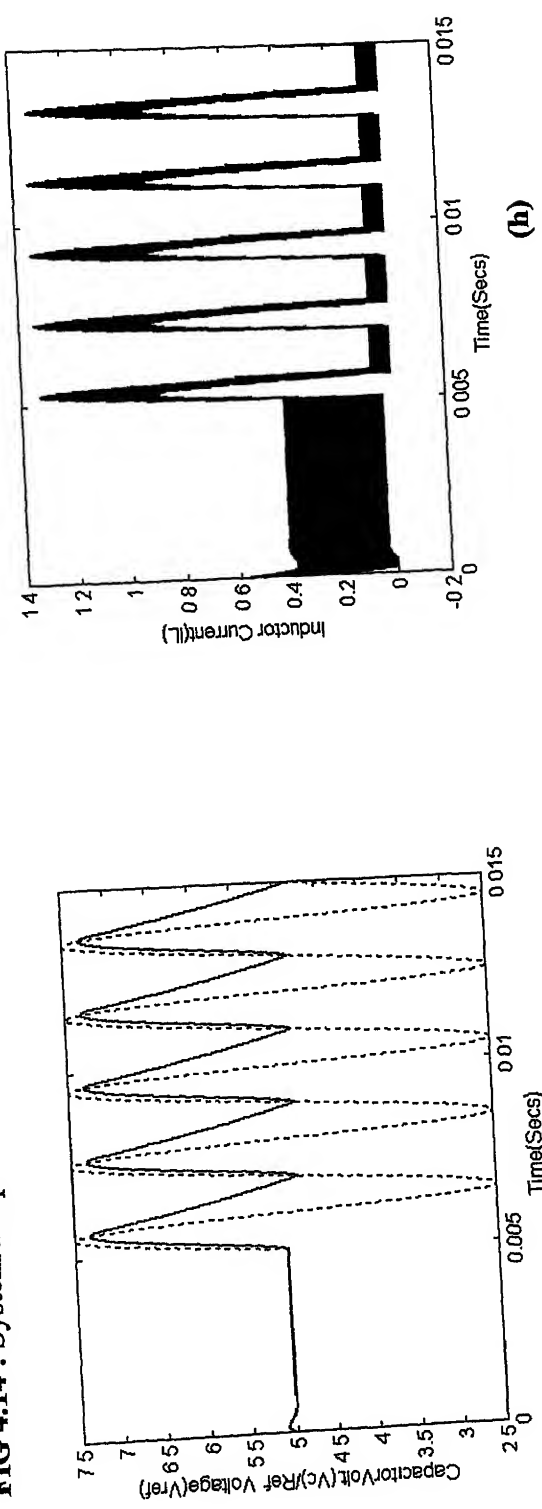
(d)

FIG 4.14 : System Response to sinusoidal variation of V_{ref} at 500 Hz of magnitude 2.5v at $R = 30$ Ohms & $V_{ref} = 20$ v.



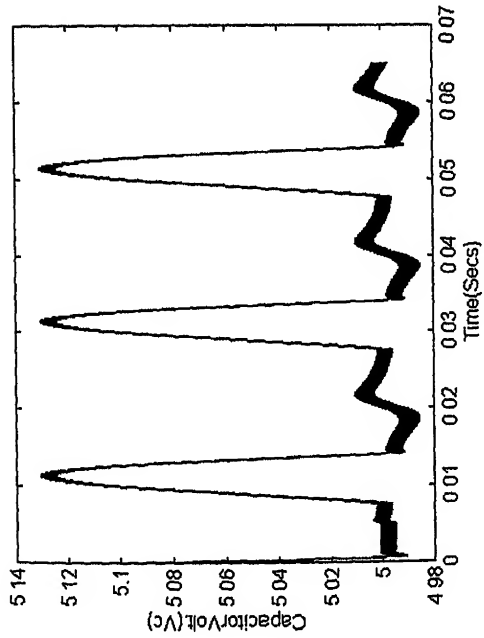
(e)

FIG 4.14 : System Response to sinusoidal variation of Vref at 5000 Hz of magnitude 2.5v at R= 30 Ohms & Vref = 5 v.

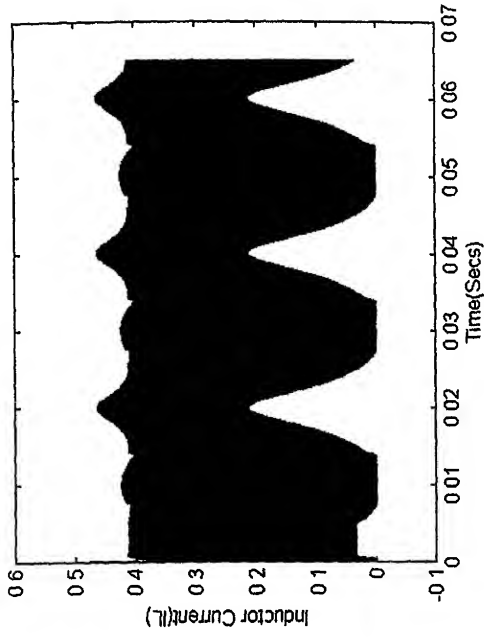


(g)

FIG 4.14 : System Response to sinusoidal variation of Vref at 500 Hz of magnitude 2.5v at R= 30 Ohms & Vref = 5 v for KFB=[1 1] & Ki=1

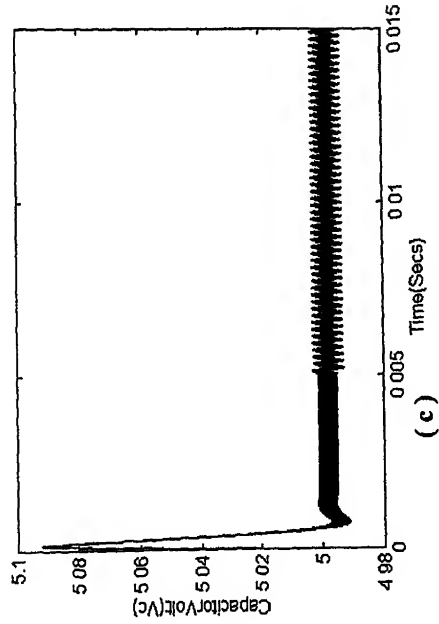


(a)

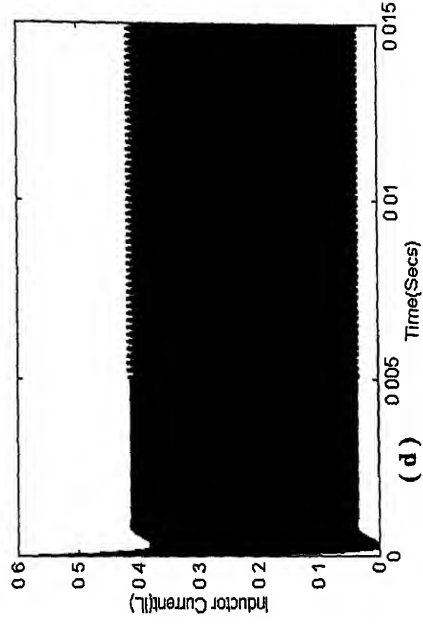


(b)

FIG 4.15: System Response to Sinusoidal variation in Vdc of 10v and 50Hz around operating point Vref=5v & R=30 Ohms



(c)



(d)

FIG 4.15: System Response to Sinusoidal variation in Vdc of 1v and 5000Hz around operating point Vref=5v & R=30 Ohms

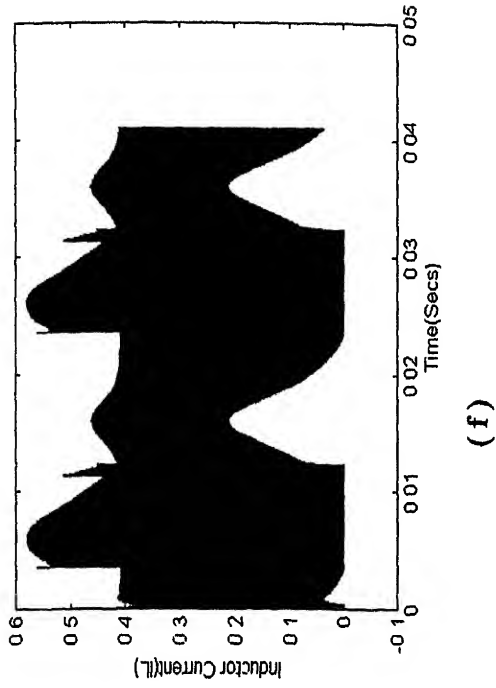
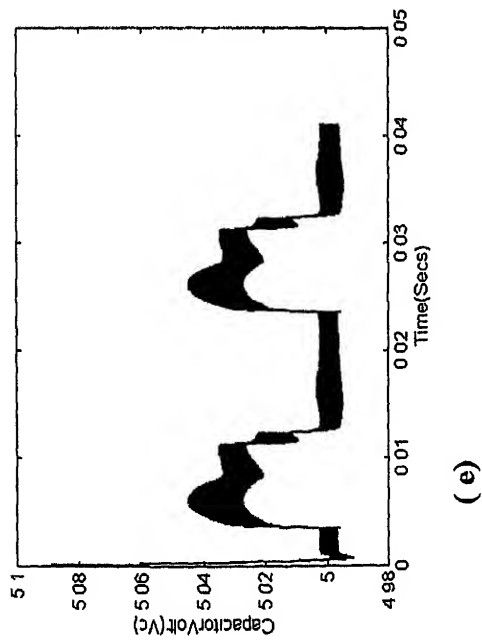


FIG 4.15: System Response to Sinusoidal Variation in Vdc at 50Hz of magnitude 10v ;around Vref=5v & R=30 Ohms for KFB=[1 1] & K_I=1

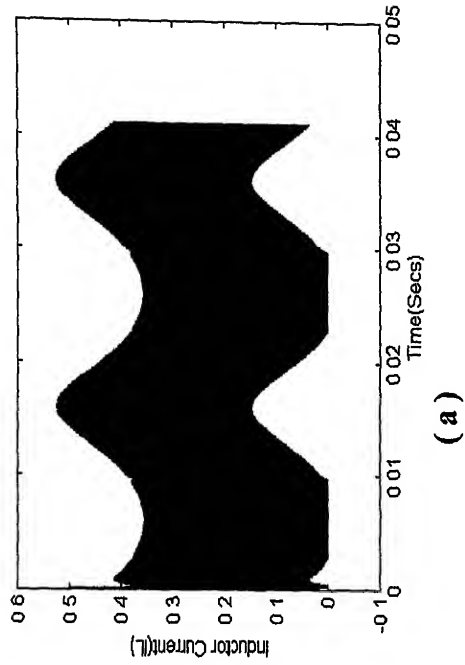
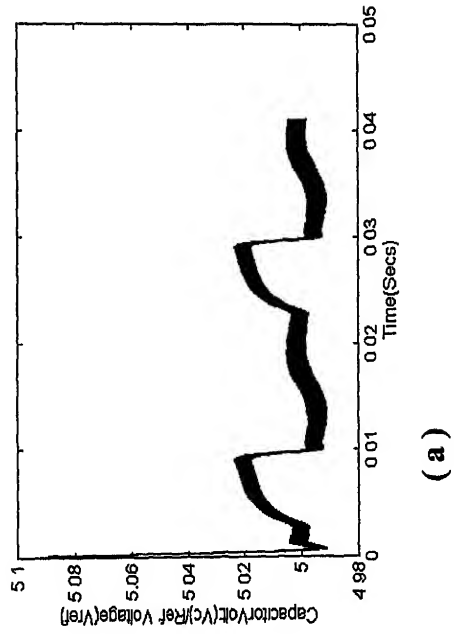
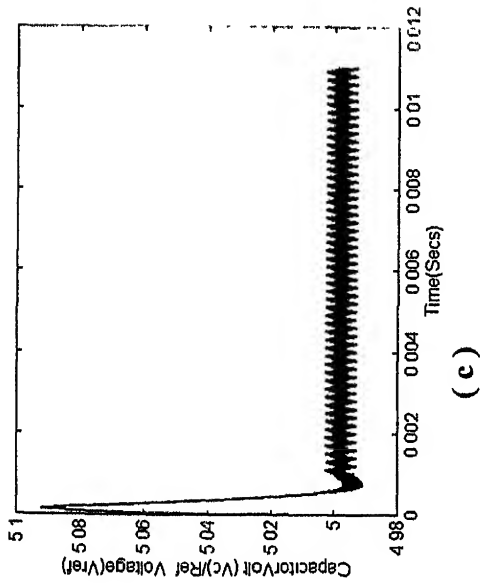
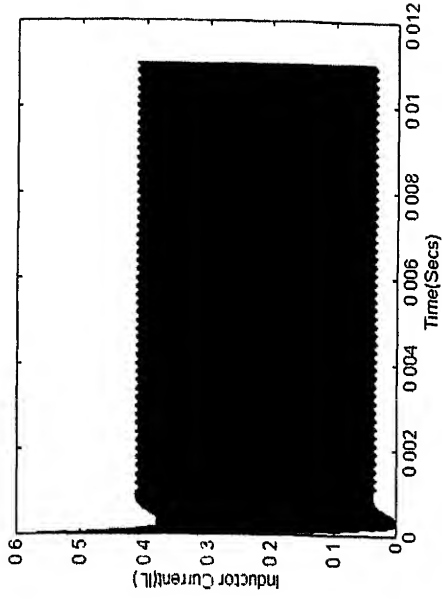


FIG 4.16: System Response to Sinusoidal Variation in R at 50Hz of magnitude 10 Ohms ;around Vref=5v & R=30 Ohms

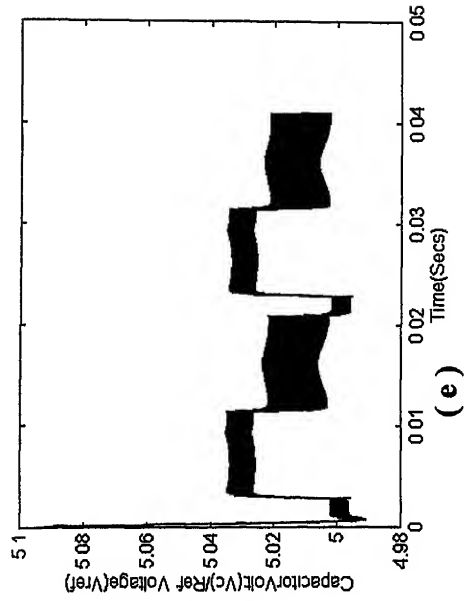


(c)

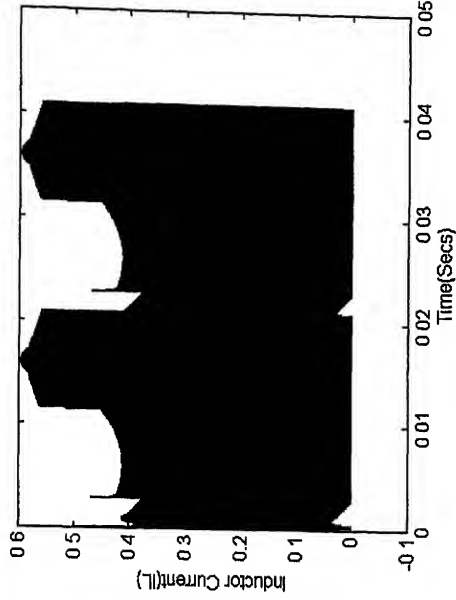


(d)

FIG 4.16: System Response to Sinusoidal Variation in R at 5000Hz of magnitude 1 Ohms ;around $V_{ref}=5v$ & $R=30$ Ohms



(e)



(f)

FIG 4.16: System Response to Sinusoidal Variation in R at 50Hz of magnitude 100ohms ;around $V_{ref}=5v$ & $R=30$ Ohms ;for $K_{FB}=[1 \ 1]$ & $K_I=1$

CHAPTER V

CONCLUSION AND FUTURE WORK :

From the modelling and the detailed analysis of the Buck-boost converter an insight into its characteristics has been achieved. Zones of continuous, boundary and discontinuous operation have been defined for a given load resistance and that during the discontinuous mode of conduction for a given load resistance R the duration of mode-2 remains constant for all values of D . This information can be used to define continuous state space averaged models and therefore the small signal models for any operating point easily. It is observed that the system satisfies the necessary and sufficient conditions of arbitrary pole placement and state feed back controller has been designed.

However, the effort to prove the fact that the state space averaged models can represent the actual converter for all kinds of perturbation has succeeded partially. For the transition of the kind DCM—DCM---DCM, DCM---CM---DCM, CM---DCM---DCM during the initial state, the transient state and the final state additional factors governing the model transition conditions need to be examined. One possibility is to examine the nature of transients in the differential equation model with particular attention being given to variation of D_1 . If this variation can be modelled then probably the information gained can be used in the state space averaged models to represent all kinds of perturbations.

Deciding the desired damping ratio to achieve optimum system response for change in V_{ref} , V_{dc} , R is difficult. Fuzzy decision making can be applied to decide close loop damping ratio by fuzzyfying the open loop response. It is observed that values of K_1 , K_2 , K_I as desired by the algorithm given in Fig. 4.7 gives satisfactory results. However optimization of the response can be done by using fuzzy gain scheduling.

REFERENCES :

1. D.M. Mitchell, "DC-DC Switching Regulator Analysis", Mc-Grawhill, 1988.
2. Katsuhito Ogata, "Modern Control Engineering", Prentice Hall, 1992.

State Vector : A vector that determines uniquely the system state $x(t)$ for any time $t \geq t_0$ once the state at $t=t_0$ is given and the input $u(t)$ for $t \geq t_0$ is specified.

State Space : The n -dimensional space whose co-ordinate axes consist of the x_1, x_2, \dots, x_n axis. Any state can be represented by a point in the state -space.

State Space Equations : Assume that a multiple input -output system involves n integers, also there are r inputs $u_1(t), u_2(t), \dots, u_r(t)$ and m outputs $y_1(t), y_2(t), \dots, y_m(t)$

Let the n outputs of the integers be defined by state variables $x_1(t), x_2(t), \dots, x_n(t)$. The system may then be described by

$$x_1(t) = f_1(x_1, x_2, \dots, x_r; u_1, u_2, \dots, u_r; t)$$

$$x_2(t) = f_2(x_1, x_2, \dots, x_r; u_1, u_2, \dots, u_r; t)$$

$$x_n(t) = f_n(x_1, x_2, \dots, x_r; u_1, u_2, \dots, u_r; t)$$

and the system outputs given by

$$y_1(t) = g_1(x_1, x_2, \dots, x_r; u_1, u_2, \dots, u_r; t)$$

$$y_2(t) = g_2(x_1, x_2, \dots, x_r; u_1, u_2, \dots, u_r; t)$$

$$y_m(t) = g_m(x_1, x_2, \dots, x_r; u_1, u_2, \dots, u_r; t)$$

$$X(t) = \begin{bmatrix} x_1(t) \\ x_2(t) \\ \vdots \\ x_n(t) \end{bmatrix} \quad f(x, u, t) = \begin{bmatrix} f_1(x_1, x_2, \dots, x_n; u_1, u_2, \dots, u_r; t) \\ f_2(x_1, x_2, \dots, x_n; u_1, u_2, \dots, u_r; t) \\ f_n(x_1, x_2, \dots, x_n; u_1, u_2, \dots, u_r; t) \end{bmatrix}$$

$$Y(t) = \begin{bmatrix} y_1(t) \\ y_2(t) \\ \vdots \\ y_n(t) \end{bmatrix} \quad g(x, u, t) = \begin{bmatrix} g_1(x_1, x_2, \dots, x_n; u_1, u_2, \dots, u_r; t) \\ g_2(x_1, x_2, \dots, x_n; u_1, u_2, \dots, u_r; t) \\ g_n(x_1, x_2, \dots, x_n; u_1, u_2, \dots, u_r; t) \end{bmatrix}$$

$$\dot{u}(t) = \begin{bmatrix} u_1(t) \\ u_2(t) \\ \vdots \\ u_n(t) \end{bmatrix}$$

$$\text{Then, } X(t) = f(x, u, t) \tag{1}$$

$$Y(t) = g(x, u, t) \tag{2}$$

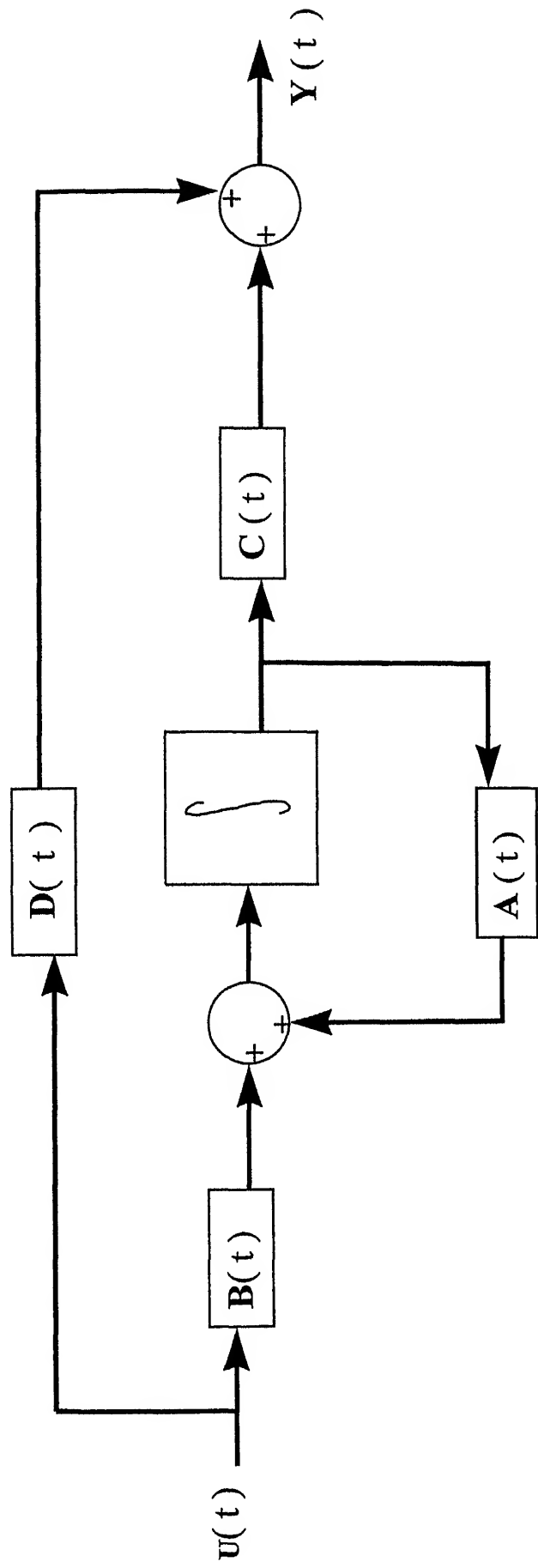


FIG A - 1 : State Space Representation of a system defined by Non - linear Differential Equation

Eq. 1 is the input Equation. and Eq. 2 is the output Equation. If vector function f and/ or g involve time t explicitly then system is called a time -varying system and if Eq. 1 and 2 are linearised about the operating point then we have the following linearized eqn.

$$\dot{X}(t) = A(t)X(t) + B(t)u(t) \quad (3)$$

$$Y(t) = C(t)X(t) + D(t)u(t) \quad (4)$$

Where $A(t)$ is called the state matrix

$B(t)$ is called the input matrix

$C(t)$ is called output matrix

$D(t)$ is called direct transmission matrix

If functions f and g do not involve t explicitly then system is called time variant system and is represented by

$$\dot{X}(t) = AX(t) + Bu(t) \quad (5)$$

$$Y(t) = CX(t) + Du(t) \quad (6)$$

Fig. A-1 gives the block diagram representation of equations.

APPENDIX B

B-1 CONCEPTS OF STATE-SPACE AVERAGING :

Let us consider the two method conduction of the converter: The system can now be represented by :-

$$X(t) = A_1 X(t) + B_1 u(t) \text{ for } n T_s \leq t \leq (n+D)T_s \quad (1)$$

$$X(t) = A_2 X(t) + B_2 u(t) \text{ for } (n+D) T_s \leq t \leq (n+1)T_s \quad (2)$$

for any cycle n .

Where $T_s = 1/f_s$

Eq. 1 cannot continuously follow Eq. 2 . Since $X[(n+D)T_s - \epsilon]$ as described by Eq. 1 cannot equal $X[(n+D)T_s]$ as described by Eq. 2, no matter how closely ϵ approaches zero. But if the switching components of the $X(t)$ waveform are excluded continuous description of a discontinuous system can be approached. Now the time-interval of Eq. 1 can include $(n+D)T_s$ and that of Eq. 2 can include $(n+1)T_s$. If the switching frequency is high enough

relative to the circuit natural frequency and the signal frequency then switching period is short enough to approximate X at $t = n T_s$ and at $t = (n+D)T_s$ as follows

$$X(nT_s) = \frac{X[(n+D)T_s] - X[nT_s]}{DT_s} \quad (3)$$

$$X(n+D)T_s = \frac{X[(n+1)T_s] - X[(n+D)T_s]}{(1-D)T_s} \quad (4)$$

Since now closed time intervals are permitted, we combine Eq. (1 and 3) & (2 and 4), to eliminate $X(nT_s)$, $X[(n+D)T_s]$

$$X(n+D)T_s = X(nT_s) + DT_s [A_1 X(nT_s) + B_1 u(nT_s)] \quad (5)$$

$$X(n+1)T_s = X[(n+D)T_s] + (1-D)T_s [A_2 X(n+D)T_s + B_2 u(n+D)T_s] \quad (6)$$

Combining Eq. 5&6 to eliminate $X[(n+D)T_s]$ we get

$$X[(n+1)T_s] = X(nT_s) + DT_s [A_1 X(nT_s) + B_1 u(nT_s) +$$

$$(1-D)T_s A_2 [X(nT_s) + DT_s [A_1 X(nT_s) + B_1 u(nT_s)]] + (1-D)T_s B_2 u(n+D)T_s \quad (7)$$

$$\text{Now } u(nT_s) = \frac{u[(n+D)T_s] - u(nT_s)}{DT_s}$$

Therefore

$$\frac{X[(n+1)T_s] - X(nT_s)}{T_s} = [A_1D + (1-D)A_2]X(nT_s) + [B_1D + (1-D)B_2]u(nT_s) + [(1-D)D T_s [A_2[A_1X(nT_s) + B_1u(nT_s)]] + [B_2u(nT_s)] \quad (8)$$

If T_s is very small LHS of Eq. 8 approximates $X(nT_s)$ and T_s terms of RHS being negligible results in

$$X(nT_s) = [A_1D + (1-D)A_2]X(nT_s) + [B_1D + (1-D)B_2]u(nT_s) \quad (9)$$

Therefore

$$A_0 = A_1D + A_2(1-D)$$

$$B_0 = B_1D + B_2(1-D)$$

B-2 LINEARIZATION OF STATE -SPACE AVERAGED MODELS :

In the linear state space averaged Eqn., if the D.C. terms of X, u, D are separated from signal frequency A-C terms. It is assumed that ac amplitudes are small enough so that the product of any two ac terms is negligible.

Substituting $X = X_o + \hat{X}$

$$u = u_o + \hat{u}$$

$$D = D_o + \hat{d}$$

(where \hat{X} , \hat{u} , \hat{d} identify the signal frequency ac terms) in Eq. 9 results in DC Eqn.

$$0 = [A_1 D + (1-D)A_2]X_o + [B_1 D + (1-D)B_2]u_o \quad (10)$$

and ac Eq.

$$\hat{X} = [A_1 D + (1-D)A_2] \hat{X} + [B_1 D + B_2(1-D)] \hat{u} + [(A_1 - A_2)]X_o + [(B_1 - B_2) u_o] \hat{d} \quad (11)$$

Defining $E = (A_1 - A_2)X_o + [(B_1 - B_2) u_o]$

Eq. 10 and 11 can be written as

$$0 = A_0 X_o + B_0 u_o \quad (12)$$

$$\hat{X} = A_0 X + B_0 \hat{u} + E \hat{d} \quad (13)$$

Adding Eq. 12 & 13 results in a linearized Eqn.

$$\hat{X} = A_0 X + B_0 \hat{u} + E \hat{d}$$

Valid for an operating point in the continuous operating zone. But in discontinuous operating zone A_0 and B_0 are defined by Eq. 3.4 and 3.5 and matrix E is defined as

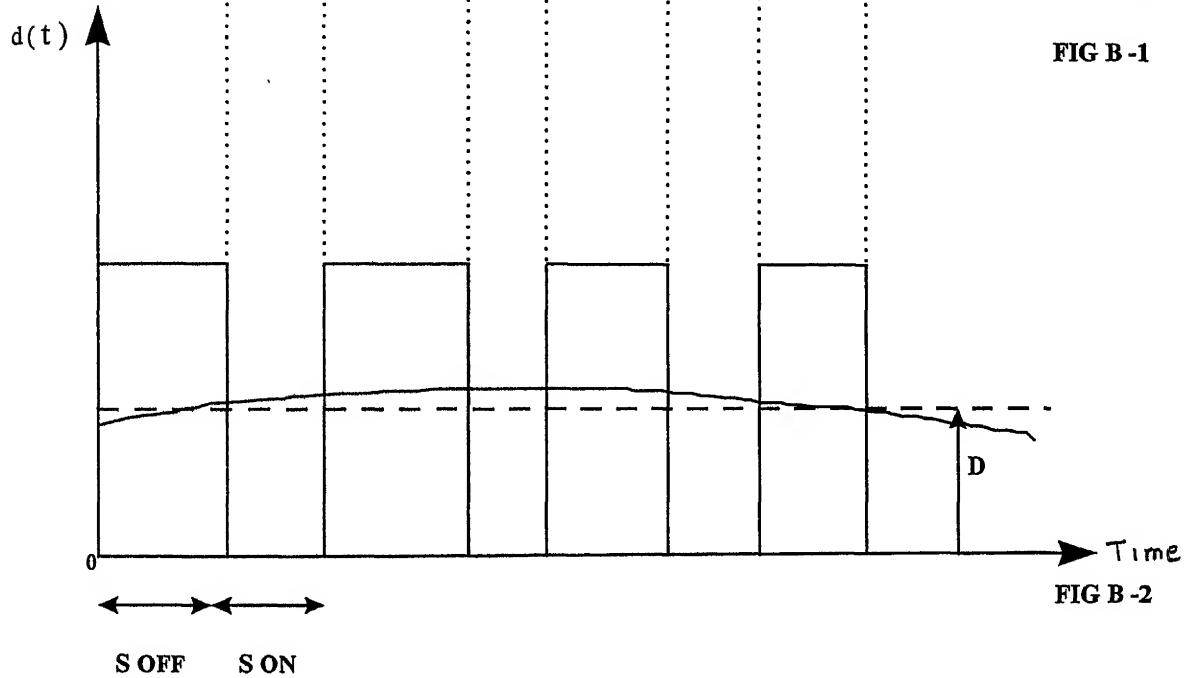
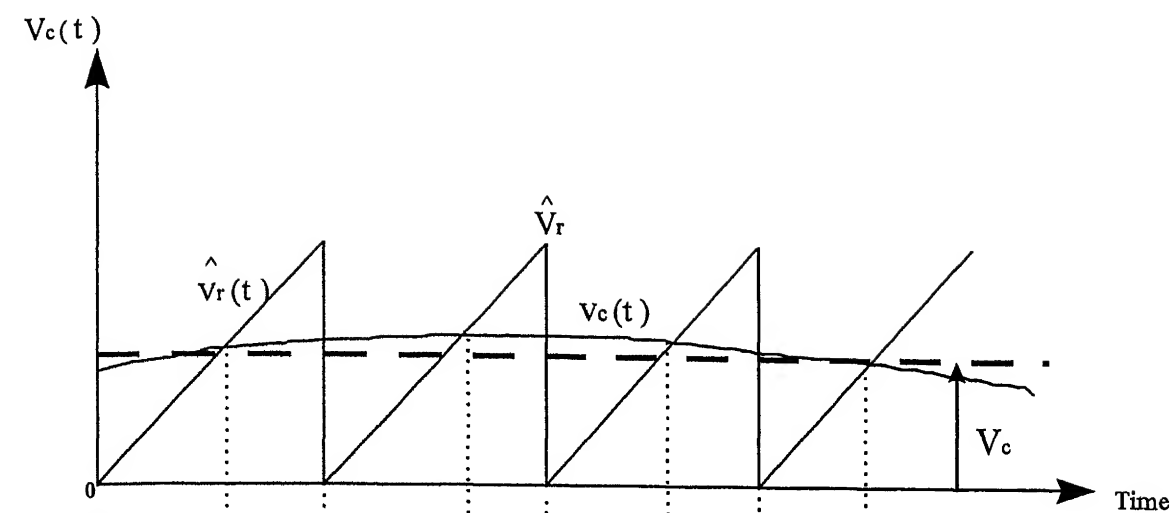
$$E = (A_1 - A_2 - A_3) X_0 + (B_1 - B_2 - B_3) u_0 \quad (14)$$

Where $X_0 = -\text{inv}(A_0) B_0 V_{dc}$

B-3 SMALL SIGNAL MODEL OF PULSE WIDTH MODULATOR :

In the direct duty ratio pulse-width modulator, the control voltage $v_c(t)$, which is output of the error amplifier is compared with a repetitive waveform $v_r(t)$, which establishes the switching frequency f_s , as in Fig. B-1. The control voltage $v_c(t)$ consists of a dc component and a small ac perturbation component

$$v_c(t) = v_c + \tilde{v}_c \quad (15)$$



Graphical Representation of functioning of Pulse Width Modulator

where $v_c(t)$ is in a range between 0 and \tilde{v}_r , as shown in Fig. B-1. $\tilde{v}_c(t)$ is a sinusoidal ac perturbation in the control voltage at a frequency ω , where ω is much smaller than the switching frequency $\omega_s (= 2\pi f_s)$. The ac perturbation in the control voltage can be expressed as

$$\tilde{v}_c(t) = a \sin(\omega t - \phi) \quad (16)$$

by means of an amplitude a and an arbitrary phase angle ϕ .

In fig. B-2, the instantaneous switching duty ratio $d(t)$ is as follows :

$$d(t) = 1.0 \text{ if } \tilde{v}_c(t) \geq v_r(t) \quad (17)$$

$$= 0 \text{ if } \tilde{v}_c(t) < v_r(t) \quad (18)$$

$d(t)$ can be expressed in terms of the Fourier series as

$$d(t) = \frac{v_c}{V_r} + \frac{a}{V_r} \sin(\omega t - \phi) + \text{other high frequency component} \quad (19)$$

The higher frequency components in the output voltage v_o due to the high frequency components in $d(t)$ are eliminated because of the low pass filter at the output of the converter,

therefore the high frequency components in Eq. 13 can be ignored. In terms of its dc value and ac perturbation :

$$d(t) = D + \tilde{d}(t) \quad (20)$$

Comparing Eq. 19 & 20

$$D = \frac{V_c}{V_r} \quad (21)$$

$$\tilde{d}(t) = \frac{a}{V_r} \sin(\omega t - \phi) \quad (22)$$

From Eq. 16 & 22, the small signal transfer function $T_m(s)$ of the Pulse Width Modulator is

$$T_m(s) = \frac{\tilde{d}(s)}{\tilde{v}_c(s)} = \frac{1}{V_r}$$

APPENDIX C

C-1 : CORRELATION BETWEEN TRANSFER FUNCTION AND STATE-SPACE EQUATIONS :

Equations 5 and 6 in Appendix A represents a system in state-space. Since transfer function is defined as the ratio of the Laplace transform of the output to the Laplace transform of the input when the initial conditions are zero, then taking $X(0)$ as zero in Laplace transform of the equation (5) in appendix A results in:

$$sX(s) - X(0) = AX(s) + Bu(s)$$

$$sX(s) - AX(s) = Bu(s)$$

$$(sI-A) (Xs) = Bu(s)$$

Multiplying both sides by $(sI-A)^{-1}$

$$X(s) = (sI-A)^{-1} Bu(s)$$

Substituting this in equation 6 Appendix A results in

$$Y(s) = [C(sI-A)^{-1} B + D] u(s)$$

And the transfer function $G(s) = C(sI-A)^{-1} B + D$ (1)

Right hand side of equation 1 involves $(sI-A)^{-1}$. Hence $G(s)$ can be written as

$$G(s) = Q(s) / |sI - A|$$

Where $Q(s)$ is a polynomial in s . Therefore $|sI - A|$ is equal to the characteristic polynomial of $G(s)$ and the eigenvalues of A are identical to poles of $G(s)$.

C-2 : SOLUTIONS OF LINEAR TIME INVARIANT VECTOR MATRIX DIFFERENTIAL EQUATIONS :

Consider the following vector matrix differential equation.

$$\dot{X}(t) = AX(t) + Bu(t) \quad (2)$$

Let $X(0) = X_0$

Where X is an n -vector

u is a r -vector

A is $n \times n$ constant matrix

B is $n \times r$ constant matrix

Equation 2 can be written as

$$\dot{X}(t) - AX(t) = Bu(t)$$

Multiplying both sides of this equation by e^{-At} results in

$$e^{-At}[X(t) - AX(t)] = \frac{d}{dt}[e^{-At}X(t)] = e^{-At}Bu(t)$$

integrating the above equation between 0 and t

$$\begin{aligned} e^{-At}X(t) &= X_0 + \int_0^t e^{-A\tau}Bu(\tau)d(\tau) \\ X(t) &= e^{At}X_0 + \int_0^t e^{A(t-\tau)}Bu(\tau)d\tau \end{aligned} \quad (3)$$

If initial time is t_0 instead of 0 then

$$X(t) = e^{A(t-t_0)}X_0 + \int_{t_0}^t e^{A(t-\tau)}Bu(\tau)d\tau$$

Where $X_0 = X(t_0)$

The response $X(t)$ is a sum of the motions due to the initial condition and those due to the forcing function. Motion due to forcing function depend on B. It is possible to choose B such that any particular motion $e^{\lambda_i t}$ cannot be excited for any input.

C-3: COMPLETE STATE CONTROLLABILITY OF CONTINUOUS TIME SYSTEMS

Solutions of linear time-invariant vector matrix differential equation defined by equation 2 is given by equation 3. Note that using the Sylvester's interpolation formula for a minimal polynomial involving only distinct roots e^{-At} can be written as *that is and how is it implied.*

$$e^{-A\tau} = \sum_{k=0}^{n-1} \alpha_k(\tau) A^k \quad (4)$$

System described by equation 2 is said to be state controllable at $t=t_0$ if it is possible to construct an unconstrained control signal that will transfer an initial state to any final state in a finite time interval $t_0 < t \leq t_1$. If every state is controllable then the system is said to be completely state controllable.

CONDITION OF COMPLETE STATE CONTROLLABILITY :

It is assumed that the final state is the origin of the state space & that the initial time $t_0=0$. Applying the definition of complete state controllability in equation 3 results in :

$$X(t_1) = e^{At_1} X_0 + \int_0^{t_1} e^{A(t_1-\tau)} B u(\tau) d\tau = 0 \quad (5)$$

$$\therefore X(0) = - \int_0^{t_1} e^{-A\tau} B u(\tau) d\tau \quad (6)$$

Substituting the value of $e^{-A\tau}$ as given by equation (4)

$$X(0) = - \sum_{k=0}^{n-1} A^k B \int_0^{t_1} \alpha_k(\tau) u(\tau) d\tau$$

Put $\int_0^t \alpha_k(\tau) u(\tau) d\tau = \beta_k$

$$X(0) = - \sum_{k=0}^{n-1} A^k B \beta_k$$

$$X(0) = - [B \quad AB \dots A^{n-1}B] \begin{bmatrix} \beta_0 \\ \beta_1 \\ \vdots \\ \beta_{n-1} \end{bmatrix} \quad (7)$$

If the system is completely state controllable then given any initial state $X(0)$, equation 6 must be satisfied. This requires that the rank of the nxn matrix consisting of n linearly independent column vectors, $[B \quad AB \dots A^{n-1}B]$ (called as the controllability matrix) be n.

C-4 NECESSARY & SUFFICIENT CONDITIONS FOR ARBITRARY POLE PLACEMENT.:

Consider the control system defined by equation.2. We assume that the magnitude of the control signal u is unbounded. If the control signal u is chosen as : $u = -Kx$, where K is the

state feedback gain matrix (1xn matrix), then the system becomes a closed loop control system as shown in Fig. 4.3(a) and the solution to equation.2 becomes

$$X(t)=e^{(A-BK)t}X(0).$$

Note that the eignvalues of matrix A-BK (which we denote μ_1 , μ_2,u_n) are the desired closed loop poles. If the system is not completely state controllable, then there are eigenvalues of matrix A-BK that cannot be controlled by state feedback. Suppose the system represented by equation 2 is not completely state controllable. Then the rank of the controllable matrix is less than n,

$$\text{or rank } [B|AB|.....A^{n-1}B] = q < n$$

This means that there are q linearly independant column vectors in the controllibility matrix, such q linearly independent column vectors are defined as f_1, f_2,f_q. Also, let n-q additional vectors $V_{q+1}, V_{q+2}.....V_n$ be such that

$$P = [f_1 \ f_2.....f_q \ V_{q+1} \ V_{q+2}.....V_n] \text{ is of rank } n.$$

Then

$$\hat{A} = P^{-1}AP = \begin{bmatrix} A_{11} & A_{12} \\ 0 & A_{22} \end{bmatrix} \quad \hat{B} = P^{-1}B = \begin{bmatrix} B_{11} \\ 0 \end{bmatrix}$$

Define $\hat{K} = KP = \begin{bmatrix} K_1 & K_2 \end{bmatrix}$

Then

$$\begin{aligned}
 |sI - A + BK| &= |P^{-1}(sI - A + BK)P| \\
 &= |sI - P^{-1}AP + P^{-1}BKP| = |sI - \hat{A} + \hat{B}\hat{K}| \\
 |sI - A + BK| &= |sI - \hat{A} + \hat{B}\hat{K}| \\
 &= \left| sI - \begin{bmatrix} A_{11} & A_{12} \\ 0 & A_{22} \end{bmatrix} + \begin{bmatrix} B_{11} \\ 0 \end{bmatrix} \begin{bmatrix} K_1 & K_2 \end{bmatrix} \right| \\
 &= |sI_q - A_{11} + B_{11}K_1 - A_{12} + B_{11}K_2| \\
 &\quad |sI_q - A_{11} + B_{11}K_1| \cdot |sI_{n-q} - A_{22}| = 0
 \end{aligned}$$

Where I_q is a q -dimensional identity matrix I_{n-q} is an $(n-q)$ dimensional identity matrix.

Notice that the eigenvalues of A_{22} do not depend on K . Thus if the system is not completely state controllable, then there are eigenvalues of matrix A that cannot be arbitrarily placed, therefore, to place the eigenvalues of matrix $A-BK$ arbitrarily, the system must be completely state controllable (necessary condition)

Next, if the system is completely state controllable [means that matrix M given by equation 9 below has rank n or has inverse], then all eigenvalues of matrix A can be arbitrarily placed (sufficient conditions). In proving the sufficient condition, it is convenient to

transform the state equation given by equation (2) into controllable Canonical form. Define a transformation matrix T by

$$T=MW \tag{8}$$

Where M is the controllability matrix

$$M = [B|AB.....|A^{n-1}B] \tag{9}$$

and

$$W = \begin{bmatrix} a_{n-1} & a_{n-2} & ----- & a_1 & 1 \\ a_{n-2} & a_{n-3} & ----- & a_1 & 0 \\ & & ----- & & \\ a_1 & 0 & & 0 & 0 \\ 1 & 1 & ----- & 0 & 0 \end{bmatrix}$$

Where the a_i 's are co-efficients of the characteristic polynomial.

$$|sI - A| = S^n + a_1 S^{n-1} + a_2 S^{n-2} + + a_{n-1}S + a_n$$

Define a new state vector \hat{X} by

$$X = T \hat{X}$$

If the rank of the controllability mark M is n (meaning that the system is controllable), then the inverse of matrix T exists and equation (8) can be modified to

$$\dot{\hat{X}} = T^{-1}AT\hat{X} + T^{-1}Bu \tag{10}$$

$$T^{-1}AT = \begin{bmatrix} 0 & 1 & 0 & \dots & 0 \\ 0 & 0 & 1 & \dots & 0 \\ \vdots & \vdots & \vdots & \ddots & \vdots \\ 0 & 0 & 0 & \dots & 1 \\ -a_n & -a_{n-1} & -a_{n-2} & \dots & -a_1 \end{bmatrix}$$

$$T^{-1}B = \begin{bmatrix} 0 \\ 0 \\ \vdots \\ 0 \\ 1 \end{bmatrix}$$

Equation (10) represents the system in controllable canonical form. Thus, given a state equation. Equation (2), it can be transformed into the controllable canonical form if the system is completely state controllable and if we transform the state vector X into state vector \hat{X} by use of transformation matrix T.

Let the set of the desired eigenvalues be u_1, u_2, \dots, u_n . Then the desired characteristic equation becomes

$$(S-u_1)(S-u_2)\dots(S-u_n) = S^n + \alpha_1 S^{n-1} + \dots + \alpha_{n-1} S + \alpha_n \tag{11}$$

Let,

$$\hat{K} = KT = [\delta_n \delta_{n-1} \dots \delta_1] \tag{12}$$

When $u = -\hat{K}\hat{X} = -KT\hat{X}$ is used to control the system given by equation (2) the system equation becomes

$$\dot{\hat{X}} = T^{-1}AT\hat{X} - T^{-1}BKT\hat{X}$$

The characteristic equation is

$$|sI - T^{-1}AT + T^{-1}BKT| = 0$$

This characteristic equation is the same as the characteristic equation for the system, defined by equation (2), when $U=-KX$ is used as the control signal. This can be seen as follows.

Since

$$\dot{X} = AX + Bu = (A - BK)X$$

The characteristic equation for this system is

$$|sI - A + BK| = |T^{-1}(sI - A + BK)T| = |sI - T^{-1}AT + T^{-1}BKT|$$

Simplifying the characteristic equation of the system in the controllable canonical form

$$\begin{aligned}
 &|sI - T^{-1}AT + T^{-1}BKT| \\
 &= \left| sI - \begin{bmatrix} 0 & 1 & \dots & 0 \\ 0 & 0 & \dots & 1 \\ -a_n & -a_{n-1} & \dots & -a_1 \end{bmatrix} + \begin{bmatrix} 0 \\ 0 \\ 1 \end{bmatrix} [\delta_n \delta_{n-1} \dots \delta_1] \right| \\
 &= \left| \begin{bmatrix} s & -1 & \dots & 0 \\ 0 & s & \dots & 0 \\ & 0 & \dots & \\ a_n + \delta_n & a_{n-1} + \delta_{n-1} & \dots & s + a_1 + \delta_1 \end{bmatrix} \right|
 \end{aligned}$$

$$s^n + (a_1 + \delta_1)s^{n-1} + \dots + (a_{n-1} + \delta_{n-1})s + (a_n + \delta_n) = 0$$

This is the characteristic equation for the system with state feedback. So it must be equal to equation (11) the desired characteristic equation. By equating the coefficients of like powers of s.

$$a_1 + \delta_1 = \alpha_1$$

$$a_2 + \delta_2 = \alpha_2$$

$$\vdots$$

$$a_n + \delta_n = \alpha_n$$

Solving the preceding equations for the δ_i 's and substituting them into equation (12), results in

$$\hat{K} = KT^{-1} = [\delta_n \delta_{n-1} \dots \delta_1] T^{-1}$$

Thus if the system is completely state controllable, all eigenvalues can be arbitrarily placed by choosing matrix K according to equation. We have thus proved that the necessary and sufficient condition for arbitrary pole placement is that the system be completely state controllable.

C-5 :

If matrix P is defined as $\begin{bmatrix} A & 0 \\ -C & 0 \end{bmatrix}$ and has rank (n+1) then the system defined by

equation 4.13 is completely state controllable as shown :

If M is defined as

$$M = [BAB \dots A^{n-1} B]$$

and if system is defined by

$$\dot{X} = AX + Bu$$

is completely state controllable and rank of matrix M is n then rank of

$$\begin{bmatrix} M & 0 \\ 0 & 1 \end{bmatrix} \quad \text{is } n+1$$

Consider

$$\begin{bmatrix} A & B \\ -C & 0 \end{bmatrix} \begin{bmatrix} M & 0 \\ 0 & 1 \end{bmatrix} = \begin{bmatrix} AM & B \\ -CM & 0 \end{bmatrix} \tag{13}$$

Since matrix P is of rank n+1 the left side of equation (13) is of rank (n+1) and

∴ RHS of equation (13) is also of rank (n+1), since,

$$\begin{bmatrix} AM & B \\ -CM & 0 \end{bmatrix} = \begin{bmatrix} A[B \ AB \ \cdots \ A^{n-1}B] & B \\ -C[B \ AB \ \cdots \ A^{n-1}B] & 0 \end{bmatrix}$$

and if system is defined by

$$\dot{X} = AX + Bu$$

is completely state controllable and rank of matrix M is n then rank of

$$\begin{bmatrix} M & 0 \\ 0 & 1 \end{bmatrix} \quad \text{is } n+1$$

Consider

$$\begin{bmatrix} A & B \\ -C & 0 \end{bmatrix} \begin{bmatrix} M & 0 \\ 0 & 1 \end{bmatrix} = \begin{bmatrix} AM & B \\ -CM & 0 \end{bmatrix} \tag{13}$$

Since matrix P is of rank n+1 the left side of equation (13) is of rank (n+1) and

∴ RHS of equation (13) is also of rank (n+1), since,

$$\begin{bmatrix} AM & B \\ -CM & 0 \end{bmatrix} = \begin{bmatrix} A[B \ AB^{-} \ \cdots \ A^{n-1}B] & B \\ -C[B \ AB \ \cdots \ A^{n-1}B] & 0 \end{bmatrix}$$

$$\begin{bmatrix} \hat{A}M & B \\ -CM & 0 \end{bmatrix} = \begin{bmatrix} \hat{A}B \hat{A}^2 B^- \dots \hat{A}^n B & B \\ -CB - CAB \dots - CA^{n-1} B & 0 \end{bmatrix}$$

$$[\hat{A} \hat{B} \hat{A}^2 \hat{B}^- \dots \hat{A}^n \hat{B}. \hat{B}]$$

Where rank of

$$[\hat{B} \hat{A} \hat{B} \hat{A}^2 \hat{B}^- \dots \hat{A}^n \hat{B}] \quad \text{is } (n+1)$$

Thus the system defined by equation 4.13 is completely state controllable and solution to it can be obtained by pole placement approach.

The state error equation can be obtained by substituting $u_v = -\hat{K}V$ in equation 4.13.

$$\dot{\hat{V}} = (\hat{A} - \hat{B}\hat{K})V$$

If the desired eigenvalues of matrix $(\hat{A} - \hat{B}\hat{K})$ or the desired closed-loop poles are specified as u_1, u_2, \dots, u_{n+1} then feedback gain matrix K_{FB} and the integral gain constant K_I can be determined.

If a_1, a_2, \dots, a_p are the co-efficients of the characteristic equation $\left| sI - \hat{A} \right|$ and $\alpha_1,$

$\alpha_2, \dots, \alpha_p$ are co-efficients of the desired characteristic equation formed by defining the desired eigenvalues u_1, u_2, \dots, u_p .

Then,

$$M = [\hat{B} \ \hat{A} \ \hat{B} \ \dots \ \hat{A}^{n-1} \ \hat{B}]$$

$$W = \begin{bmatrix} a_{p-1} & a_{p-2} & \dots & a_1 & 1 \\ a_{p-2} & a_{p-3} & \dots & -a_1 & 1 & 0 \\ a_1 & 1 & 0 & 0 & 0 \\ 1 & 0 & 0 & 0 & 0 \end{bmatrix}$$

$$T = MW$$

$$\hat{K} = [K_1, K_2, \dots, K_{p-1} - K_1] = [\alpha_p - a_p \alpha_{p-1} - a_{p-1} \dots \alpha_1 - a_1] T^{-1}$$

$$=[KFB \ - \ K_1]$$

Where $KFB = [K_1 K_2 \dots K_{p-1}]$

A

113199

EE-1998-M-SAC-ANA

Date Slip

This book is to be returned on the
date last stamped

A

113199

To be issued after 17 MAY 1998

